

UNIVERSITY OF CAPE COAST

MEASUREMENT AND MODELING OF EXPOSURE LEVELS OF
RADIOFREQUENCY EMISSIONS FROM FOURTH GENERATION LONG
TERM EVOLUTION BASE STATIONS IN THREE REGIONS IN THE
SOUTHERN PART OF GHANA

ABDUL-RAZAK FUSEINI

2020

© Abdul-Razak Fuseini
University of Cape Coast

UNIVERSITY OF CAPE COAST

MEASUREMENT AND MODELING OF EXPOSURE LEVELS OF
RADIOFREQUENCY EMISSIONS FROM FOURTH GENERATION LONG
TERM EVOLUTION BASE STATIONS IN THREE REGIONS OF THE
SOUTHERN PART OF GHANA

BY

ABDUL-RAZAK FUSEINI

Thesis Submitted to the Department of Physics of School of Physical Sciences,
College of Agriculture and Natural Sciences, University of Cape Coast, in Partial
Fulfilment of the requirements for the award of Doctor of Philosophy degree in
Physics

JANUARY, 2020

DECLARATION

Candidate's Declaration

I hereby declare that this thesis is the result of my own original research and that no part of it has been presented for another degree in this university or elsewhere.

..... Date:

Abdul-Razak Fuseini
(Candidate)

Supervisors' Declaration

We hereby declare that the preparation and presentation of the thesis were supervised in accordance with the guidelines on supervision of thesis laid down by the University of Cape Coast.

..... Date:

Dr. J. K. Amoako
(Principal Supervisor)

..... Date:

Dr. A. Twum
(Co-Supervisor)

ABSTRACT

The analysis of electric field strengths and power densities at one hundred and fifty (150) Fourth Generation Long Time Evolution (4G LTE) base stations in three urban and densely populated regions of the southern part of Ghana (Greater Accra, Ashanti and Western) was carried out using an Anritsu Spectrum Master coupled to a handheld log-periodic antenna. The measurements were taken around the base stations and at public access points, chosen to represent the highest levels of exposure to which a person might be subjected to. The results of electric field strength measurement for the various base stations varied from as low as $8.52\text{E-}09 \pm 8.52\text{E-}10$ mV/m from a site in the Western region to as high as $2.81\text{E-}02 \pm 2.81\text{E-}03$ mV/m from a site in the Ashanti region. The corresponding power densities were $3.42\text{E-}08$ mW/m² and $1.13\text{E-}01$ mW/m² respectively. The results however, comply with the ICNIRP recommended limits of 38.89 V/m and 4 W/m² for electric field strength and power density for 800 MHz frequency band respectively. The results also showed a good correlation between measurement and theoretical models for the prediction of power density levels at base station, even though the levels from the measured results were on the average less than that of the predicted values.

KEYWORDS

Electromagnetic radiation

Ionising radiation

Long-Term Evolution

Non-ionising radiation

Radiofrequency

Telecommunication

ACKNOWLEDGEMENTS

My warmest gratitude goes to my supervisors Dr. Joseph Kwabena Amoako and Dr. Anthony Twum whose efforts ensured that this research work sees the light of day. May the merciful Angels of God be with them always. I wish to acknowledge Dr. Philip Deatanyah for his help in developing the model. My profound gratitude also goes to the Radiation Protection Institute of the Ghana Atomic Energy Commission for the equipment's used for the field work.

I also wish to acknowledge the staff of the Non-ionising section of Health Physics and Instrumentation Centre of the Radiation Protection Institute for their help during the field work. I thank them for the help offered me and I wish them God's blessings.

DEDICATION

This work is whole-heartedly dedicated to my mum, siblings, wife and lovely sons (Amjad and Aarif) for their prayers and support throughout the course.

	Page
DECLARATION	ii
ABSTRACT	iii
KEY WORDS	iv
ACKNOWLEDGEMENTS	v
DEDICATION	vi
LIST OF TABLES	xi
LIST OF FIGURES	xii
LIST OF ABBREVIATIONS	xv
CHAPTER ONE: INTRODUCTION	
Background to the study	1
Statement of the Problem	3
Objectives of the study	5
Justification of the study	5
Scope of the study	7
Structure of Thesis	8
Chapter Summary	8

CHAPTER TWO: LITERATURE REVIEW

Introduction	10
Electric Field	11
Magnetic Field	12
Near and Far Fields	13
Antenna Theory	14
Antenna Types	14
Some Characteristics of Antennas	28
Electromagnetic Wave Equation	30
Electromagnetic Spectrum	32
Non-Ionising Radiation	33
Biological Effect of Non-ionizing Radiation	36
Biological Effects of Radiofrequency	37
Use of RF for Communication Purpose	39
The Architecture of LTE Network and Working Principle	50
Related Works	52
Chapter Summary	54

CHAPTER THREE: METHODOLOGY

Introduction	55
Study Area	55
Materials	58
Methodology	60
Uncertainty Estimation	63
Mathematical Model	65
Chapter Summary	68

CHAPTER FOUR: RESULTS AND DISCUSSION

Introduction	69
Field Measurement	69
Mathematical model	81
Validation of Mathematical Model	81
Comparison of Model with Empirical Model	82
MATLAB Model	84
Chapter Summary	86

CHAPTER FIVE: SUMMARY, CONCLUSIONS AND
RECOMMENDATIONS

Introduction	88
Summary	88
Conclusions	89
Recommendations	90
Recommendations to the Policy Maker	
Recommendations to the Operator	
Recommendations for future research work	
REFERENCES	93
APPENDICES	107
APPENDIX 1A: GREATER ACCRA REGION; ELECTRIC FIELD STRENGTH AND POWER DENSITIES.	107
APPENDIX 1B: ASHANTI REGION; ELECTRIC FIELD STRENGTH AND POWER DENSITIES.	108
APPENDIX 1C: WESTERN REGION; ELECTRIC FIELD STRENGTH AND POWER DENSITIES	109
APPENDIX 2A: SITES WHERE MEASUREMENTS WERE TAKEN IN	

GREATER ACCRA REGION	111
APPENDIX 2B: SITES WHERE MEASUREMENTS WERE TAKEN IN	
ASHANTI REGION	112
APPENDIX 2C: SITES WHERE MEASUREMENTS WERE TAKEN IN	
WESTERN REGION	114
APPENDIX 3: MATLAB PROGRAMME CODE	115
APPENDIX 4: PUBLICATION	130

LIST OF TABLES

Table	Page
1: Comparison of work to other LTE studies	80
2: Uncertainty estimation budget	86

LIST OF FIGURES

Figure	Page
1: A Diagram of a Wave Showing Electric and Magnetic Fields	11
2: A Photograph of an Isotropic Antenna	15
3: A Photograph of a Turnstile Antenna, or Crossed-Dipole Antenna	16
4: A Photograph of a Corner Reflector Antenna	17
5: A Photograph of a Patch Antenna	18
6: A Photograph of a Monopole Antenna	19
7: A Photograph of a Collinear Antenna Array	20
8: A Photograph of a Yagi–Uda Antenna	20
9: A Photograph of a Log-Periodic Antenna	21
10: A Photograph of a Reflective Array	22
11: A Schematic Diagram of the Phased Array Antenna	22
12: A Photograph of a Curtain Array Antenna	23
13: A Photograph of a Batwing Antenna	23
14: A Photograph of a Microstrip Antenna	24
15: A Photograph of a Large Loop Antenna	24
16: A Photograph of a Biconical Antenna	25
17: A photograph of a Discone antenna	26

18: A Photograph of an Aperture Antenna	26
19: A Photograph of a Traveling Wave Antenna	27
20: The Electromagnetic Spectrum Showing the different bands	34
21: A Photograph of a 1G Phone	43
22: A Photograph of a 2G Phone	44
23: A Photograph of a 3G Phone	45
24: A Photograph of a 4G Phone	46
25: Architecture of LTE Network	51
26: Map Showing Sites where Measurements were taken in Greater Accra Region	56
27: Map Showing Sites where Measurements were taken in Ashanti Region	57
28: Map Showing Sites where Measurements were taken in Western Region	58
29: A Photograph of an Anritsu Spectrum Master, Model MS2720T	59
30: A Photograph of Log-Periodic Antenna, Model TS-6021	60
31: A Typical Exposure Scenario in the Far-Field of an Antenna	66
32: Graph of Electric Field Strength Variation with Site Numbers in the Greater Accra Region	70
33: Graph of Mean Electric Field Strength Variation with Site Numbers in the Greater Accra Region	71

34: Graph of Power Density Variation with Site Numbers in the Greater Accra Region	71
35: Graph of Mean Power Density Variation with Site Numbers in the Greater Accra Region	72
36: Graph of Electric Field Strength Variation with Site Numbers in the Ashanti Region	73
37: Graph of Mean Electric Field Strength Variation with Site Numbers in the Ashanti Region	74
38: Graph of Power Density Variation with Site Numbers in the Ashanti Region	74
39: Graph of Mean Power Density Variation with Site Numbers in the Ashanti Region	75
40: Graph of Electric Field Strength Variation with Site Numbers in the Western Region	76
41: Graph of Mean Electric Field Strength Variation with Site Numbers in the Western Region	77
42: Graph of Power Density Variation with Site Numbers in the Western Region	77

43: Graph of Mean Power Density Variation with Site Numbers in the Western Region	78
44: Verification of Results from Field Measurement with the Results from the Model	82
45: Comparison of Results from Field Measurement with the Results from the Model	83
46: Resulting MATLAB Model Graphical user Interphase Showing the Various Inputs and Outputs Functions	85

LIST OF ACRONYMS

1G	First Generation
2G	Second Generation
3G	Third Generation
4G	Fourth Generation
LTE	Long Term Evolution
4G LTE	Fourth Generation Long Term Evolution
ICNIRP	International Commission for Non-Ionising Radiation Protection
EMR	Electromagnetic Radiation
RF	Radio Frequency
MRI	Magnetic Resonance Imaging
GSM	Global System for Mobile Communications
UMTS	Universal Mobile Telecommunication System
HSPA	High-Speed Packet Access
FDMA	Frequency Division Multiple Access
TDMA	Time Division Multiple Access
CDMA	Code-Division Multiple Access

WCDMA	Wideband Code Division Multiple Access
CDMA-EVDO	Code-Division Multiple Access-Evolution Data Optimize
3GPP	Third Generation Partnership Project
ITU	International Telecommunication Union
NMT	Nordic Mobile Telephone
IP	Internet Protocol
GPRS	General Packet Radio Service
WiMAX	World Wide Interoperability for Microwave Access
WLAN	Wireless Local Area Network
OFDMA	Orthogonal Frequency-Division Multiple Access
CSFB	Circuit-Switched Fallback
MSC	Mobile Switching Centre
OTT	Over-The-Top
PDN	Packet Data Network
EPC	Evolved Packet System
HSS	Home Subscriber Server
MME	Mobile Management Entity
SGW	Serving Gateway

CN	Control Network
QoS	Quality of Service
IR	Infrared
MW	Microwave
UV	Ultraviolet radiation
ELF	Extremely Low Frequencies
IARC	International Agency for Research on Cancer
FM	Frequency Modulation
AM	Amplitude Modulation
NTT	Nippon Telegraph and Telephone
SVLTE	Simultaneous voice and Long Term Evolution
GPS	Global Positioning System
LPA	Log Periodic Antenna

CHAPTER ONE

INTRODUCTION

Background to the study

Electromagnetic radiation (EMR) is the transmission or emission of energy which is in the form of waves or particles through a material medium or space (Purcell & Morin, 2013). The radiations may come from natural or artificial sources. The waves, however, consist of both electric and magnetic energy oscillating perpendicularly together with the speed of light (Browne, 2013). They have characteristics such as frequency, wavelength or energy (Constantine, 2005). The distance between two successive peaks of a wave is termed as a wavelength. Its unit of measurement is meters (m). Frequency-This has to do with the number of waves that are formed in a particular span of time (Giancoli, 1988). When the wavelengths are short, the frequency will be higher, because it will take a shorter amount of time for one cycle to pass and hence will have a higher amount of energy. Similarly, when the wavelength is longer, lower frequency will be produced, since it will take each cycle longer time to complete and therefore has low energy (Browne, 2013).

EMR is either considered as ionising or non-ionising and this depends on the amount of energy radiated by the particles (Moulder, 2007). Ionising radiation possess enormous energy to be able to remove electrons from atoms or molecules, and so it is able to breakdown a chemical bonds (Woodside, 1997). Examples of ionising radiation include; Alpha (α), Beta (β), and Gamma (γ) radiations. Other

examples are X-rays from medical radiography examinations and muons, mesons, positrons, neutrons and other particles that constitute the secondary cosmic rays that are produced after primary cosmic rays interact with Earth's atmosphere (Woodside, 1997).

Non-ionising radiation is said to be the type of electromagnetic radiation which has limited amount of energy to be able to ionise atoms or molecules-that is, to entirely eject an electron from an atom or molecule (Browne, 2013). The energy possessed by particles of non-ionising radiation is minimal, and so are only able to cause vibrational, rotational or change the configuration of the electronic valence shell of atoms and molecules. Instead of the production of charged ions while moving through matter. It is only recently that some possible effects from non-thermal form of non-ionising radiation on living tissues have been studied (Moulder, 2007). However, different non-ionising radiation types are observed to have different biological effects (Woodside, 1997). Visible light, microwaves, near ultraviolet, infrared and radio waves, are all forms of non-ionising radiation. Radiofrequency (RF) electromagnetic radiation is a type of non-ionising radiation which spans from a frequency of 3 kHz – 300 GHz on the electromagnetic spectrum (Moulder, 2007). RF field show the existence of electromagnetic or RF energy.

RF energy is employed in the telecommunications industry for usage in the provision of radio and television broadcasting, radio communications for security services, cellular telephones and microwave point-to-point links. The non-communication uses of RF energy are microwave ovens, industrial heaters and

sealers and air traffic control and military applications (Browne, 2013). RF is also used in magnetic resonance imaging (MRI).

In the telecommunication industry, RF is used for the purposes of both voice and data communication. The latest in Ghana is the 4G LTE wireless data technology. 4G refers to fourth generation of wireless data transmission networks which is developed by the telecommunication industry for the provision of greater speeds and additional bandwidth for everyday mobile device operations, such as messaging and video calling whilst LTE, an abbreviation for Long-Term Evolution, which is marketed as 4G LTE, is a standard for wireless communication of high-speed data for data terminals and mobile phones. It is based on the Global System for Mobile Communication (GSM)/Enhanced Data Rates for GSM Evolution (EDGE) and Universal Mobile Telecommunication System (UMTS)/High Speed Packet Access (HSPA) network technologies, by increasing the capacity and speed of radio interface together with a core network improvements (Rappaport, 2002). This technology is developed by the Third Generation Partnership Project (3GPP)

Statement of the Problem

Mobile telecommunication is fast developing with time and new technologies introduced to replace/augment old ones to be able to facilitate the users more. These technologies however, could come with some effects due to the emissions of electromagnetic fields.

Studies indicate that there have been growing concerns with regards to some biological effects (heating of body surface, disturbance of nerves, raised body

temperature, vertigo and nausea) associated with RF emissions not only in Ghana but the world as a whole (Amoako, Fletcher & Darko, 2009; Begüm & Çetin, 2016). The emergence of 4G LTE which is a new technology, has come to widen the scope of communication. Operating on a frequency of 800 MHz, it is expected that some significant amount of RF levels would be emitted from the antennas.

Now, mobile phone is not only a device used for talking but more or less portable computer that serves different purposes. The number of mobile phone users in Ghana rose to 34.57 million as of March, 2018 from 30.36 million in December, 2014 (National Communications Authority, [NCA, 2018]).

4G LTE offers higher data rates with seamless roaming. The mobile phone user can communicate without any disturbance while switching the coverage network. This user, however, have most of their mast sited in densely populated areas, schools and hospitals. Residents and the general public could therefore, be subjected to exposure of RF radiations.

There is currently no record of any study with regards to this technology to determine whether a potential health hazard could exist with respect to the transmitting antennas even though much work has been done for the previous generations of technologies (thus 900 MHz, 1800 MHz and 2100 MHz), sited in densely populated areas, schools and hospitals (Deatanyah, Amoako, Abavare & Memeh, 2018).

Objectives of the study

The main objective of this work was to conduct RF radiation safety assessment and its effects on people within the vicinity of 4G LTE base stations in three regions of the southern part of Ghana.

Specific Objectives:

1. Measurement of RF levels around 4G LTE base stations.
2. Computation of the electric field strengths and the power densities emitted from 4G LTE antennae's and the results compared to the International Commission on Non-ionizing Radiation Protection (ICNIRP) and the International Telecommunication Union (ITU) recommended guidelines.
3. Develop a model to estimate the power densities of transmitting antennas.
4. To acquire baseline data for future comparison.

Justification

Thousands of cell sites are mounted all over the country which are from different telecommunication companies, operating at different frequencies and technologies. There are about five (5) companies in Ghana currently operating 4G LTE. These are: Surfline Ghana Limited, Blu Telecommunication, Busy Ghana Limited, Mobile Telecommunication Network (MTN) Ghana Limited and recently Vodafone Ghana Limited.

MTN Ghana Limited which is the network that this work was carried out on, alone has 2083 4G LTE cell sites in the country, out of which 1675 are located

in the Greater Accra, Ashanti and Western regions and these sites are located in densely populated residential areas, near schools and hospitals.

This has brought about a lot of agitations from the public with regards to health and safety issues as far as the RF radiation emitted from these antennae are concern. The newest assertion is that the 4G technology is numerous times more of a health hazard as compared to any of its forerunners. Protestors have been echoing that the telecommunication companies are very much in the known of the possible consequences that this technology comes with but keeping mute due to the fear of hurting their revenue margin. They rather, only point out the great benefits and conveniences that the technology offers us. This technology makes use of more bandwidth than 2G and 3G which means additional exposure to radiation (Begüm & Çetin, 2016). For this technology to function effectively, additional high masts have to be mounted and linked to each other. This is alleged to produce much radiation than earlier, which may be the source of some health concerns at a later time (Begüm & Çetin, 2016). Although no definitive suggestion has been made up yet but a good number of people living or working for lengthy hours in the vicinity of telephone masts have raised concerns about the swift emergence of mysterious headaches, attacks of nausea and blurry vision (Begüm & Çetin, 2016). Medical practitioners handling these cases have also attested to the fact that these numbers are actually in the rise for some time now with only the use of 2G and 3G. This may possibly become more serious with the erection of 4G masts (Begüm & Çetin, 2016). Even though 4G offers us numerous services than 2G and 3G might ever do, it comes with some possible harmful health matters as well (Begüm & Çetin, 2016).

There is however no evidence to prove that, but only suggestions indicating that there are some biological effects associated with exposure to RF radiation (International Commission on Non-Ionising Radiation Protection [ICNIRP], 2010).

This study would therefore, come up with some data with regards to the levels of emissions of RF from the 4G LTE telephone masts and the results compared with international standards. A model would also be developed to estimate future emission levels with regards to the transmitting antennas. The results from the measurement will be used to validate the model.

Scope of the Study

This study was designed to measure RF emission levels from fifty (50) 4G LTE base stations in each of the Greater Accra, Ashanti and Western regions of Ghana. The measurements were done around sites that were located near hospitals, schools and highly populated residential areas, at a height of about 1.5 m above the ground and to represent the adult human body but keeping a straight line of vision with the RF source (Simon and Alejandro, 2007). The signals were however measured during the day (peak hours), at five (5) different points around the mast (at a distance of 10 m, 30 m 50 m, 70 m and 100 m from the masts) and six minutes weighted averaging time was used for all measurements as recommended by ICNIRP for RF exposure (Browne, 2013).

Structure of Thesis

The rest of the chapters are organized as follows:

Chapter one included the background of the study, statement of the problem, objectives of the study, justification and scope of the study.

Chapter two would give a detailed explanation of electromagnetic radiation and a literature review of related studies. Chapter three includes materials and methodology employed in the study and a mathematical model that has been developed for the prediction of power density of RF radiation of a transmitting antenna. The results that were obtained from the previous chapter would be discussed in chapter four. Chapter five, which is the final chapter would comprise of conclusion and some recommendations.

Chapter Summary

This chapter introduces the reader to electromagnetic radiation and how it is employed in the telecommunication industry for the purpose of communication, most importantly 4G LTE. The research problem underlying this study had been explained. The objectives, the study aimed to achieve were stated. The justification of the study was also given. The scope within which the study was carried out was also discussed. Finally, the chapter gave an account to how the study was arranged.

4G LTE is the latest technology in the telecommunication industry as far as Ghana is concerned. MTN alone had 2183 sites with 77% of them located in the Ashanti, Greater Accra and Western Regions. Most of which are located near schools, hospital and in densely populated residential areas. This brought a lot of

agitations from the public with regards to health and safety issues associated with RF emissions from the antenna's. This study sought to determine whether the levels from these sites are within the recommended levels of ICNIRP or not. A mathematical model was also developed to predict the power density of RF emissions from transmitting antenna's.

CHAPTER TWO

LITERATURE REVIEW

Introduction

Classically, EMR basically are waves (photons) transmitting through space-time or a material medium, carrying electromagnetic radiant energy (3.0×10^8 m/s) but in a form of sinusoidal waves (Alessandro, 2013). The fields oscillate perpendicularly to each other and to the direction of wave propagation (Alan, 2014). Electromagnetic radiation may come from natural sources for instance the sun, earth and ionosphere or from artificial sources like in broadcasting, telecommunication and microwaves. The waves are generated whenever charged units are fast-tracked and they usually carry energy away from their source particle. They are able to impart this quantity to any matter they interact with (Browne, 2013)

EMR is associated to waves which are able to radiate by themselves, without the continuous reliance on the charge unit of which they were generated from, since they have achieved sufficient distance from those charges that produced them (Cloude, 1995).

Electric Field

It refers to the area around an electric charge where an electric force is applied on charge unit. It can therefore, be defined as the electric force per unit charge (Tipler, 1999).

$$\text{Mathematically, electric field, } E = \frac{F}{q} \quad (1)$$

Where F is electric force in Newtons and q is charge in Coulombs. An electric field has both magnitude and direction and can be represented by lines of force, or field lines (Purcell, 2011) as shown in Figure 1. It has an International System (SI) of unit of Newtons per coulomb (N/C), or volts per meter (V/m).

The direction of the force that is exerted on the positive test charge is taken to be the direction of the field (Purcell & Morin, 2013). The electric field is radially outward from a positive charge and radially in toward a negative point charge (Tipler, 1999).

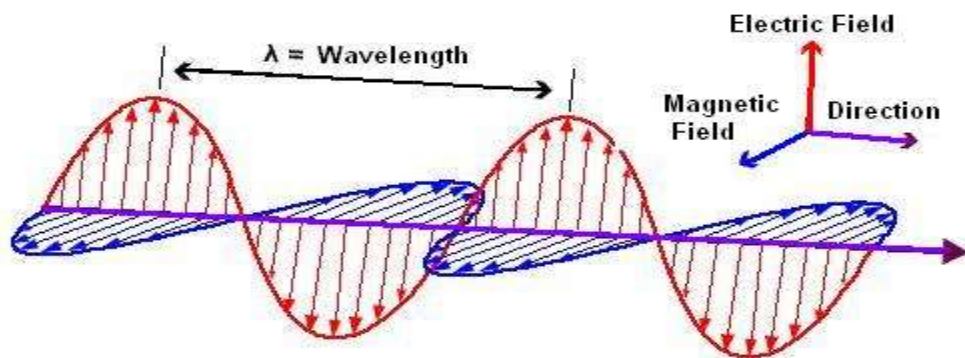


Figure 1: A diagram of a wave showing electric and magnetic fields (Tipler,1999)

Magnetic Field

The region around a magnet within which a magnetic force is exerted, is referred to as a magnetic field. It is produced by moving charged units (Purcell & Morin, 2013). The magnetic flux line shows the presence and strength of a magnetic field. The direction of the magnetic field is also indicated by these lines (Purcell & Morin, 2013). It has both magnitude and direction at any given location, therefore it is denoted by a vector field (Purcell, 2011). The term actually refers to two different but very linked fields with symbols B (magnetic induction or magnetic flux density) and H (magnetic field strength) (Purcell & Morin, 2013). Amperes per meter is the unit of measurement of H while teslas or newtons per meter per ampere is the unit of measurement for B . In a vacuum H and B are the same apart from measurement units; but when it comes to a material that has magnetization, B is solenoidal (having no divergence in its spatial dependence) while H is irrotational (curl-free) (Purcell & Morin, 2013)

Magnetic fields are created by the movement of charged units and fundamental magnetic moments of basic particles (Jiles, 1998). Magnetic fields are mostly experienced as a force produced through the use of permanent magnets in everyday life (Purcell, 2011).

Far Fields and Near Fields

Far-field (Fraunhofer region) is the area where the charged units performs as a normal electromagnetic radiation and so electromagnetic radiation is generally said to be a far-field (Constantine, 2005). That area is predominantly electric or magnetic fields with electric dipole characteristics (Rappaport, 2002).

The near-field region (Fresnel region) refers to the electromagnetic field near the charges and the currents that produce them (Constantine, 2005). This region is made up of different field types which may be considered as a collection of these fields with a fixed phase association (Constantine, 2005).

The borderline amid these regions is largely undefined, so it is subject to the wavelength that is being produced and the size of the emitting element (John, 1998).

There is a reduction in the transmitted power with the square of the distance. The absorption of the field do not feed back into the transmitter, in the far-field region of an antenna. While in the near field area, the is being absorbed by the source and this affects the load of the transmitter (John, 1998).

In the far-field area, the electric or magnetic portion of the charge is produced or related to a variation in the other. The relation between them is the wave impedance. But the fields in a near field area can exist separately and one can also dominate the other (Knoll, 1979).

Antenna Theory

In radio engineering, an antenna is said to be the boundary amid which the radio waves are broadcasting via space and the electric currents propagating in metallic conductors, with the use of a transmitter or receiver (Graf, 1999).

In transmission, the antenna receives the electric current that is to be supplied at its terminals by a radio source, the energy from the current is then radiated by the antenna as electromagnetic waves (radio waves). At the reception unit, the antenna receives the waves and generate an electric charge at the terminals, which is then sent to a receiver and amplified. Antennas are very essential units of all radio gadgets (Pattanaik, 2012).

Basically, an antenna is an collection of conductors (elements), which are electrically linked to the receiver or transmitter. Antennas are usually produced to transmit and receive radio waves equally in all directions or specifically in a particular direction (Farahani, 2008).

Antenna types

Antenna are usually designed with specialized properties and used for a particular functions. They can be grouped in various ways. The classification here is according to common operating principles.

An isotropic antenna (isotropic radiator): It is a theoretical antenna that is able to radiate signal power equally in all directions (Farahani, 2008). This antenna is used to validate the directionality or gain of real antennas by the application of a model. No actual antenna has the radiation pattern of an isotropic antenna and so it

only serves as a reference for checking other antenna types (Dragan, Khalil, Sergey & Andres, 2012)

An isotropic antenna is often mistaken as an omnidirectional antenna. But an isotropic antenna transmits power equally in all dimensions, whereas an omnidirectional antenna transmits power equally in all horizontal directions, but the power that is being transmitted differs with angle of elevation, which reduces to nothing on the antenna's axis (Farahani, 2008).

Isotropic antennas are usually made with the use of a number of elements and are used for the measurement of the electric field strength or general testing other antennas (Dragan et. al., 2012). Figure 2 shows a photograph of an Isotropic antenna



Figure 2: A photograph of an Isotropic antenna

Dipole: This is a typical antenna on which some types of antennae are designed from (Bevelaqua, 2015). It is made up of two conductors that are evenly arranged with one side connected to a transmitter or receiver (Abdullah, Samadder, Imon and Ahmed, 2015). The half-wave dipole which is more accessible is and has two resonant elements which are about a quarter wavelength long (Amandeep, Abhishek, Jitender & Basudeo 2014). This antenna transmits greatly in directions

that are perpendicular to the antenna's axis. These antennae are used as omnidirectional antennas but are also the basis for the creation of other directional antennas (Abdullah, et. al., 2015).

A turnstile antenna, or crossed-dipole antenna- It is a radio antenna that has a set of two undistinguishable dipole antennas that are erected at an angles of 90° to each other (as shown in Figure 3). This antenna is applied in two modes (Farahani, 2008). It is able to radiates radio waves that have been horizontally polarized perpendicular to its axis (normal mode) or radiates radio waves that have been circularly polarized along its axis (axial mode) (Bevelaqua, 2015). Superturnstile or batwing antennas are specialized normal mode turnstile antennas and are applied in television broadcasting (Xuart, Ziolkowski & Park, 2015). The axial mode turnstiles antennas are used in satellite ground station antennas in the Very High Frequency (VHF) and Ultra High Frequency (UHF) bands.



Figure 3: A photograph of a turnstile antenna, or crossed-dipole antenna

A corner reflector antenna- This is a kind of directional antenna and is used at VHF and UHF frequencies (Stutzman & Thiele, 2012). It is made up of a dipole

element that is erected an angle of mostly 90° in front of the flat rectangular reflecting screens (as shown in Figure 4). These antennas are usually used as, point-to-point communication links, data links for wireless Wide Area Networks (WANs), and UHF television receiving antennas (Stutzman & Thiele, 2012).



Figure 4: A photograph of a corner reflector antenna

A patch antenna- It is a type of radio antenna which is erected on a flat surface (Ashok, Sheeba & Rhishika, 2013). It is made up of a flat rectangular metal sheet (as shown in Figure 5) that is erected on a larger metal sheet (Farahani, 2008). The discontinuities at the ends of the truncated edges of the microstrip transmission lines are the mechanism of the radiation (Anushi, Yash, Aditya & Shashank, 2015). This antenna is largely practical at frequencies of microwave levels; the patches are small since the wavelengths are short (Anushi, et. al., 2015). They are generally used in portable wireless devices due to the ease with which they can be fabricated on printed circuit boards (Ashok, et. al., 2013). Multiple patch antennas on the same substrate are used in the designing of high gain and phased arrays antennas (Anushi, et. al., 2015).



Figure 5: A photograph of a patch antenna

Monopole antenna is mainly made up of a single conductor like a metal rod that is usually erected above the ground or an unnatural conducting surface (Lusekelo, 2013) which can be seen in Figure 6. The feedline is connected in such a way that one side is attached to the conductor while the other to an unnatural ground plane (ground) (Lusekelo, 2013). The quarter-wave is the most common monopole antenna type and it is erected over ground plane (Das, 2016). The radiation pattern in monopole is omnidirectional and so are used for coverage of a particular region. Minor monopoles are usually applied in nondirectional antennas on movable radios (Lusekelo, 2013).



Figure 6: A photograph of a Monopole antenna

Array antennas: These antennas are made up of a number of antennas which works like a single antenna (Bruno, 2013). A number of driven elements which are identical, dipoles and feed in phase are used to produce broadside arrays (Haydar, Al-Tamimi & Salah, 2016). Parasitic arrays are dipoles with a driven element and a parasitic element that transmits radiation along its lines (Bruno, 2013). Below are some types of Array antennas:

a) A collinear antenna array- An array of dipole antennas is referred to as a collinear antenna array. They are always mounted in such a way that the elements of the antenna are placed parallel and collinear to each other (Das, 2016) as illustrated in Figure 7. Collinear antenna arrays are high gain omnidirectional antennas. (Stutzman & Thiele, 2012).

Collinear dipole arrays- These are mostly used in land mobile radio systems. Thus base station antennas that communicate via a mobile two-way radios. Broadcasting also makes use of these antenna types (Stutzman & Thiele, 2012).



Figure 7: A photograph of a collinear antenna array

b) A Yagi–Uda antenna also known as a Yagi antenna- this type of antennas are said to be directional antennas and consists of a number of elements that are arranged parallel to each other in a line (Balanis, 2011) (as shown in Figure 8). They have a driven element that is attached to the transmitter or receiver with the use of a transmission line (Balanis, 2011).

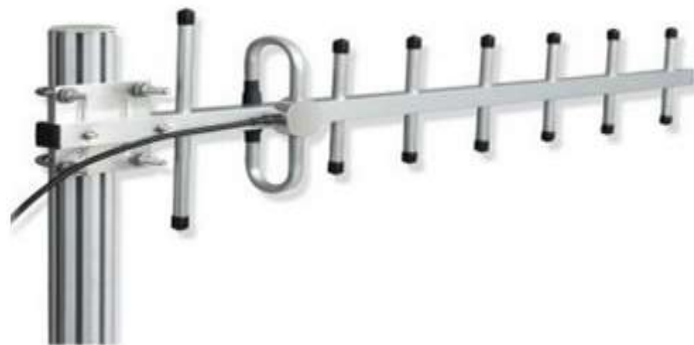


Figure 8: A photograph of a Yagi–Uda antenna

c) Log-periodic antenna – It is mostly mistaken as the Yagi-Uda, even though it has a lower gain than that of a Yagi of similar size (Sudesh, Kshitij & Amit, 2015). It is made up of a number of dipole elements and a boom that increases gradually in length (which is illustrated in Figure 9) and are linked with a transmission line that has a polarity which is alternating (Hemant and Girish, 2018). It is a type of directional antenna and also has an extensive bandwidth. And so most perfect as a television antenna (Sudesh et. al., 2015).



Figure 9: A photograph of a Log-periodic antenna

d) Reflective array: This is also a type of directional antenna. A number of driven elements are erected opposite a flat surface which is able to reflect radio waves in a preferred route (Dragan et. al., 2012). This type of antennas are used in frequency bands of VHF and UHF (Bevelaqua, 2015). Figure 10 shows a reflective array antenna.



Figure 10: A photograph of a Reflective array antenna

e) Phased array: This type of antenna is a high gain and applicable in frequencies that are electronically steerable like UHF and microwave (Stutzman & Thiele, 2012). Figure 11 shows an illustration of a Phased array antenna.

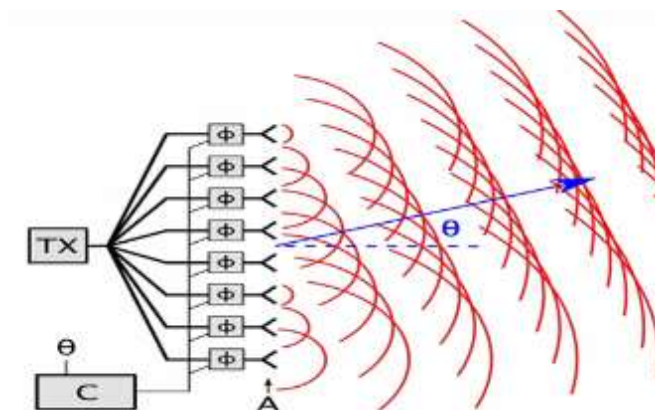


Figure 11: A schematic diagram of the Phased array antenna

f) Curtain array: These are transmitting antennas that has a large multi-element directional wire and are very useful in the shortwave radio bands (Sreedhar, 2014) as can be seen in Figure 12.



Figure 12: A photograph of a Curtain array antenna

g) Batwing or super turnstile: It is a unique type of antenna that is used in the broadcasting of television and consists of couples of dipoles and radiators that resembles bat wings (Ochala & Okene, 2011) as shown in Figure 13.



Figure 13: A photograph of a Batwing antenna

h) Microstrip: It is an antenna that is fabricated with the use of a microstrip technique on a printed circuit board (PCB) (as shown in Figure 14) (Anushi, et. al., 2015). This antenna is for internal purposes and used at frequencies of microwave level. (Stutzman & Thiele, 2012).

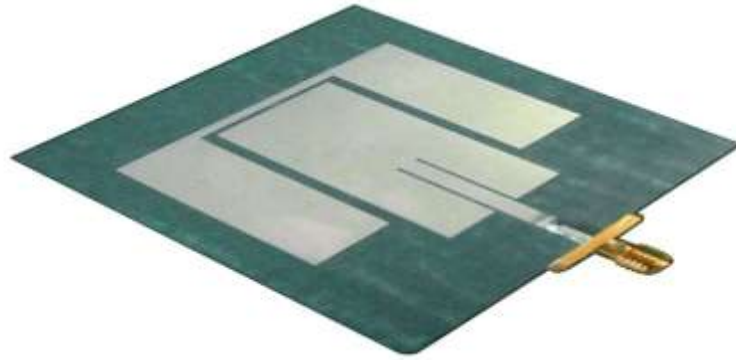


Figure 14: A photograph of a Microstrip antenna

Loop antennas: These antennas are made from a coiled wire (Balanis, 2011). They are moderately insensitive to noise that are generated electrically since they rather interact with the magnetic field but not electric field of the radio wave (Dragan et. al., 2012).

Loop antennas are classified as either large or small loops

a) Large loops: These are types of antennas which has loops with a circumference of a full wavelength as indicated in Figure 15. They have very high resistance of radiation and so excellent antenna efficiency (Dragan et. al., 2012).



Figure 15: A photograph of a large loop antenna

b) Small loops – These antennas have smaller loops than the large loop antennas. Their loop is able to be altered so as to enable them resonant, when it is essential (Das, 2016). These loops are referred to as magnetic loops but when they are enabled to resonant then they are referred to as tuned loops (Dragan et. al., 2012).

Conical Antennas

a) Biconical antennas- These are basically dipole antennas with a broadband and exhibits three octaves or more of a bandwidth (as shown in Figure 16) (Khadar & Sneha, 2017). The bowtie antenna is the most common type and it is a two dimensional which is most appropriate for use in short-range UHF television reception. They are also known as butterfly antennas (Das, 2016).

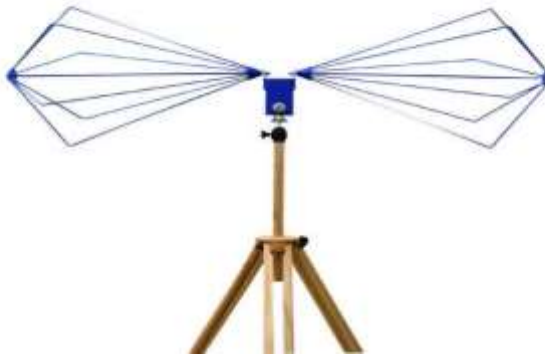


Figure 16: A photograph of a Biconical antenna

b) Discone antenna- This antenna is a semi biconical and has a plane disc that is erected above the cone (Khadar & Sneha, 2017) which is illustrated in Figure 17.



Figure 17: A photograph of a Discone antenna

Aperture Antennas- These are the major class of directional antennas and are used at frequencies of microwave levels (300 MHz - 300 GHz) and above (Balanis, 2011). They are made up of a small dipole antenna within a large guiding structure that is three-dimensional and has an aperture to release waves. Examples of aperture antennas are parabolic, horn, slot lens and dielectric resonator (Dragan et. al., 2012) and can be seen in Figure 18.



Figure 18: A photograph of an Aperture antenna

Travelling wave: Unlike the other types of antennas, the travelling wave antennas do not resonant and so they have inherently broad bandwidth (Balanis, 2011). In a traveling wave antenna which is basically a wire antenna (as shown in Figure 19), the voltage and wave propagate in a particular direction (Balanis, 2011). The Beverage, Rhombic, Helical and Leaky are all types of the Travelling wave antenna.



Figure 19: A photograph of a Traveling wave antenna

Some Characteristics of Antennas

Bandwidth

This the span of frequencies at which the antenna performs with regards to some characteristics to achieve the desired standards. An antenna functions well enough over wide bandwidth (Sreedhar, 2014). The impedance of the antenna is poor outside its range to be able to transmit or receive signals (Farahani, 2008).

Effective area or aperture

An antenna aperture area is the region that is offered for signals to be received or radiated and it is an essential unit of the antenna that oversees its function (Dragan et. al, 2012).

Radiation pattern

An antenna's radiation pattern basically describes the strength of the waves radiated by the antenna at varied angles in the far-field (Stutzman, 2012). A three-dimensional graph is mostly used to represent it or polar plots (Das, 2016).

Efficiency

A transmitting antenna's efficiency is the relationship between the absorbed power by the antenna at its terminals and the power that is transmitted in varied directions (Balanis, 2011). The heat that is generated from the power is supplied to the terminals of the antenna but not radiated. (Das, 2016).

Polarization

Polarization is the orientation of the electric field of an electromagnetic wave with regards to the earth's surface and this depends on the orientation and physical structure of the antenna (Balanis, 2011). When a straight wire antenna is erected vertically, it will have one polarization and a distinct polarization when erected horizontally. Polarization is mostly elliptical (that is it differs over time).

Impedance matching

To attain highest power transfer, matching the impedance of the complex conjugate of a receiver/transmitter to the antenna impedance system is required (Sreedhar, 2014). However, the required impedance matching probably will not agree with the dynamic output impedance of the transmitter. Transmitter and some receivers have supplemental adjustments which are able to cancel some amount of reactance to twist the match when the intended impedance is not normal resistive (Balanis, 2011).

Directivity

Directivity has to do with the capacity of an antenna to be able to direct energy in a specified position when transmitting or receiving energy better (Wayne, et. al., 2013). For static condition, the directivity of an antenna is used to focus radiation in a specified position, but in a dynamic conditions, the antenna has to radiate correspondingly in all directions (Balanis, 2011).

Gain

The antenna's gain in a particular route is the quantity of energy that is radiated to that particular route compared to the energy that an isotropic antenna would radiate in the same route when the same input power is used to drive it (Balanis, 2011).

Electromagnetic wave equation

This is a second-order partial differential equation that is able to explain the transmission of electromagnetic waves through a material medium or in a vacuum. These waves are predicted by the Maxwell's equations also known as the classical laws of electricity and magnetism (Grellier et. al, 2017).

Maxwell's equations are able to explain how the electric and magnetic fields are created by charges, currents, and changes of each other. One essential aspect of these equations is that fluctuating electric and magnetic fields transmitting at speed of light can also be demonstrated by them. The equations are named after the physicist and mathematician James Clerk Maxwell (Krane, 1988). The homogeneous form of the equation, in terms of either the electric field E or the magnetic field B , takes the form:

$$\left(\nabla^2 - \mu\varepsilon \frac{\partial^2}{\partial t^2}\right) E = 0 \quad (2)$$

$$\left(\nabla^2 - \mu\varepsilon \frac{\partial^2}{\partial t^2}\right) B = 0 \quad (3)$$

$$\text{where } c = \frac{1}{\sqrt{\mu\varepsilon}} \quad (4)$$

$$\nabla \cdot E = 0 \quad (5)$$

$$\nabla \times E = -\frac{\partial B}{\partial t} \quad (6)$$

$$\nabla \cdot B = 0 \quad (7)$$

$$\nabla \times B = \mu\epsilon \frac{\partial E}{\partial t} \quad (8)$$

Taking the curl of the curl equations in 5-8 gives:

$$\nabla \times (\nabla \times E) = -\frac{\partial}{\partial t} (\nabla \times B) = -\mu\epsilon \frac{\partial^2 E}{\partial t^2} \quad (9)$$

Using the vector identity

$$\nabla \times \nabla \times A = \nabla (\nabla \cdot A) - \nabla \cdot \nabla A \quad (10)$$

where A is a vector field.

$$\text{Since } \nabla \cdot E = \nabla \cdot B = 0 \text{ (in free space)} \quad (11)$$

$$\nabla \times \nabla \times E = -\nabla^2 E \quad \text{and} \quad \nabla \times \nabla \times B = -\nabla^2 B \quad (12)$$

The wave equation is obtained as equation (13) and (14)

$$\frac{\partial^2 E}{\partial t^2} - C_0^2 \cdot \nabla^2 E = 0 \quad (13)$$

$$\frac{\partial^2 B}{\partial t^2} - C_0^2 \cdot \nabla^2 B = 0 \quad (14)$$

Where $C_0 = \frac{1}{\sqrt{\mu_0 \epsilon_0}} = 2.99792458 \times 10^8 \text{ m/s}$ is the speed of light in free space.

Electromagnetic Spectrum

The electromagnetic spectrum consists of electromagnetic waves arranged in order of increasing frequency and decreasing wavelength: radio waves, microwaves, infrared radiation, visible light, ultraviolet radiation, X-rays and gamma rays (Krane, 1988).

The waves are described by any of the following three physical properties: the frequency f , wavelength λ , or photon energy E (Konya & Nagy, 2012). Wavelength is inversely proportional to the wave frequency and so gamma rays have very short wavelengths while radio waves have very long wavelengths (May and Woods, 1979). Photon energy is directly proportional to the wave frequency, so gamma ray photons have the highest energy, whilst radio wave photons have very low energy (May & Woods, 1979). This is illustrated by equations (15) and (16).

$$f = \frac{c}{\lambda} \quad (15)$$

$$f = \frac{E}{h} \quad (16)$$

$$E = \frac{hc}{\lambda} \quad (17)$$

Since (15) = (16)

The frequency ranges of the spectrum are divided into separate bands, and the electromagnetic waves within each band are referred to by different names; beginning from the low frequency end of the spectrum to that of the end, these are:

radio waves, microwaves, infrared, visible light, ultraviolet, X-rays, and gamma rays, (John, 1998) as shown in figure 20.

Each of the electromagnetic waves in these bands have an exceptional characteristic, such as how they are produced, how they interact with matter, and their practical applications (Konya & Nagy, 2012).

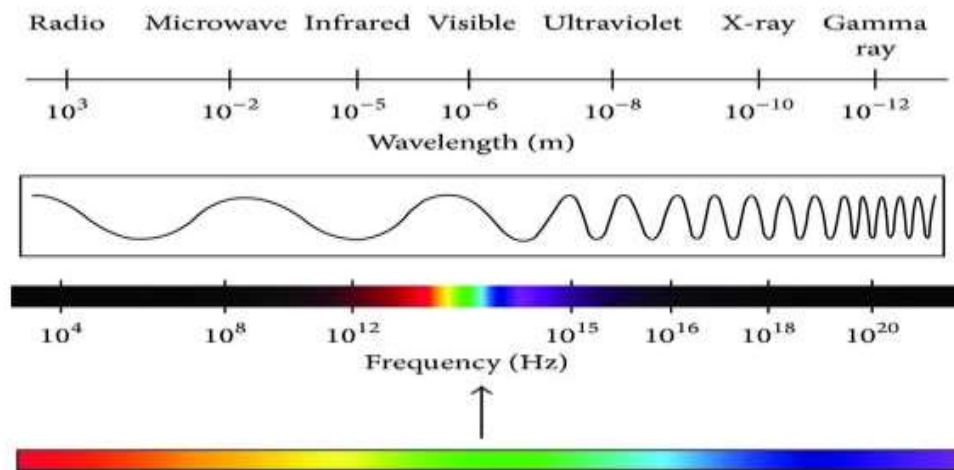


Figure 20: The electromagnetic spectrum showing the different bands (John, 1998)

Non-ionising radiation

These are radiations whose kinetic energy is minimal in order to create charged ions when moving through matter (ICNIRP, 1998). Although considered less dangerous than ionising radiation, overexposure to non-ionising radiation can cause biological issues (Hammett, 1997). The border line between ionising and non-ionising radiations occurs in the ultraviolet part of the electromagnetic spectrum (Balzano, Garay and Manning, 1995). Radiation in the ultraviolet band and at lower energies (to the left of ultraviolet) is called non-ionising radiation,

while at the higher energies to the right of the ultraviolet band is called ionising radiation (Hammett, 1997).

Types of Non-ionizing radiation

Ultraviolet radiation (UV)

Ultraviolet light is a form of non-ionising radiation that can be found in the range of the EM spectrum between visible light and X-rays (Balzano, Garay & Steel, 1978). It has frequencies of about 3000 THz and 750 THz and wavelengths of about 400 nm to about 10 nm (Balzano, et. al, 1978). This radiation is generated either by heating of a material to incandescence or by the excitation of a gas discharge in either a closed or open arc (Seybold, 2005). The main source of natural UV radiation is the sun which is a huge incandescent mass (Balzano, et. al, 1978). It has a lots of medical and industrial applications. However, it could also cause damage to living tissues (Hitchcock & Patterson, 1995).

Visible light

This can be found in the middle of the spectrum of EM. Thus between infrared and ultraviolet (Martin et. al, 2007). It has a wavelength of about 380 nm - 750 nm and this is equivalent to a frequency span of 790 THz - 400 THz (Balzano, et. al, 1978). Visible light is basically defined as the wavelengths that are noticeable to most human eyes (Christopher, 2008)

Infrared (IR)

Infrared can be found in the span of the EM spectrum between microwaves and visible light (Christopher, 2008). A wavelength between $0.7 \mu\text{m}$ and $300 \mu\text{m}$ and corresponds to a frequency range between 430 to 1 THz (Balzano, et. al, 1978). This light is not visible to human eyes, nonetheless could be felt as heat if its intensity is highly sufficient (Haykin & Moher, 2002)

Microwave (MW)

Microwaves have their wavelengths spanning from as short as 1 mm to as long as 1 m and this corresponds to a frequency span of 300 MHz to 300 GHz (Ashwani & Vijay, 2016). Microwaves are most appropriate for high-bandwidth communications, radar and as a heat source for microwave ovens and industrial applications (Hitchcock, 2004).

Radio waves

Radio waves are a class of EM radiation which have their wavelengths in the EM spectrum longer than that of an infrared light (Petersen, 2002). They equally move at the speed of light like all other electromagnetic waves. Naturally occurring radio waves are generated by lightning, or by certain astronomical objects (Jung-Sim, Yong-Seung, Tae & Sang-Wook, 2008). Radio waves that are generated artificially are mostly used for fixed and mobile radio communication, broadcasting, radar and other navigation systems, satellite communication, computer networks and innumerable other applications (Hitchcock, 2004). They span from a frequency of 3 kHz to 300 MHz on the EM spectrum (Browne, 2013).

Biological Effects of Non-ionizing Radiation

Biological effect can only occur when there is a measurable change in a biological system after there has been an introduction of some stimuli (Vladimir & Frank, 2017). When there is an observation of a biological effect in itself does not essentially mean that there exist any biological hazard or health effect (Kyung-Taek & Cheol-Hong, 2014). It becomes a safety hazard only when it is able to causes a detectable impairment to the health of the individual or to his/her offspring (Kyung-Taek & Cheol-Hong, 2014). This could be physiological, biochemical or behavioural changes in an organism, tissue, or cell (Kyung-Taek & Cheol-Hong, 2014; Dutkiewicz et. al, 2011). Non-ionizing radiations often interact with tissues through the generation of heat (Guowang, Jens, Sung & Slimane, 2016). The hazard usually depends on its ability to penetrate the body and the absorption characteristic of the type of tissue (Dutkiewicz, et. al, 2011).

There are a lot of uncertainties with regards to the severity of effects of both acute and chronic exposure to the various types of non-ionising radiations (Dutkiewicz, et. al, 2011). The public is most concerned about the risk of Extremely Low Frequencies (ELF), RF and MW but the greatest risk to them probably is from natural UV radiation (Hitchcock & Patterson, 1995).

The potential biological effects with regards to non-ionising radiation section of the EM spectrum can be categorized into:

1. The optical radiation portion that is the section electron excitation can occur and it is made up of visible light and infrared light.
2. The section that the wavelength that is smaller than the body and so heating occurs through induced currents. The effects with this section are not well understood and even mostly denied. It is made up of MW and higher-frequency RF.
3. The section with the wavelength that is much larger than that of the body and heating occurs through induced currents seldom. This section is made up of Lower-frequency RF, power frequencies, and static fields.

Biological Effects of Radiofrequency

Radiofrequency radiation ranges from 3 kHz-300 GHz on the electromagnetic spectrum. Some of its sources are: mobile phones, cordless phones, long-distance telecommunication, air traffic control system, police and military radar, television broadcast system, Frequency Modulation (FM), and Amplitude Modulation (AM) (Sharmila, 2015). The International Agency for Research on Cancer (IARC) of the World Health Organization (WHO) recently released a statement indicating that radiofrequency electromagnetic fields are possibly carcinogenic to humans (IARC, 2013).

The term given to a biological effect that can result from heating of tissues by RF radiation is referred to as Thermal effect (Pattanaik, 2012). It is a well-known fact that, RF radiation exposure can be harmful at very high levels, since it is able to rapidly heat biological tissue (Guowang, et. al, 2016). When the electromagnetic energy is absorbed by the tissue it is converted into heat through several molecular

interaction mechanisms, like molecular polar rotation (water proteins, and amino acids), polarization of space charge and ionic conduction (Nicola & Leslie, 2009).

The intensity of the radiation, the duration of the exposure, and the water content of the tissue and its ability to dissipate heat determines the amount of heat to be produced (Pattanaik, 2012). Biological objects are mostly of complex exterior and interior geometry that are made up of several layers (eg, skin, fat, muscle, bone) with varying electrical properties (dielectric constant and conductivity) (Guowang, et. al, 2016). Due to this, the internal energy deposition is mostly not uniform and so local differences in thermal gradients and the rise of temperature rates occur (Pattanaik, 2012). The body size and orientation to the radiation field, and on the frequency and polarisation of the radiation strongly indicates the absorption rate of the energy (Sharmila, 2015). Maximum absorption in the RF region of the electromagnetic spectrum by small individuals and children occurs at a higher frequency as compared to average sized adults, even though they have similar body averaged peak specific absorption rate values (Sharmila, 2015).

There are two areas of the body, which are particularly vulnerable to RF heating. The eyes and the testes, due to the comparative absence of available blood movement to dissipate the extra heat load (Guowang, et. al, 2016). The evidence for harmful biological effects with regards to exposure to relatively low levels of RF, thus levels that are lower than those that are not able to generate heat is unproven (Guowang, et. al, 2016). These effects are said to be nonthermal effects (Sharmila, 2015). It is therefore widely accepted that further research is needed to

determine whether there are effects to human health at these levels and their possible relevance, if any (Guowang, et. al, 2016).

Use of RF for communication purpose

Radiofrequency waves that are generated artificially are used for fixed and mobile radio communication, broadcasting, radar and other navigation systems, communications satellites, computer networks and a lot of other applications (Ashwani & Vijay, 2016). The radio transmitters generate the waves and received by radio receivers (Ashwani & Vijay, 2016). Each frequency of a radiofrequency wave, has its own propagation characteristic in the earth's atmosphere. Long waves are able to diffract around obstacles like mountains and follow the contour of the earth (ground waves), shorter waves reflect off the ionosphere and return to earth beyond the horizon and much shorter wavelengths bend or diffract very little and travel on a line of sight, so their propagation distances are limited to the visual horizon (Seybold, 2005).

The International Telecommunication Union (ITU) is an international body that coordinates the artificial generation and use of radiofrequency waves in order to prevent interference between different users and this is strictly by law (Anu, Pulkit, Sachin, Mohita & Meghna, 2013)

Reflection, refraction, polarization, diffraction, and absorption takes place when RF waves are moving through different environments (Seybold, 2005). The combinations of these phenomena experienced by frequencies in the atmosphere

are different for each, therefore some radio bands are more useful for specific purposes than others (Seybold, 2005). Basically four different techniques of radio propagation of communication are used by Practical systems:

a) Line of sight: Receiving antenna receive RF waves that travel in a straight line from the transmitting antenna and does not really need a cleared sight path (Christopher, 2008). Lower frequencies RF waves are able to move through buildings and other obstructions (Seybold, 2005).

b) Indirect propagation: RF waves have the ability to reach points above the line-of-sight through diffraction and reflection (Christopher, 2008). RF waves diffract and so bend around obstructions such as buildings and vehicles (Haykin & Moher, 2002). The waves also reflect from surfaces of walls, ceilings, vehicles and the ground (Seybold, 2005). These propagation phenomena occur in short-range radio communication systems such as cell phones, cordless phones, walkie-talkies, and wireless networks (Christopher, 2008). Multipath propagation is the disadvantage of this mode, since it makes the waves to interfere, which causes fading and other reception problems (Seybold, 2005)

c) Ground waves: Due to diffraction, waves that are polarized vertically are able to bend beyond hills and mountains and propagate over the horizon at lower frequencies (Haykin & Moher, 2002). This makes it possible to communicate with submarines hundreds of feet underwater and over most of the earth (Seybold, 2005)

d) Skywaves (skip): At shortwave wavelengths and medium wave, radio waves are able to reflect off conductive layers of charged particles in the ionosphere, making

it possible for waves directed at an angle into the sky to return to earth beyond the horizon; Skywave propagation depends basically on atmospheric conditions and it is most reliable at night and during winter (Ellingson, 2016).

In radio communication systems, information is carried across with the use of RF waves (Ellingson, 2016). The information to be sent is in the form of a time-varying electrical signal and is applied to a radio transmitter, in the form of an audio signal or a video signal (Altgelt, 2005). In the transmitter, an electronic oscillator generates an alternating current which oscillates at a radio frequency called the carrier (Singh, 2016) since it is supposed to "carry" the information through the air.

The information signal then modulates the carrier, altering some aspect of it (Altgelt, 2005). This modulated carrier is then amplified and applied to an antenna and the oscillating current pushing the electrons in the antenna back and forth, creating oscillating electric and magnetic fields, which radiate the energy away from the antenna as RF waves. The information is then carried by the RF waves to the receiver.

At the receiver, the electrons in the receiving antenna are pushed back and forth by the oscillating electric and magnetic fields of the incoming RF waves and so creates tiny oscillating voltage in the receiving antenna that are a weaker replica of the current (Ellingson, 2016). The voltage is then applied to the radio receiver, which extracts the information signal. The receiver then uses a bandpass filter to separate the desired radio signal from all the other signals picked up by the antenna, and then amplifies it, before finally extracting the information-bearing modulation signal in a demodulator. The recovered signal is sent to a loudspeaker or earphone

to produce sound, or a television display screen to produce a visible image, or other devices. There has been a lot of developmental changes with regard to the use of RF for communication purposes such as first generation (1G), second generation (2G), third generation (3G), fourth generation long term evolution (4G LTE) and fourth generation (4G). Below is a brief description of the generation of mobile communication:

First generation (1G): Figure 21 shows a photograph of a 1G phone. It was launched in Japan by Nippon Telegraph and Telephone (NTT) in 1979 as the first commercially automated cellular network, initially for the metropolitan area of Tokyo alone (ITU/MIC, 2004). They were able to expand to cover the whole population of Tokyo within five years to become the first nationwide 1G network (Mekala, Sai & Nayakanti, 2016). Nordic Mobile Telephone (NMT) system was able to launch in Denmark, Finland, Norway and Sweden simultaneously in 1981 (Petersen, 2002). They were the first to feature international roaming of mobile phone network (Petersen, 2002). In 1983, Ameritech (Chicago based) launched the first 1G network in the USA using the Motorola DynaTAC mobile phone. Most countries then followed including the UK, Mexico and Canada in the early to mid-1980s (Petersen, 2002)

Analogue was the structure of this technology and so could be used for voice calls only (Mekala, et. al, 2016). It had a 25 MHz frequency band allocation for signals from the base station to the cell phone and vice versa (Mekala, et. al, 2016).

It made use of the Frequency Division Multiple Access (FDMA) systems, which is a technology whereby the total amount of spectrum is divided in a number

of channels and so each channel is assigned to a different user with a 30 kHz bandwidth (Petersen, 2002). There was however a problem of lack of accommodation due to this (Mekala, et. al, 2016). It also had problems with interference and attenuation (Petersen, 2002).



Figure 21: A Photograph of a 1G phone

Second generation (2G): With the coming on board of more people due to publicity, the 1G network could no longer fulfil the needs of customers (Petersen, 2002). Hence, there was a need to introduce new ideas and techniques to solve the problem. That brought the development of the 2G network technology (Figure 22 shows a photograph of a 2G phone). It was obvious from the characteristics that accommodation and good service would be provided for more customers, with great security and also deal with the problems of interference and attenuation (Petersen, 2002).

Radiolinja was the first company to launch the 2G technology commercially in Finland in 1991. (Petersen, 2002). It was a digitally encrypted communication system rather than analogue and so data could be transferred via a cell phone (like simple text messaging and multimedia messaging system) in addition to voice calls.

2G made use of the Time Division Multiple Access (TDMA) systems, which is a technology that allows different users to share a common frequency by allocating different time slots to each user (Petersen, 2002).



Figure 22: A Photograph of a 2G phone

Third generation (3G): Figure 23 shows a photograph of a 3G phone. It was first launched commercially by NTT DoCoMo in Japan on 1st October, 2001 (Nicola and Leslie, 2009). In December the same year Europe also launched its 3G in Isle of Man by Max Telecom. The 3G employs either Code-Division Multiple Access (CDMA) or Wideband Code Division Multiple Access (WCDMA).

CDMA is a technique in which the data bits are modulated by high-frequency orthogonal sequence of bits to spread the signals over a large frequency band (Guowang, 2016). Multiples of such signals from different users are then transmitted over the same frequency band. In order to retrieve a signal, a receiver must have the same spreading sequence, which is multiplied to this composite signal in a process called despreading (Guowang, 2016). This makes CDMA very secured and robust. It was used in 3GPP2 standards such as CDMA and Code-Division Multiple Access-Evolution Data Optimize (CDMA-EVDO) standards.

WCDMA spreads the signals over even a higher bandwidth (Ayyappan and Kumar, 2011). It was used in 3GPP standard such as Universal Mobile Telecommunication System (UMTS) to High-Speed Packet Access (HSPA+). Where the available bandwidth was 5 MHz compared to 1.5 MHz used in CDMA (Guowang, 2016). It improved the following in the previous generation;

- 1) Low data rates.
- 2) Congestion at peak hours.
- 3) Resource wastage.
- 4) Poor spectral efficiency.
- 5) Interference and attenuation.



Figure 23: A Photograph of a 3G phone

Fourth generation (4G): It is the fourth generation of wireless mobile telecommunication technology which succeeded 3G. Even though 3G is relatively good, after its introduction mobile phone users started to agitate for improved image processing, speed of processors and other services (Hina, 2016). This made the International Telecommunication Union (ITU) to come up with some set of standards for 4G in March, 2008 requiring all services described as 4G to adhere to a particular set of speed and connection standards (ITU-R, 2010). For mobile

gadgets including smart phone and tablets, connection speed needs to have a peak of 100 Mbit/s and for stationary uses such as hotspots, at least 1 Gbit/s (ITU, 2004). Applications like 3D games, high-definition mobile TV, video conferencing and 3D television are being provided by 4G at the expected speed (Hina, 2016).

4G has also been able to provide a common platform for different wireless networks and they are connected through one Internet Protocol (IP) core and this has also ensured a drastic reduction in latency (Djemai, Hadjila and Feham, 2011). This technology has also integrated all wireless technologies and doing away with the need for a new uniform standard for the different wireless systems such as: Universal Mobile Telecommunication System (UMTS), World Wide Interoperability for Microwave Access (WiMAX), General Packet Radio Service (GPRS) and Wireless Local Area Network (WLAN) (Djemai et. al, 2011).

Due to the increase in data rates of this technology, cell phones are designed to perform higher applications but not only for calls. For instance, it can be used in telemedicine where a patient sends his/her vital statistics (like temperature, glucose level and blood pressure) to a doctor online (Kyriacou, et.al, 2003). Figure 24 shows a photograph of a 4G phone.



Figure 24: A Photograph of a 4G phone

Fourth generation long term evolution (4G LTE): As the number of users and their demands started growing, communication networks evolved from 1G to 4G LTE. The radio part was significantly enhanced from Global System for Mobile Communication (GSM) to HSPA+ (Haykin & Moher, 2002). The focus was now shifted towards better spectral efficiency by using higher modulation models (Guowang, 2016). Most of the problems were solved in 3G but there was the need to deal with the following;

- 1) Exhaustion of spectrum.
- 2) Very high data rates.
- 3) High spectral efficiency.

This led to Orthogonal Frequency-Division Multiple Access (OFDMA) which is the technology employed in LTE and it encodes digital data on multiple carrier frequencies (Guowang, 2016). It comes with several advantages over WCDMA such as;

- 1) Bandwidth scalability.
- 2) Carrier aggregation.
- 3) Low Inter-Symbol Interference (ISI).

It uses orthogonal subcarriers equally spaced at 15 kHz (Guowang, 2016). Users are provided with the subsets of these carriers for data transmission. Unlike FDMA and TDMA, it allows the user to access variable bandwidth depending upon

the resource availability (Guowang, 2016). Also, since the subcarriers are orthogonal there are no band guards between them (Guowang, 2016).

The standard was developed by the 3rd Generation Partnership Project (3GPP) which is the producers of 3G as a means of achieving 4G, since the standards that were set by ITU for the 4G looked outrageous and difficult to achieve (Aret, Haardt, Konhauser, and Mohr, 2001).

It was however, first proposed by NTT DoCoMo of Japan in 2004 and studies commenced officially in 2005 (Anu, et. al, 2013). But the LTS/SAE Trial Initiative (LSTI) alliance was founded in May, 2007 as a global collaboration between vendors and operators with the aim of verifying and promoting the new standard to ensure that the technology was introduced as quickly as possible (Sharmila, 2015). The standard was however finalized in December, 2008 and commercially deployed in Oslo and Stockholm simultaneously on December 14, 2008 by TeliaSonera as the first publicly available LTE service as a data connection with a USB modem (Anu, et. al, 2013). The modem devices were manufactured by Samsung (dongle GT-B3710), and the network infrastructure with SingleRAN technology created by Huawei (in Oslo) and Ericsson (in Stockholm) (Sharmila, 2015). A spectral bandwidth of 10 MHz (out of the maximum 20 MHz), and Single-Input and Single-Output transmission was used (Guowang, 2016). The deployment should have provided up to 50 Mbit/s downlink and 25 Mbit/s in the uplink (Sharmila, 2015). However, introductory tests showed a 42.8 Mbit/s downlink and 5.3 Mbit/s uplink in Stockholm (Sharmila, 2015).

Samsung was the first to launch LTE mobile phone with the Samsung SCH-r900 on September 21, 2010 and the Samsung Galaxy Indulge being the world's first LTE smartphone starting on February 10, 2011 (Anu, et. al, 2013).

The LTE standard supports only packet switching with its all-IP network. Voice calls in GSM, UMTS and CDMA2000 are circuits switched, so with the adoption of LTE, carriers will have to re-engineer their voice call network (Anu, et. al, 2013).

There are four approaches to mobile broadband voice:

1) Circuit-switched fallback (CSFB): LTE only provides data services, and when a voice call is to be made or received, it will fall back to the circuit switch domain (Jose, Salil, Mutaz and Ishwinder, 2013). With this solution, operators only need to upgrade the Mobile Switching Centre (MSC) instead of deploying the IP Multimedia Subsystem (IMS), and therefore, can provide services quickly. But the disadvantage of this approach is longer call setup delay (Anu et. al, 2013). However, the CSFB solution is suitable as an interim solution prior to the deployment of IMS supported services (Jose, et. al, 2013).

2) Simultaneous voice and LTE (SVLTE): The handset works simultaneously in this approach (that is LTE and circuit switched modes) with the LTE mode providing data services and the circuit switched mode providing the voice service (Jean-Gabriel, 2014). This is a solution based solely on the handset, which does not have special requirements on the network or require the deployment of IMS either.

The disadvantage of this solution is that the phone can become expensive with high power consumption (Anu, et. al, 2013).

3) The third approach is based on the usage of over-the-top (OTT) services, using applications like Skype and Google Talk to provide LTE voice service (Jean-Gabriel, 2014). LTE boasts of features such as broad bandwidth, low latency, being always-online, and All-IP, creating natural convenience for the development of OTT and making OTT voice calls almost barrier-free (Anu, et. al, 2013).

4) The fourth approach is the IMS-based VoLTE. IMS has become the main network's standard architecture in the All-IP era because it supports multiple access modes and a wide range of multimedia services (Lav, 2014). It is based on the IMS network, with specific profiles for control and media planes of voice service on LTE defined by GSMA (Anu, et. al, 2015). Voice service is being delivered as data flows within the LTE data bearer in this approach (Lav). VoLTE has about three times the voice and data capacity of 3G UMTS and about six times 2G GSM (Lav, 2014). Moreover, it frees up bandwidth due to the fact that VoLTE's packets headers are smaller than those of unoptimized VoIP/LTE (Anu, et. al, 2013).

The Architecture of LTE Network and Working Principle

Figure 25 shows an architecture of the LTE network. In order to achieve the goals of this technology, the architecture of this network is different from the previous wireless data transfer network. The LTE standard supports packet switching with its all-IP network only (Okene, 2017). This is because it is designed to provide seamless Internet Protocol (IP) connectivity between user equipment

(UE) and the packet data network (PDN), without any interruption to the end users' applications if in motion (Dhathri and Krishna, 2017). Evolved UTRAN (E-UTRAN) is the air interface of LTE upgrade path for mobile networks (Tara, 2011), and it is accompanied by an evolution of the non-radio aspects under the term "System Architecture Evolution" (SAE), which includes the Evolved Packet Core (EPC) network. Together LTE and SAE comprise the Evolved Packet System (EPS). This network also uses an evolved node B, essentially an LTE base station (eNodeB), a Mobile Management Entity (MME), a Home Subscriber Server (HSS), a Serving Gateway (SGW), and a Packet data network Gateway (PGW). These are all part of the EPC except eNodeB.

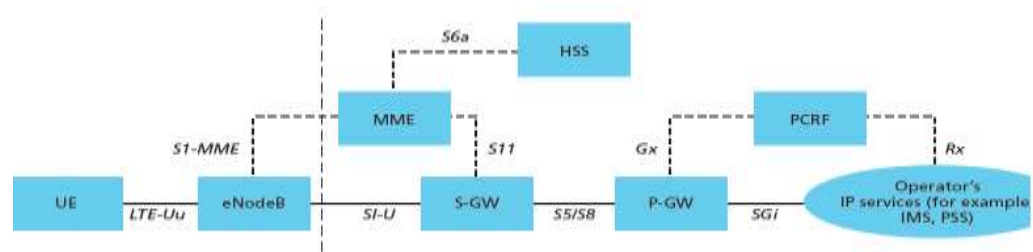


Figure 25: Architecture of LTE Network (Sesia, Toufik and Baker, 2011).

EPS is to provide the user with IP connectivity to a PDN for accessing the internet, as well as for running service such as Voice over IP (VoIP) (Sesia et.al, 2011). Usually, an EPS bearer is associated with a Quality of Service (QoS). In order to provide different QoS streams or connectivity to different PDNs, multiple bearers can be established for a user (Tara, 2011). Figure 25 shows the general network architecture, which includes the network elements and standardized interfaces. At a high level, the network is comprised of the Control Network (CN),

thus EPC and the access network E-UTRAN. Whereas the CN comprises several logical nodes, the access network is made up of only one node, eNodeB, which connects to the UEs. Each of the network elements is interconnected by an interface that is standardized in order to allow multi-vendor interoperability. This offers network operators the opportunity to source different network elements from different vendors. In fact, network operators can choose to split or merge these logical network elements depending on commercial considerations during their physical implementations (Sesia, et.al, 2011).

Related studies

A lot of research work has been carried out in the area of electromagnetic field levels and have been reported in literature. The studies in this field can be grouped into two. Thus, field measurement and mathematical models (Rappaport, 2002). Amoako et. al, (2009) measured and analysed radiofrequency radiations from some mobile phone base stations in Ghana. This is categorized under field measurement. Mathematical models give good estimation of situations to real world solutions (Lin, 2002). There are two forms of mathematical modeling approaches: empirical and theoretical (Rappaport, 2002). Theoretical models mostly depend on fundamental laws of wireless channels such as the electrical properties of the ground but empirical models are dependent on radio frequency measurements of the wireless channels.

The empirical models can be physical models, empirical or Monte carlo which is a statistical method and so makes use of statistics and distribution functions (Okumura, 1960). Okumura, 1960 revealed that when there is no line of

sight to a transmitter, the attenuation of the voltage that is being received approximates a ray distribution. Okumura, 1960 also came out with a correction factor for the correction of the field strengths.

The Okumura model is formally expressed as:

$$L = L_{FSL} + A_{MU} - H_{MG} - H_{BG} - \sum K_{correction} \quad (18)$$

Where: L = Median path loss (dB), L_{FSL} = The free space loss (dB),

A_{MU} = Median attenuation (dB) , H_{MG} = Mobile station antenna height gain factor,

H_{BG} = Base station antenna height gain factor and $K_{correction}$ = Correction factor gain

account for the type of terrain (such as type of environment, water surfaces, isolated

obstacle). The nature of a settlement, the type of buildings and trees also have a lot

of effect on the rate of propagation of the radio waves. Previous studies have

indicated that the waves are able to diffract down from the buildings (Parsons, 2000

& Okumura, 1960). Ikegami, Yoshida, Takeuchi, and Umehira, 1984 developed a

method to account for the diffractions on rooftop transmitters (Ikegami, et. al,

1984). Pande, Choudhari and Pathak, 2012, Willis and Kikkert, 2005, and Neto

Yang, and Glover 2010, have all published some works with regards to propagation

of radio waves in free space and two array models. The assumption free space

models make is that there are no reflections and obstructions in both transmitters

and receivers. There are a lot of reflections, diffractions and obstructions in the

environment and so these attenuate the signals (Mao, Anderson, & Fidan, 2007).

Rappaport 2002, revealed that the impact of vegetation and location accounts for

signal power decrease with distance (Rappaport, 2002). In order to predict the path

loss, a log-distance model which is a radio propagation model that predicts the path loss, a signal encounters inside a building or densely populated areas over distance was developed (Liao & Sarabandi, 2005).

Chapter Summary

The concept of radiation as electric and magnetic fields, as well as far and near fields were discussed. The non-ionising section of the EM spectrum was viewed into details, discussing the biological effects of non-ionising radiation and more precisely radio frequency. The use of RF for communication purposes was also taken into consideration, taken into account 1G, 2G, 3G, 4G and 4G LTE. The architecture and working principle of LTE was also viewed. Matters arising from related literature points to the fact that, this study can be grouped into field measurement and mathematical models.

CHAPTER THREE

MATERIALS AND METHODOLOGY

Introduction

This chapter describes the materials and methods used for the research work. Electric field levels were measured around 50 sites each (at a distance of 10 m, 30 m, 50 m, 70 m and 100 m from the base of the mast), in the Greater Accra, Ashanti and Western Regions. These are shown in Figures: 26-28 respectively. The description of how the power densities of the various sites were also deduced and the uncertainty estimation technique has also been described.

The chapter also gives a description of the mathematical model that has been developed for the prediction of power densities from transmitting antennas.

Study Area

a) Greater Accra Region: This region has the smallest area of Ghana's 16 administrative regions, occupying a total land mass of 3,245 square kilometres or 1.4 per cent of the total land area of Ghana (Ghana Statistical Service [GSS], 2019). It is located at 5.8143° N latitude and 0.0747° E longitude and bordered on the north by the Eastern Region, on the east by the Volta Region, on the south by the Gulf of Guinea, and on the west by the Central Region. This is the second most populated region, after the Ashanti Region, with a population of 4,010,054 in 2010, accounting for 16.3 per cent of Ghana's total population (GSS, 2019). Figure 26 is a map that shows the location of sites around which the measurements were taken in the region.



Figure 26: A map showing sites where measurements were taken in the Greater Accra region

b) Ashanti Region: It is the third largest of the 10 administrative regions, occupying a total land surface of 24,389 km² (9,417 sq mile) or 10.2 per cent of the total land area of Ghana (GSS, 2019). It lies between longitudes 0.15 W and 2.25 W, and latitudes 5.50 N and 7.46 N. However, it is the most populated region in the country with a population of 4,780,380 according to the 2010 census, accounting for 19.4% of Ghana's total population (GSS, 2019). The regional capital is Kumasi and it's the largest city in the region. Figure 27 is a map that shows the location of sites around which the measurements were taken in the region.



Figure 27: A map showing sites where measurements were taken in the Ashanti region

c) Western Region: The region spreads from the Cote D'Ivoire border in the west to the Central region in the east and it is located at 5.499998 N latitude and - 2.499998 W longitude (GSS, 2019). The region experiences the highest rainfall in Ghana and has fertile soils. There are a number of small and large-scale gold mines and offshore oil platforms which dominate the Western Region economy. Figure 28 is a map that shows the location of sites around which the measurements were taken in the region.



Figure 28: A map showing sites where measurements were taken in the Western region

Equipments

The materials used in carrying out the research included:

Anritsu Spectrum Master, Model MS2720T

Figure 29 shows a handheld spectrum analyzer with a range of 9 KHz to 43 GHz and a serial number 1338067, manufactured in the United States of America. It provides quick and accurate measurement of results. This was verified by comparing with other measuring devices and it also offers other functions such as high-accuracy power meter and an optional GPS receiver (Anritsu, 2015). The design is incorporated with Burst Detect and so allows users to measure signals as low as 200 μ s in a span up to 15 MHz, which makes finding directions on such

signals easier and productive. The optional GPS receiver is very sensitive and able to lock to the GPS network even inside some buildings. Once locked to the GPS network, its accuracy is better than 25 ppb and maintains better than 50 ppb for up to 72 hours after disconnecting the GPS antenna (Anritsu, 2015).

It has an optional full band tracking generators which are able to provide up to 20 GHz level output power in the range of 0 to -40 dBm in 0.1 dB steps.



Figure 29: A photograph of an Anritsu Spectrum Master, Model MS2720T

Log Periodic Antenna (LPA) model TS-6021

Figure 30 shows a photograph of a LPA. It offers uncompromising performance (Mushiake, 1999). The LPA has been optimised using a cutting edge genetic algorithm and an electromagnetic simulation tool. It has a very great gain and efficiency that gives the highest directional sensitivity from 600 MHz to 21 GHz with a nominal gain of 5-8 dBi to 21 GHz and an exceptional performance and also has a superior front to back ratio of 21GHz and beyond (Anritsu, 2015). This antenna offers the finest direction finding sensor for localizing the origin of

transmitting equipment and also it is able to cover frequencies that one need to locate.



Figure 30: A photograph of log-periodic antenna model TS-6021

Methodology

Radiofrequency (RF) signals were measured around one hundred and fifty (150) Fourth Generation Long Term Evolution (4G LTE) base stations in three regions in the southern part of Ghana (namely Greater Accra, Ashanti and Western Regions), which were all urban and densely populated areas.

The measurements were carried out using an Anritsu Spectrum Master, model MS2720T which was coupled to a handheld Log Periodic Antenna (LPA) model TS-6021. These were done at 5 different points around each mast at a height of 1.5 m and a distance of 10 m, 30 m, 50 m, 70 m and 100 m from the base of the masts, since emission levels from the antenna's within these distances are considered relatively high. The maximum hold function is used on the spectrum analyser such that the highest emission level at each location will be recorded.

The spectrum master had in-built antenna factors and associated cable factors that were able to correct the measured electric field strength. The points at which the measurements were taken around the base stations were chosen based on the direction of the antennae (sector). Also, all the measurements were made at public access points and the points were chosen to represent the highest levels of exposure to which a person might be subjected to, considering the positions of antennas and also to make sure that there were little or no reflecting objects and few overhead conductors like power lines and buildings with metal roofs as much as possible. These locations were however found by a quick sweep of the area using the measuring equipment. The selected sites were chosen to cover schools, hospitals and highly populated residential areas, since vulnerable people can easily be found here.

The antenna was connected to the spectrum master with the aid of an RF cable which had a load impedance of 50 Ω . The data was then downloaded after each day's measurement onto a lap-top computer. The spectrum master software that had been installed on the computer was used to determine the corresponding electric field strength in dB (mV/m) which is a quantitative expression of the intensity of an electric field at a particular location.

$$E = V_0 + K + A_c \quad (19)$$

where E is the electric field strength in dB (mV/m),

V_0 is the output voltage of the antenna in dB (mV), K is the antenna factor in dB (m^{-1}) and A_c is the attenuation of the antenna signal path in dB.

The corrected electric field strength was then converted into Volts per meter (V/m) taking into consideration polarization according to equation 20.

$$E(V/m) = 10\left\{\left(\frac{E(dB\mu V/m)}{20} - 120\right)\right\} \quad (20)$$

An average of all the 5 points at which the measurements were taken at each site was then calculated using equation 21.

$$Mean, \bar{x} = \sum_{j=1}^n \frac{x_j}{n} \quad (21)$$

Where x_j is the possible outcomes and n is the number of measurements

The intention of the measurements was to determine if the RF EME over the frequency bands of 800 MHz of the cell site comply with the public exposure limits of 38.89 V/m recommended by ICNIRP (ICNIRP, 2010).

The power density (in Wm^{-2}) which is the amount of power (time rate of energy transfer) per unit volume was calculated using equation 22.

$$S = \frac{E^2}{Z_0} \quad (22)$$

where: E is the electric field strength in V/m, S is the power density in W/m^2 and Z_0 is the impedance in Ω . For free space, impedance is 377 Ω . In determining compliance with ICNIRP equation 23 was used.

$$\sum_1^N \frac{S_1^{meas}}{S_1^{guid}} = \frac{S_1^{meas}}{S_1^{guid}} + \frac{S_2^{meas}}{S_2^{guid}} + \dots + \frac{S_N^{meas}}{S_N^{guid}} < 1 \quad (23)$$

Where S^{meas} is the measured (calculated) power density and S^{guid} is the guidance or reference power density and checked with the public exposure limits of 4 W/m² as recommended by ICNIRP (ICNIRP, 2010).

Uncertainty Estimation

The uncertainty of a measurement is the range within which the true value or the conventional true value of the measured quantity is likely to lie at the stated level of confidence (Weltner, Weber, Grosjean & Schuster, 1986) and in this case a confidence level of 95% was used.

Variance and Standard deviation

Random error is partly responsible for the deviation of individual measurements from the mean value (Weltner, et. al, 1986). The deviations become minimal as the measurement turns more exact and reliable and so, that made it possible to predict the reliability of the measurement. This was achieved by considering the deviations of the individual measurements from the mean. That is generally termed as variance using equation 24.

$$S^2 = \frac{1}{n} \sum_{i=1}^n (x_i - \bar{x})^2 \quad (24)$$

The Standard deviation was calculated by taking the square root of the variance so as to measure the dispersion of the measurements.

$$\text{Standard deviation, } S = \sqrt{\frac{1}{n} \sum_{i=1}^n (x_i - \bar{x})^2} \quad (25)$$

Error in the mean

There was the need to know whether the dispersion of the mean value was smaller than that of the individual values or not. The dispersion of the mean value is most essential, since that determines the reliability of the results.

The variance of the mean value is given as:

$$(SM)^2 = \frac{s^2}{n} \quad (26)$$

The standard deviation of the mean value is given as:

$$SM = \frac{s}{\sqrt{n}} \quad (27)$$

The standard uncertainty, $U_{(xi)}$ which is the standard deviation of the mean (SM) and the sensitivity coefficient, C_i (Instruments Uncertainty) was evaluated for the estimate x_i of each quantity. The combined standard uncertainty, $U_c(y)$ of the estimate y of the measured was calculated as a weighted root sum square (r.s.s):

$$U_c(y) = \sqrt{\sum_{j=1}^n (C_j + U_{(xj)})^2} \quad (28)$$

The expanded measurement uncertainty U_e was calculated as:

$$u_e = 2u_c \quad (29)$$

Mathematical model

Description of the model

Maxwell's equation is the fundamental equation that is used to study the electromagnetic field propagation with respect to transmitter power and the power density taking into account the distances away from the transmitters as described in Chapter two. Figure 32 shows a 4G LTE antenna, responsible for the transmission and receiving of radio frequency signals which were mounted on a telephone mast at a particular height, H and emitting RF radiations directed towards a man of height, h_1 standing at a distance, d from the antenna.

In order to determine the power density that has been emitted from the antenna at a given time and at a particular distance from it, the electric field strength was measured from which the power density could be evaluated.

Purpose of the Model

The model that has been developed is able to predict the power density of RF radiation around mobile telephone masts in the far-field region (up to 100 m from the mast) for regulatory purposes or in epidemiology studies. This model would be applicable to all generations of telecommunication technologies in predicting the power densities including those that are yet to be developed.

Assumptions and limitations of the model

Although, this model is very reliable in the prediction of power densities, some assumptions were made.

1. The man is in a direct line of sight to the antenna.
2. There are no reflection of radiations from the ground and buildings/trees.
3. The configuration of the transmitter may also be changed at the site and so worst case transmitter power was assumed.
4. Also in field work, losses due to cable and mismatch are corrected for by the spectrum analyzer. In the case of the model, high power is used in compensation for the losses.
5. Also, uncertainties due to tilt angle and position were not accounted for.

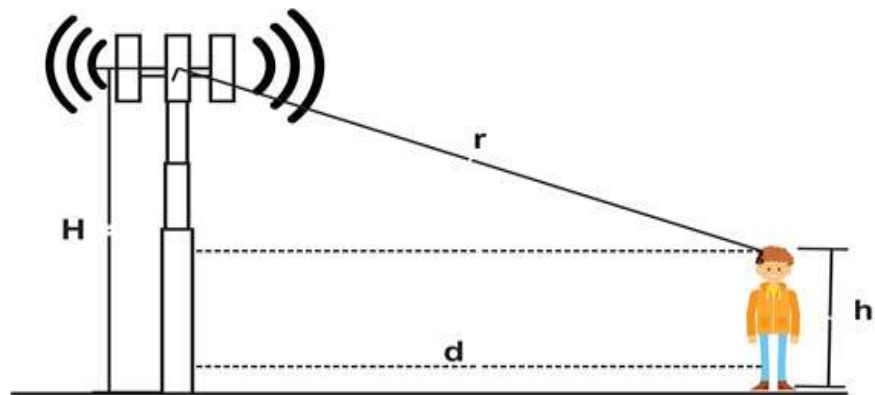


Figure 31: A typical exposure scenario in the Far-field of an antenna

Calculation of Power density

The magnitude of the E-field (E_n) contributed by a single point source is calculated by multiplying the scaled amplitude of radiation by the square root of the transmitted power and the antenna gain:

$$|E_n| = \frac{\sqrt{P} \times G}{r} (V/m) \quad (30)$$

where $G(\beta_T, \varphi)$ is the gain of the antenna,

$$r \text{ is the radial distance, given by } r = \sqrt{h^2 + d^2} \quad (31)$$

where $h = (H - h_1)$ is the height of the antenna from the reference point and d is the distance from the base of the mast to public compliance boundary.

From Kraus and Marhefka, (2001), the gain is modified to suit the assumptions of this study in equation (32) (Kraus and Marhefka, 2001).

$$G \simeq \frac{100}{D(\beta_T, \varphi)} \quad (32)$$

The vertical Half Power Beam Width (HPBW) is determined using, $\beta_T = \vartheta - \alpha_t$, where ϑ is Vertical Beam Width and α_t is the tilt angle. φ in equation 32 is the Horizontal Beam Width

The total E-field at a given observation point was calculated from the sum of the E-fields due to each of the N independent point sources in the collinear array as shown in the equation 33.

$$|E_n| = \frac{\sqrt{P} \times \left(\frac{100}{D(\beta_T, \varphi)} \right)}{r} \quad (33)$$

The tilt angle is a function of the vertical beam width and the mechanical tilt of the antenna to the required coverage area. The resulting vertical HPBW β_T is given by:

$$\beta_T = (\vartheta - \alpha_t) \quad (34)$$

The Power density is calculated using equation 30.

$$\text{Power Density, } S = \left(\frac{1}{2}\right) \left(\frac{1}{377}\right) |E|^2 \quad (35)$$

Substituting equation 33 into 35 gives:

$$S = \left(\frac{N_s}{2}\right) \left(\frac{1}{377}\right) \left\{ \frac{\left| \sqrt{P} \left(\frac{100}{(\vartheta - \alpha_t)(\varphi)} \right) \right|}{r} \right\}^2 \quad (36)$$

N_s is number of transmitters

Chapter Summary

The study covered three Regions in the Country: Ashanti, Greater Accra and Western Regions. These Regions had the highest number of base stations. The measurements were carried out using an Anritsu Spectrum Analyzer which was coupled to a handheld Log Periodic Antenna. These were done at 5 different points around each mast at a height of 1.5 m and a distance of 10 m, 30 m, 50 m, 70 m and 100 m from the base of the masts. The selected sites were chosen to cover schools, hospitals and highly populated residential areas and all the measurements were made at public access points. The measured electric field was converted to Volts per meter (V/m). The uncertainty associated with the measurement was estimated and the power density calculated. A mathematical model was developed to predict the power density of RF radiation around mobile telephone masts in the far-field region for regulatory purposes or in epidemiology studies.

CHAPTER FOUR

RESULTS AND DISCUSSIONS

Introduction

In this section, the results of the electric field strengths and power densities from the 50 base stations in each of the 3 regions studied, are presented. Figures 33, 34, 37, 38, 41 and 42 show variations in electric field strengths with the site location numbers while Figures 35, 36, 39, 40, 43 and 44 show variations in power density with their respective site location numbers. These results were compared to ICNIRP reference levels and earlier generations of technology as well as some work done on LTE.

The model developed was also validated and compared to empirical models as shown in Figures 45 and 46 respectively. The uncertainty estimation budget is also presented in Table 2.

Field Measurement

Greater Accra Region

The results of the compliance electric field measurement for the various base stations in the Greater Accra Region used for this work varied from as low as $3.85 \text{ E } -08 \pm 3.85 \text{ E } -09 \text{ mV/m}$ at site 46 which had a mean value of $1.42 \text{ E } -07 \pm 1.42 \text{ E } -08 \text{ mV/m}$ and a maximum value of $3.14 \text{ E } -07 \pm 3.14 \text{ E } -08 \text{ mV/m}$ to as high as $1.17 \text{ E } -02 \pm 1.17 \text{ E } -03 \text{ mV/m}$ at site 40 which had a mean value of $8.30 \text{ E } -03 \pm 8.30 \text{ E } -04 \text{ mV/m}$ and a minimum value of $5.65 \text{ E } -03 \pm 5.65 \text{ E } -04 \text{ mV/m}$.

The corresponding power densities of site 46 were; a minimum of $1.54 \text{ E } -07 \text{ mW/m}^2$, a mean of $5.68 \text{ E } -07 \text{ mW/m}^2$ and a maximum of $6.39 \text{ E } -07 \text{ mW/m}^2$. The site was located along the Tema-Aflao highway and the area was mainly a residential area with few factories.

The corresponding power densities of site 40 were $3.33 \text{ E } -02 \text{ mW/m}^2$ as the mean and $2.27 \text{ E } -02 \text{ mW/m}^2$ and $4.71 \text{ E } -02 \text{ mW/m}^2$ as the minimum and maximum respectively (Details of these can be seen in appendix 1A). The mast is located in the middle of estate buildings and it's close to a beach and a lagoon. It was originally a fishing village. Figures 32, 33, 34 and 35 show typical results. This relatively high results could be attributed to the fact that the community may have gadgets that support the technology and made the antenna's on the mast very active during the time of measurement as compared to the other areas.

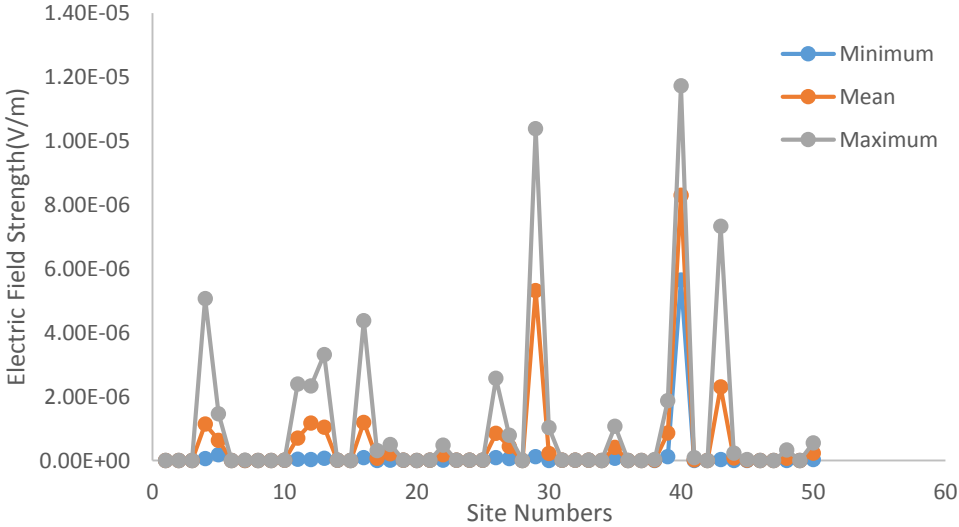


Figure 32: Graph of electric field strength variation with site numbers

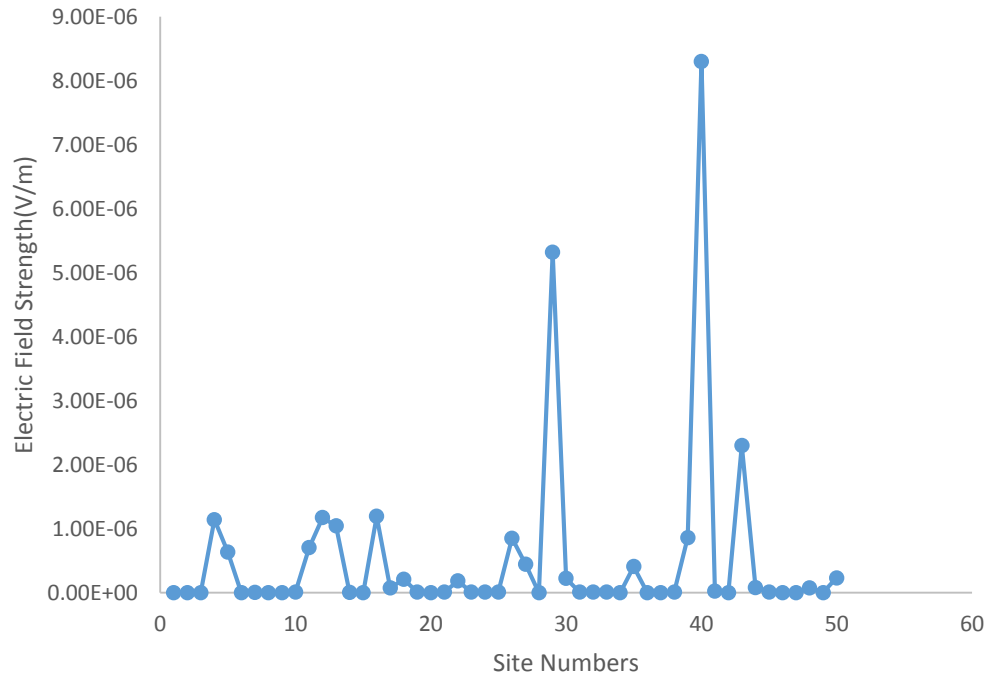


Figure 33: Graph of mean electric field strength variation with site numbers

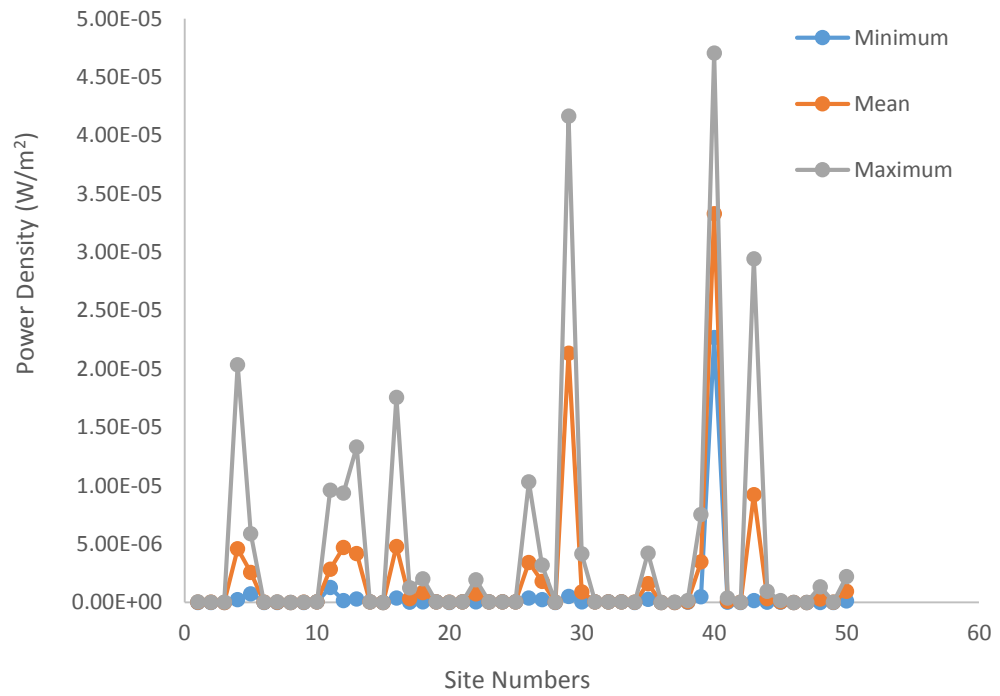


Figure 34: Graph of power density variation with site numbers

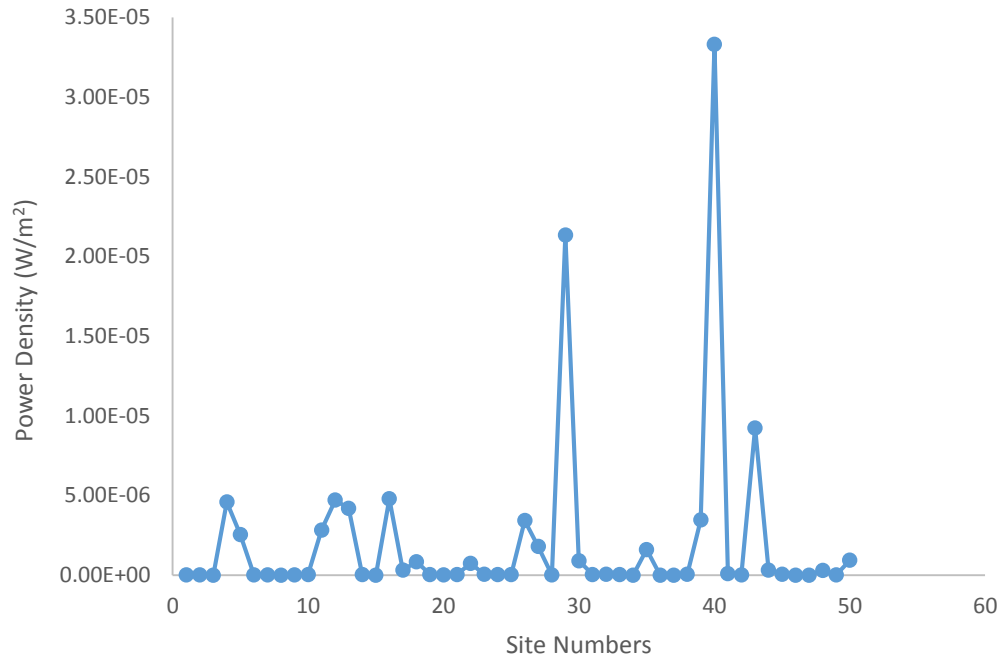


Figure 35: Graph of mean power density variation with site numbers

Ashanti Region

The minimum compliance electric field strengths from this region was recorded at site 23 which was $1.43 \text{ E } -08 \pm 1.43 \text{ E } -09 \text{ mV/m}$. It had a mean value of $1.46 \text{ E } -07 \pm 1.46 \text{ E } -08 \text{ mV/m}$ and a maximum of $4.46 \text{ E } -07 \pm 4.46 \text{ E } -08 \text{ mV/m}$. The mean corresponding mean power density of the site was $5.86\text{E}-08 \text{ mW/m}^2$ with a minimum and maximum of $5.74 \text{ E } -08 \text{ mW/m}^2$ and $1.79 \text{ E } -06 \text{ mW/m}^2$ respectively. The site was located in a community along the Kumasi-Mampong road. The highest compliance electric field strength was however recorded as $3.80 \text{ E } -02 \pm 3.80 \text{ E } -03 \text{ mV/m}$ with a minimum of $3.83 \text{ E } -04 \pm 3.83 \text{ E } -05 \text{ mV/m}$ and a mean of $1.25 \text{ E } -02 \pm 1.25 \text{ E } -03 \text{ mV/m}$ at site 11. The site was very close to the main Kumasi Township and the area had an undulating terrain. The relatively high level recorded at location 11 could be as a result of a convergence of the greater

part of the beam at that spot during measurement and due to the populous nature of the community people has gadgets that support the technology and made the antenna's active. The area is mainly for residential purposes with some shops for businesses. The corresponding power densities for the site were $1.54 \text{ E } -03 \text{ mW/m}^2$ as minimum, $4.93 \text{ E } -02 \text{ mW/m}^2$ as mean and $1.52 \text{ E } -01 \text{ mW/m}^2$ as maximum (Details of these can be seen in appendix 1B). This is shown by Figures 36, 37, 38 and 39 which had a variation factor of 2 million from the lowest to that of the highest.

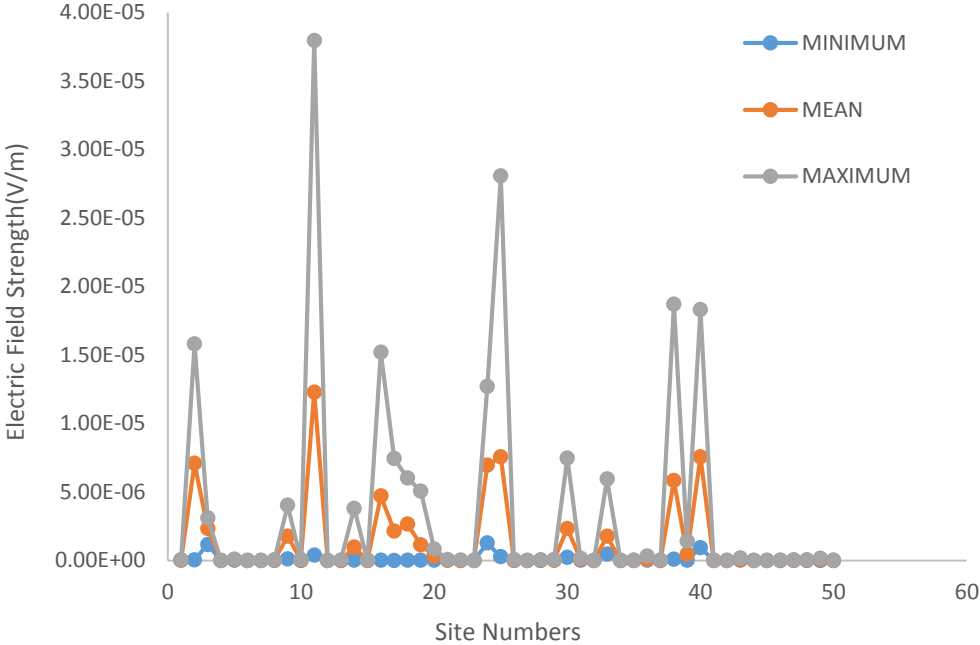


Figure 36: Graph of electric field strength variation with site numbers

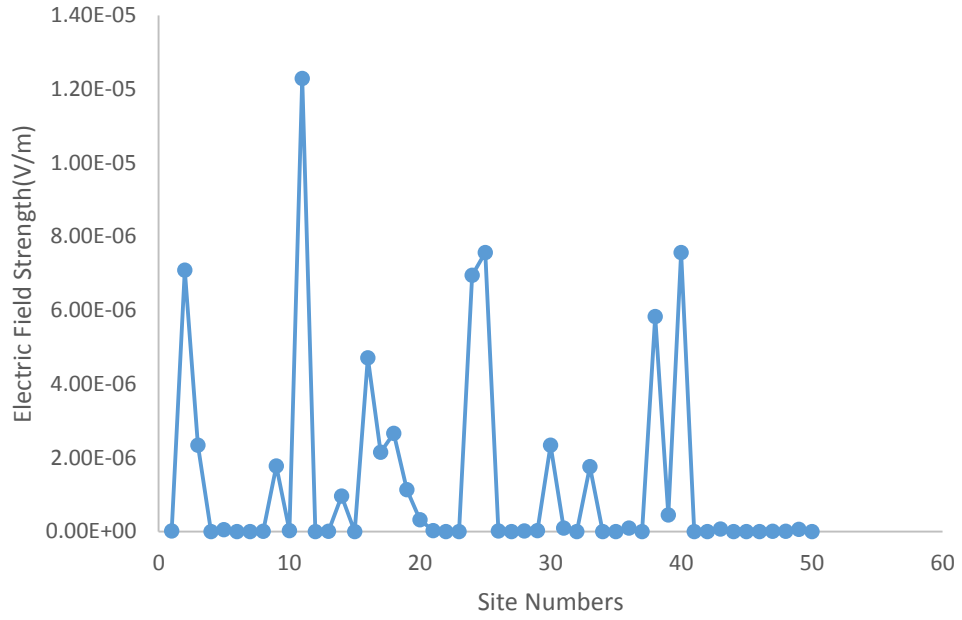


Figure 37: Graph of mean electric field strength variation with site numbers

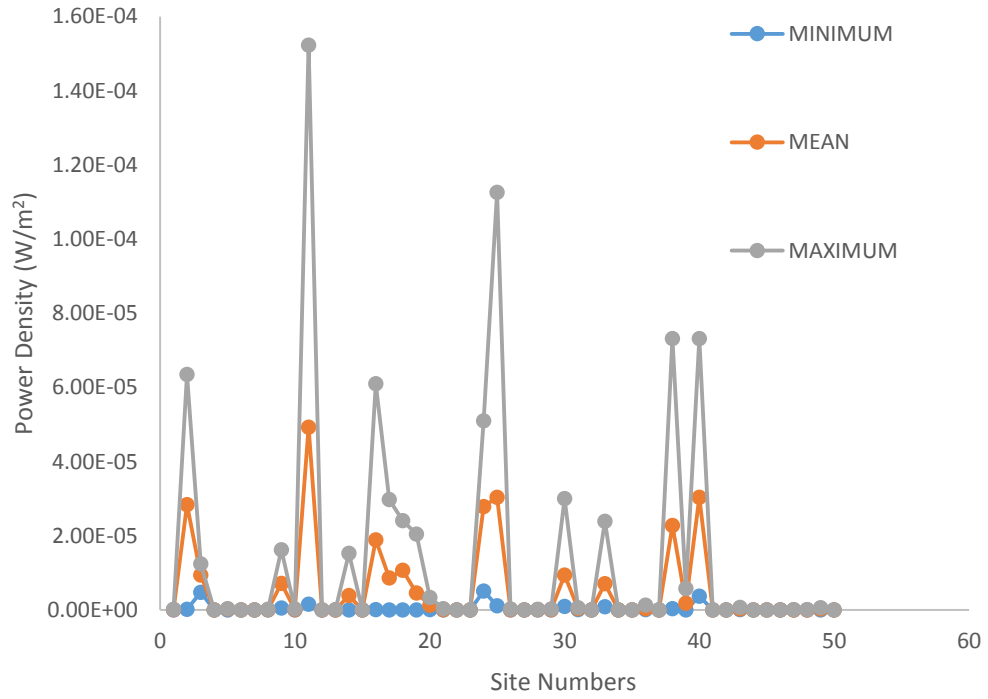


Figure 38: Graph of power density variation with site numbers

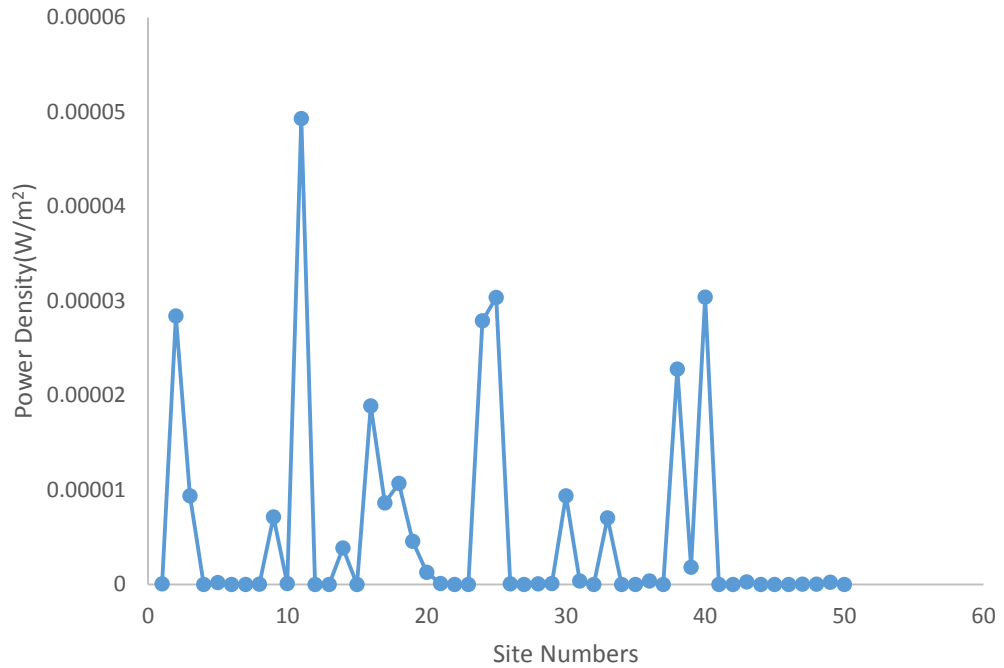


Figure 39: Graph of mean power density variation with site numbers

Western Region

The minimum compliance electric field strength value for this region was recorded at site 19 which was $8.52 \text{ E } -09 \pm 8.52 \text{ E } -10 \text{ mV/m}$ and had a mean and maximum values of $9.05 \text{ E } -09 \pm 9.05 \text{ E } -10 \text{ mV/m}$ and $9.87 \text{ E } -09 \pm 9.87 \text{ E } -10 \text{ mV/m}$ respectively. This site was located in the Bia East district. The corresponding power densities for this site were $3.42 \text{ E } -08 \text{ mW/m}^2$ as minimum, $3.63 \text{ E } -11 \text{ mW/m}^2$ as mean and $3.96 \text{ E } -08 \text{ mW/m}^2$ as maximum. However, the maximum electric field strength value was recorded at site 9. The site was located in a residential community in the Takoradi metropolis. The minimum electric field strength value was $4.86 \text{ E } -09 \pm 4.86 \text{ E } -07 \text{ mV/m}$ and $4.52 \text{ E } -04 \pm 4.52 \text{ E } -05 \text{ mV/m}$ and $1.97 \text{ E } -03 \pm 1.97 \text{ E } -04 \text{ mV/m}$ as mean and maximum respectively

(Details of these can be seen in appendix 1C). The corresponding power densities for this site were $1.59 \text{ E } -05 \text{ mW/m}^2$ as minimum, $1.81 \text{ E } -03 \text{ mW/m}^2$ as mean and $7.79 \text{ E } -03 \text{ mW/m}^2$ as maximum. Figures 40, 41, 42 and 43 shows typical results.

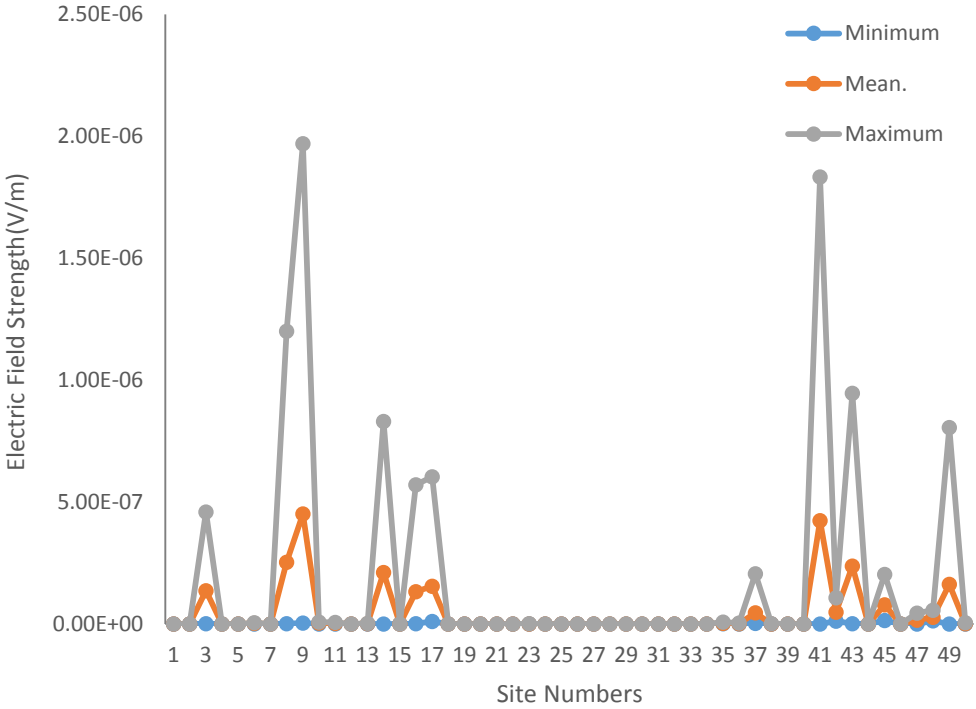


Figure 40: Graph of electric field strength variation with site numbers

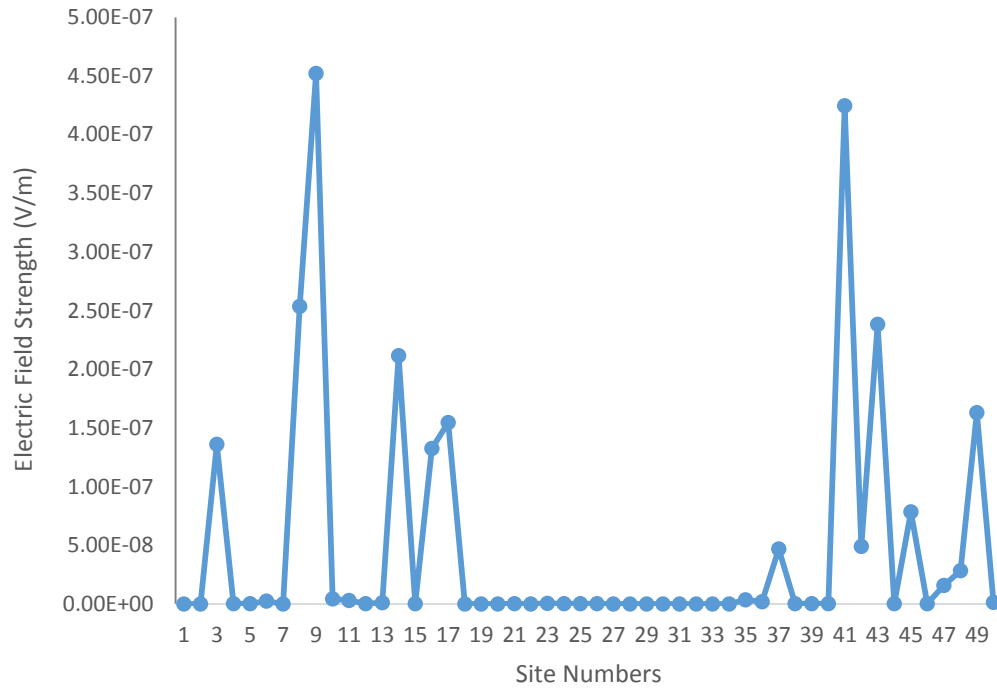


Figure 41: Graph of mean electric field strength variation with site numbers

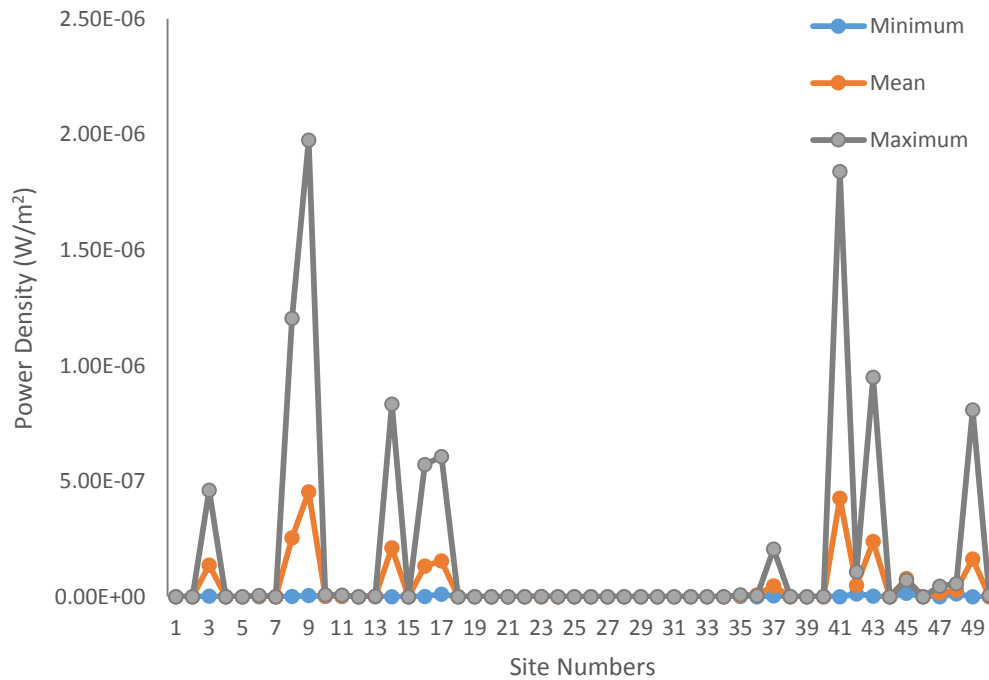


Figure 42: Graph of power density variation with site numbers

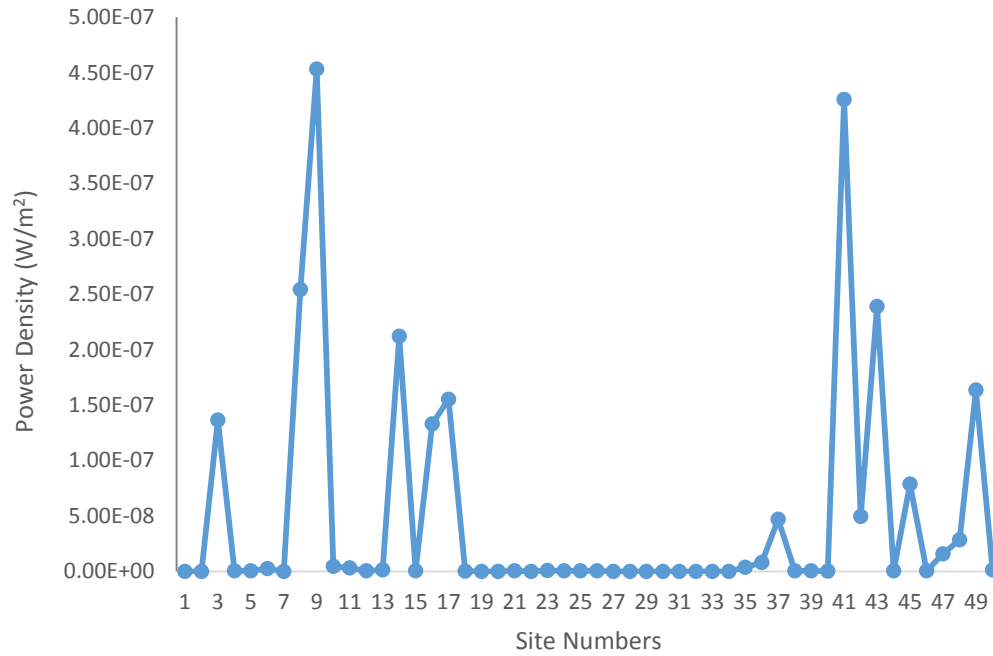


Figure 43: Graph of mean power density variation with site numbers

From Figures 32-43, it was evident that the highest electric field strength and power density were recorded in the Ashanti Region with a highest mean value of $1.25 \text{ E } -02 \pm 1.25 \text{ E } -03 \text{ mV/m}$ and $1.52 \text{ E } -01 \text{ mW/m}^2$ respectively at site 11.

Specifically, the highest electric field strength was 0.001% of the recommended limit of 38.89 V/m (ICNIRP, 2010) and the highest power density measured within the vicinity of the masts was 0.004% of the recommended limit of 4 W/m^2 (ICNIRP, 2010).

The results of this study were compared to Deatanyah et. al, (2018) who also measured and analyzed radiofrequency radiations from selected base stations in Ghana (Deatanyah et. al, 2018). Their average electric field strength for GSM

900 (1G) was 266.13 ± 23.83 mV/m, GSM 1800 (2G) was 414.43 ± 115.61 mV/m and UMTS 2100 (3G) was 366.54 ± 61.83 mV/m. The average power densities from Deatanyah et.al, (2018) were 0.1879 ± 0.0238 mW/m² for GSM 900, 0.4556 ± 0.1797 mW/m² for GSM 1800 and 0.3564 ± 0.0850 mW/m² for UMTS 2100. This indicates that the results from this work were relatively lower than theirs by a factor of 2.5 and could be attributed to the fact that most people do not have gadgets that support 4G LTE in the country and so the antennae on the mast were less active during the measurement as compared to those of 1G, 2G and 3G that they worked on.

The results were also compared to Chen and Lin, 2014. They also measured Electric fields emitted from LTE Base Stations in an Urban Area in Taiwan and their maximum power density was 1.853 mW/m² and so appeared higher than those measured in this study by a factor of 12.

Comparing the results to Mimoza et. al, 2017, where measurements were done at 138 locations around 20 LTE mobile base stations. The results were found to be relatively high by a factor of 3.5 when compared to this study. The maximum from this work was 0.004 % of the ICNIRP reference level of 4 W/m² (ICNIRP, 2010) compared to 0.014 % reported by Mimoza et al, 2017 (Mimoza et al, 2017). Further comparison to other works in Sweden (Mimoza et al, 2017) and the United Kingdom (Mimoza et al, 2017) revealed relatively higher values for both the mean and maximum values respectively recorded by this work as indicated in table 1.

Table 1: Comparison of work to other LTE studies

Country	Frequency (MHz)	ICNIRP Reference (Wm ⁻²)	Power Density (mWm ⁻²)		Compliance (%)
			Maximum	Mean	
Ghana	800	4.0	0.15	0.05	0.004
Kosovo	1810 - 1825	9.0	1.26	0.19	0.014
Sweden	2600	10	1.52	0.10	0.015
UK	2600	10	0.59	0.10	0.006

Also, there was generally a higher level of compliance of the results with the ICNIRP limits. But this does not mean that there was no possibility of a biological effect from these sites when one was exposed to them for long, since the person would be absorbing some of these radiations.

However, the compliance levels need to be improved by the installation of masts in some areas and reducing the power from the existing ones. These sites are: 2, 3, 9, 11, 16, 17, 18, 19, 30 and 40 in Ashanti region, sites: 4, 12, 13, 16, 29, 40 and 43 in Greater Accra region and sites: 8, 9 and 41 in Western region, as they appear higher than the rest by a factor of about 50000. As can be seen in figures 32-43.

Mathematical model

Validation of mathematical model

Figure 44 shows the variations between the results from the model and that from the real time measurement. The pink legend represent the field measurement while the blue represents the model. With a correlation coefficient (r) of 0.8, it signifies that the two compared works have a strong perfect positive relationship; when one variable moves in higher or lower, the other moves in the same direction with a similar magnitude. But the results of the model appear to be relatively higher than those from the field measurements and this could be attributed to the fact that worst case transmitter power were assumed, since the configuration of the transmitter may be changed and also to take care of the losses.

From the correlation coefficient, the coefficient of determination (r^2) which quantifies the proportion of the variation in one variable explained by the other was 0.64. It was evident that the results obtained from the field measurement are comparable to those of the model (theoretical) results. The results from the model were also analysed statistically to determine how well they agree with the field measurement. A mean of 3.78 E -07 and a standard deviation of 3.29 E -07 were obtained. From these two, the percentage Standard deviation was calculated as 12.95%. They were generated using equation (31) with data accessed from regulatory authority.

$$\text{Percentage Standard deviation} = \text{abs}\left(\frac{\text{mean} - \text{std.deviation}}{\text{mean}}\right) \times 100\% \quad (37)$$

The result of the percentage standard deviation indicated that the model is strong enough for predicting the power density in the vicinity of transmitting antenna's.

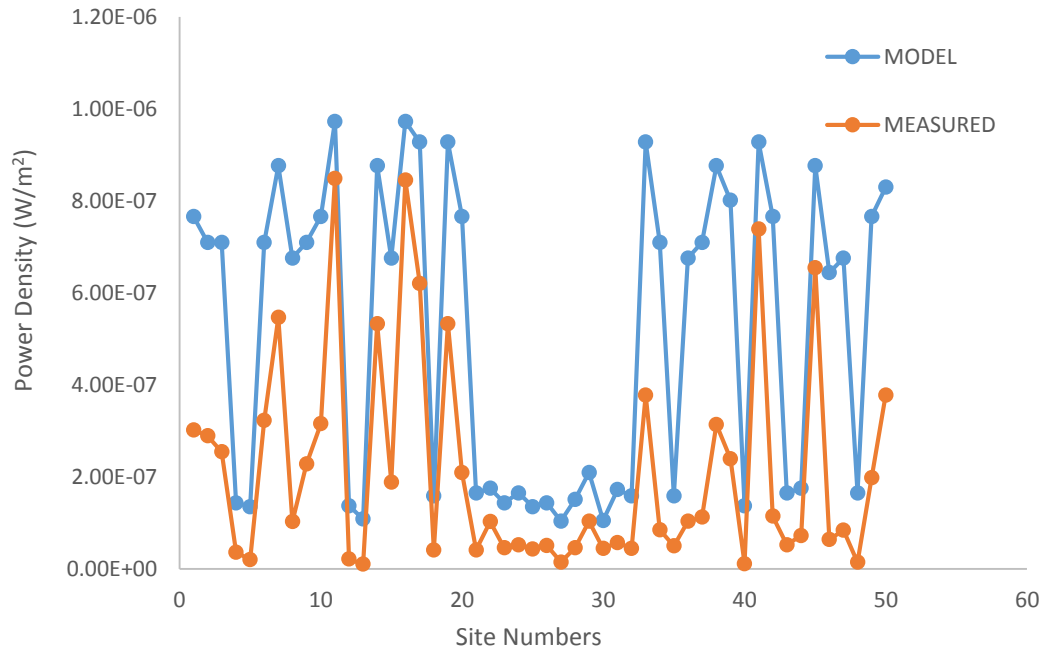


Figure 44: Verification of results from field measurement with the results from the model

Comparison of model with empirical model

Figure 45 shows that the results obtained from this work (model) were comparable to that of the free space wave propagation model. The grey legend represent the free space model (Pabari, J. P., Acharya, Y. B., Desai, U. B., Merchant, S. N., Krishna, B. G., 2010; Rappaport, 2002 and Parsons, 2000) while the pink legend represents this study. The model developed was good and gives sufficient, reliable and consistent results to predict exposure in the environment. A lot of the models available in literature (Pabari et. al, 2010) put much emphasis on

the prediction of the propagation signals and attenuation but this study focusses on the usage of the propagation information to predict exposure to the general population.

The free space wave propagation model assumes that the transmitter and receiver, use line-of-sight communication and does not take into account obstruction or reflection of any form. The equation for the free space model by Friis (Friis, 1946) is given as:

$$P_r = \frac{P_t G_t G_r \lambda^2}{16\pi^2 d^2} \quad (38)$$

Where P_t and P_r are transmitter and receiver powers, G_t and G_r are gains of transmitter and receiver antennas, λ is wavelength of operation and d is distance from the transmitter.

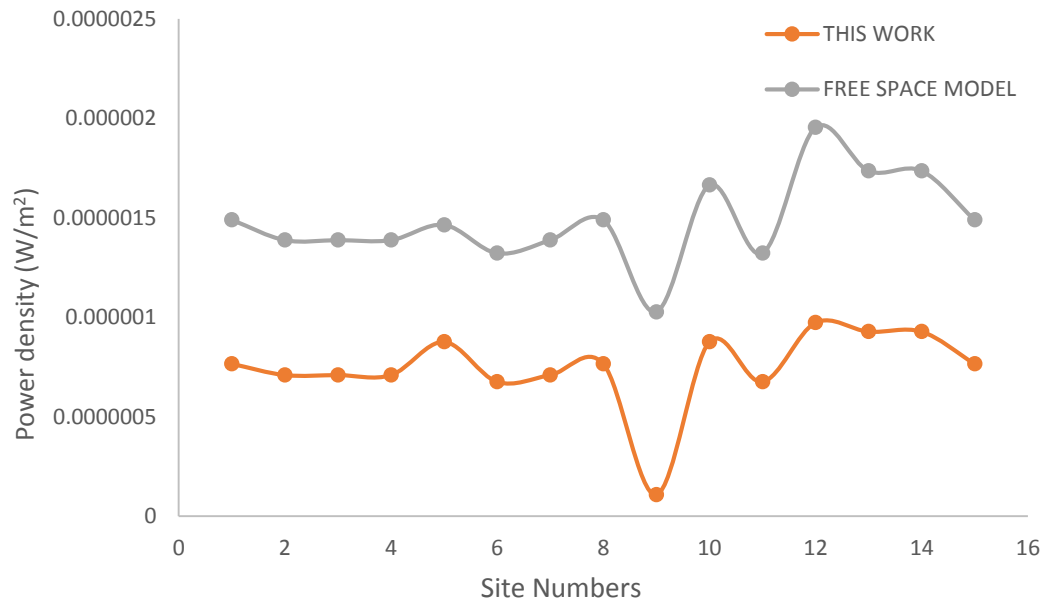


Figure 45: Comparison of results from this study with Friis model (Friis, 1946)

MATLAB Model

The information obtained from the field work was used together with developed theory to develop a predictive model using MATLAB 9.0 (MathWorks, 2016) as shown by Figure 46 and a programming code in Appendix 3.

The prediction of the model is based on input data from regulatory authority, which is provided by the manufacturer of the antenna for safety assessment before the antenna is mounted in the field. The following input data is needed to calculate the output parameters:

1. The frequency of operation of the antenna as assigned by the NCA.
2. The number of antenna elements.
3. The vertical and horizontal half-power beam width of the antenna.
4. The tilt angle of the antenna.
5. The transmission power of the antenna.
6. The distance of interest from the base of the antenna.
7. The mounting height of the antenna from the ground.
8. Human height.

When the information is fed into the model, the gain button, electric field strength button, power density button and the compliance button are required for their respective function.

The graphical output also provides the distance from the mast, the height of the mast and a three dimensional electric field strength with a colour scale.

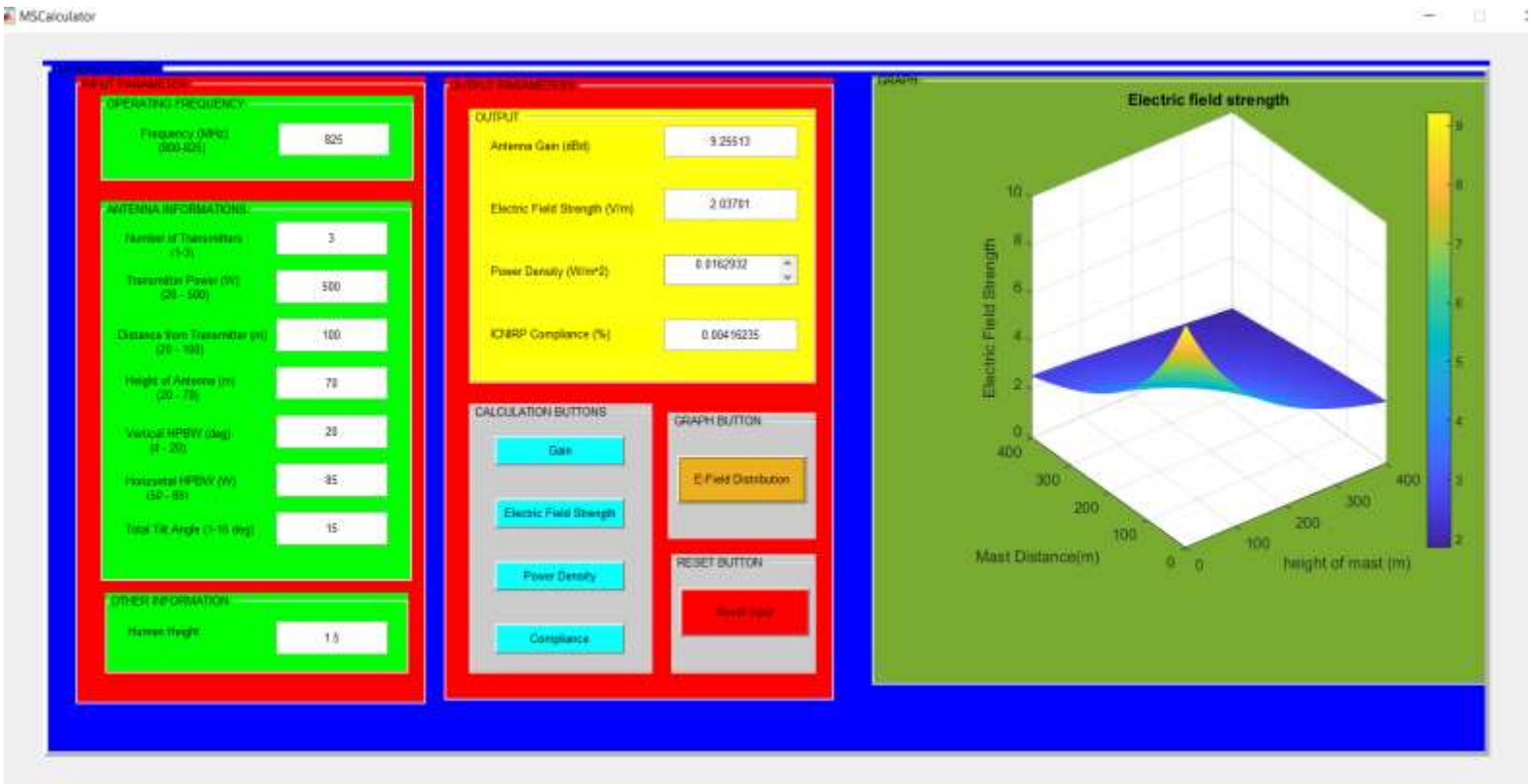


Figure 46: Resulting MATLAB model graphical user interphase showing the various inputs and outputs function

Table 2: Uncertainty Estimation budget

Uncertainty sources	Uncertainty Type	Estimate (%)	Probability Distribution	Divisor	Standard Uncertainty (%)
Spectrum Analyzer					
Amplitude accuracy	B	5.92	Rectangular	2.00	2.96
Resolution Bandwidth (1 Hz to 3 MHz)	B	0.20	Normal	2.00	0.10
Device-Under-Test					
Mismatch (Analyzer and Antenna)	B	3.64	U-shape	1.41	2.58
Antenna calibration factors	B	5.95	Normal	2.00	2.98
Cable correction factor	B	1.45	Rectangular	1.73	0.84
Measurement Repeatability	A	0.10	Normal	2.00	0.05
Measurement Uncertainty					
Combined uncertainty (%)					5.00
Expanded Uncertainty (95 %)			Coverage factor 2		10.00

Chapter Summary

An average of the electric field strengths were determined for each of the sites that were studied. The power densities were then evaluated from that. The highest electric field strength and power density were however, recorded in the Ashanti Region with a highest mean value of $1.25 \text{ E }^{-02} + 1.25 \text{ E }^{-03} \text{ mV/m}$ and $1.52 \text{ E }^{-01} \text{ mW/m}^2$ respectively at a site close to Kumasi township (site 11). The results were then compared to works done in Ghana on the previous generation of technology as well as other works done on 4G LTE elsewhere. The model been

developed was validated with some field measurements and also compared to Friis free space model.

CHAPTER FIVE

SUMMARY, CONCLUSIONS AND RECOMMENDATIONS

Introduction

This chapter presents the summary of the results of the electric field strengths and power densities and how they varied in each of the regions that were studied. How they compared with ICNIRP reference levels and other related works done.

The chapter also gives some conclusions based on the level of RF radiation that were measured at the field and some recommendations for policy makers, operators and for future research work.

Summary

The study involved the measurement of radiofrequency signals with the use of an Anritsu Spectrum Master coupled to a handheld Log Periodic Antenna, around one hundred and fifty (150) 4G LTE base stations mounted near schools, hospitals and in densely populated areas in three (3) Regions, in the southern part of Ghana (Greater Accra, Ashanti and Western). The measurements were done at five different locations (10 m, 20 m, 50 m, 70 m and 100 m) from the mast at a height of 1.5 m from the ground. The electric field strengths and power densities were calculated.

In the Greater Accra Region, the compliance electric field strength and power density varied from as low as $3.85 \text{ E } -08 \pm 3.85 \text{ E } -09 \text{ mV/m}$ and $1.54 \text{ E } -07 \text{ mW/m}^2$ to as high as $1.17 \text{ E } -02 \pm 1.17 \text{ E } -03 \text{ mV/m}$ and $4.71 \text{ E } -02 \text{ mW/m}^2$

respectively. While in the Ashanti Region the compliance electric field strength and power density ranges from $1.43 \text{ E }^{-08} \pm 1.43 \text{ E }^{-09} \text{ mV/m}$ and $5.74 \text{ E }^{-08} \text{ mW/m}^2$ to $3.80 \text{ E }^{-02} \pm 3.80 \text{ E }^{-03} \text{ mV/m}$ and $1.52 \text{ E }^{-01} \text{ mW/m}^2$ respectively. Also in the Western Region the compliance electric field strength and power density varied from as low as $8.52 \text{ E }^{-09} \pm 8.52 \text{ E }^{-10} \text{ mV/m}$ and $3.42 \text{ E }^{-08} \text{ mW/m}^2$ to $1.97 \text{ E }^{-03} \pm 1.97 \text{ E }^{-04} \text{ mV/m}$ and $7.79 \text{ E }^{-03} \text{ mW/m}^2$ respectively.

These results were however much lower than the recommended ICNIRP reference levels of 38.89 V/m and 4W/m^2 for electric field strength and power density respectively at a frequency of 800 MHz. Also, the results when compared to works done on the previous generations of technology (1G, 2G and 3G) in the country, appeared lower than them by a factor of 2.5, which shows that this technology is better than its predecessors. The results were also lower than other LTE studies by a factor of 3.5.

A model was also developed for the estimation of power density of transmitting antennas without one having to visit the site to take measurements.

Conclusion

The results from the base stations has given an indication as to the level of emissions that people are exposed to in these communities. Even though, the results appear lower than the ICNIRP reference levels that does not mean the absence of biological effects and so they could be able to cause biological effects but not health effects.

The results obtained from the study gave a clear indication of the level of radiofrequency emission that was expected in the regions that were not studied. Since the topography in the country was similar and the same frequency and conditions are used by the telecommunication companies throughout the country.

The model been developed would also be very effective in prediction of power density of transmitting antenna.

The results would also serve as a baseline data for comprehensive work on 4G LTE in the country.

The results were also essential as they gave an indication of an increase in telecommunication gadgets without an equivalent rise in the number of base stations so as to reduce the exposure levels and to improve the quality of service in the country.

Recommendations

There is an increasing importance of telecommunication to the growth and development of the country. But the swift growth of this industry in recent years has brought a lot of concerns with regards to the exposure levels of RF emissions from the telephone masts that are sited near schools, hospitals and densely populated residential areas. Certain requirements should therefore be put in place in order to ensure that public safety standards are not compromised.

Recommendations to the Policy Maker

Policy makers should make sure that Operators:

1. Provide the necessary data with regards to health and safety aspects of RF transmitters.
2. Design sites such that the public cannot access them.

Recommendations to the Operator

1. Signals with strong intensity should not be made to land on existing or planned establishment of a community sensitive location/facility e.g., school compound, a hospital, and residential areas,
2. Antennas mounted on roof-top must be elevated above the height of people who may access the roof.

Recommendations for future research work

1. Similar research should be carried out in the regions that were not covered.
2. Measurement of radiofrequency levels around the telephone masts should also be carried out during the night to assess the variations of exposure from daytime readings
3. Work should also be done at sites that has 1G, 2G, 3G and 4G LTE antennas to determine the total amount of RF levels.
4. The variation of transmitter configuration and the tilt angles should be incorporated into future versions of the model.
5. Follow up studies should also be carried out on sites that recorded higher levels of radiation by making use of the location coordinates and other data

provided by this study. This is to verify whether the telecommunication company has reduced the power from those antennae.

REFERENCES

- Abdullah A, Samadder A, Imon A, and Ahmed S. M. Z (2015): 3D Design and Gain Analysis of Dipole Antenna with Integrated Frequency Level. *IEEE Communication and Network Security*.
- Alan J. Sangster (2014): Electromagnetic Foundations of Solar Radiation Collection, *Springer International publishing*, Switzerland.
- Alan M, Sam H, Karen B and Peter C, (2012): *An introduction to radiation protection, 6th edition*, Tylor and Francis group, US.
- Altgelt, C. A (2005): "The World's Largest "Radio" Station" hep.wisc.edu. High Energy Physics @ UW Madison.
- Amandeep B, Abhishek T, Jitender S and Basudeo P (2014): Analyzing the Different Parameters of Dipole Antenna, *IJEEE*, Spl. Issue 1.
- Amoako J. K., Fletcher J. J. and Darko E. O (2009): Measurement and analysis of radiofrequency radiations from some mobile phone base stations in Ghana. *Radiation Protection Dosimetry* (2009), No. 135(4), 256–260
- Anu R, Pulkit N, Sachin K R Mohita A and Meghna K (2013): Network advancement in 4G: TD-LTE Technology. *International Journal of Engineering and Computer Science*.
- Anushi A, Yash R, Aditya K and Shashank S (2015): Comparative study of different Feeding Techniques for Rectangular Microstrip Patch Antenna. *IJIREEICE*, 3509.

- Anritsu (2015) High Performance Handheld Spectrum Analyzer manual. Morgan Hill, USA
- Aret K, Haardt M, Konhauser W, and Mohr W. (2001): The future of wireless communications beyond the third generation. *Wireless Personal Communications* 23: 121–135.
- Ashok K. K, Sheeba K and Rhishika K (2013): microstrip patch antenna using crown and sierpienski fractal slot. *International Journal of Advance Research In Science And Engineering, IJARSE*, Issue No.10.
- Ashwani K and Vijay D (2016): Electromagnetic Spectrum and Its Impact on Human Life. *International Journal of All Research Education and Scientific Methods (IJARESM)* ISSN: 2455-6211, Issue 8
- Ayyappan K and Kumar R. (2011): Impact of Convolutional Coding on Downlink Performance of WCDMA Network. *IJCA* (14):14–19.
- Balanis, Constantine A. (2011). *Modern Antenna Handbook*. John Wiley and Sons
- Balzano, Q., Garay O. and Manning, T.J. (1995): *Electromagnetic energy exposure of simulated users of portable cellular telephones*. *IEEE Transactions on Vehicular Technology* 44(3):390 - 403
- Balzano Q., Garay O., and. Steel, F.R (1978): Energy Deposition in Simulated Human Operators of 800-MHz Portable Transmitters. *IEEE Transactions on Vehicular Technology* Volume: 27 , Issue: 4 , Page: 174 – 181.

- Begüm K. E and Çetin K (2016): Comparison of Signal Strengths of 2G/3G/4G Services on a University Campus. *IJAMEC.270710*
- Bevelaqua P. (2015): *Antenna arrays: performance limits and geometry optimization* (Doctoral thesis, Arizona State University), <http://www.antenna-theory.com>.
- Browne M. (2013): *Physics for Engineering and Science*, 2nd ed. McGraw Hill/Schaum, New York.
- Chen Hsing-Yi and Lin Tsung-Han (2014): Simulations and Measurements of Electric Fields Emitted from a LTE Base Station in an Urban Area. *International Journal of Antennas and Propagation*. Article ID 147341, 10 pages
- Christopher H. (2008). *Essentials of radio wave propagation*, Cambridge University Press, U.S.A
- Cloude S. (1995): *An Introduction to Electromagnetic Wave Propagation and Antennas*. Springer International publishing, Switzerland.
- Constantine A. B (2005): *Antenna Theory: Analysis and Design*, 3rd edition, John Wiley and sons, inc., publication, US
- Das S. K. (2016): *Antenna and Wave Propagation*. Tata McGraw-Hill, U. S. A.
- Deatanyah P., Amoako J.K, Abavare E.K.K and Menyeh A. (2018): Analysis of electric field strength and power around selected mobile base stations. *Radiation Protection Dosimetry* (2018), pages: 1–8

- Dhathri R. P and Krishna M. S (2017): SIFM: A network architecture for seamless flow mobility between LTE and WiFi networks – Analysis and Testbed Implementation. *Journal of CoRR* abs/1702.07489
- Djemai, A. M. Hadjila and Feham, M. (2011): Performance Analysis of the Interconnection between WiMAX and UMTS Using MIH Services in MIPv6, *Computer Science and Network Security*.
- Dragan P, Khalil E. K. D, Sergey V. T and Andres P (2012): Antenna Models for Electromagnetic Compatibility Applications. *International Journal of Antennas and Propagation* Volume 2012, Article ID 591643, 2 pages doi:10.1155/2012/591643
- Dutkiewicz J., Cisak E., Sroka J., Wójcik-Fatla A. and Zajac V. (2011): Biological agents as occupational hazards. *Ann Agric Environ Med*. 2011;18(2):286–293
- Ellingson S. W (2016): *Radio Systems Engineering*. Cambridge University Press, U.S
- Farahani S (2008): *Zigbee wireless network and transceivers*. Newness U.S
- Friis, H.T. (1946): A Note on a Simple Transmission Formula. *IRE Proc.*: 254–256.
- Giancoli, D.C. (1988): *Physics for Scientists and Engineers*, 2nd ed. Prentice Hall, U.S

- Graf R. F. (1999): *Modern Dictionary of Electronics*. 7th edition, Typeset by Laser Words, Madras, India Printed in the United States of America
- Grellier J, Atkinson W, Bérard P, Bingham D, Birchall A, Blanchardon E, Bull R, Guseva Canu I, Challeton-de Vathaire C, Cockerill R, Do MT, Engels H, Figuerola J, Foster A, Holmstock L, Hurtgen C, Laurier D, Puncher M, Riddell AE, Samson E, Thierry-Chef I, Tirmarche M, Vrijheid M, Cardis E. (2017): Risk of lung cancer mortality in nuclear workers from internal exposure to alpha particle-emitting radionuclides. *Journal of Epidemiology*; 28(5):675-684.
- GSS (2019): 2010 population and housing census. technical report, Ghana Statistical Service, Accra.
- Guowang M, Jens Z, Sung K. W and Slimane B (2016): *Fundamentals of Mobile Data Networks*, Cambridge University Press, U.S.A.
- Hammett, W. F. (1997): *Radio Frequency Radiation, Issues and Standards*, McGraw-Hill, New York.
- Haydar M. Al-Tamimi, Salah Mahdi (2016): A Study of Reconfigurable Multiband Antenna for Wireless Application. *International Journal of New Technology and Research (IJNTR)* Volume-2: 125-134
- Haykin S. and Moher M. (2002): *Modern Wireless Communications*, Pearson Education, Inc. Singapore.

- Hemant K and Girish K (2018): A broadband planar modified quasi-yagi using log-periodic antenna. *Progress In Electromagnetics Research Letters*, Vol. 73, 23–30,
- Hina F. (2016): 4G LTE Network Growth in India and Security Issue in Network. *IJCSNS International Journal of Computer Science and Network Security*, Vol.16 No.11
- Hitchcock R. T. (2004): Radio-frequency and Microwave Radiation. *Environmental health perspectives*. DOI: 10.1002/0471435139
- Hitchcock R. Timothy and Patterson Robert M. (1995): *Radio-Frequency and ELF electromagnetic energies*. John Wiley and Sons, New York.
- IARC May 31, (2013): *Non-ionising radiation, part 2*. 102, Lyon, France. IARC press. ISBN 9789283213253. Retrived from <https://www.ncbi.nlm.nih.gov/books>
- ICNIRP (1998): *Guidelines for limiting exposure to time varying Electric, Magnetic field and Electromagnetic fields (up to 300 GHz)*. Health Physics 74, No.4, : 494-522
- ICNIRP (2010): *Guidelines for limiting exposure to time varying Electric, Magnetic field and Electromagnetic fields (up to 300 GHz)*. Health Phys 99(6):818-836

- Ikegami, F., Yoshida, S., Takeuchi, T., and Umehira, M. (1984): *Propagation factors controlling mean field on urban streets*. IEEE transactions on antennas and propagation, 32(8):822–829.
- ITU Internet Reports: (2004, September): *The Portable Internet*. Geneva, Switzerland
- ITU/MIC (2004, 4-5 March): *workshop on shaping the future mobile information society*, Seoul, Korea
- ITU-R 21 (2010, October): *IMT-Advanced 4G standards to usher new era of mobile broadband communications*. Geneva, Switzerland.
- Jean-Gabriel R. C. L. (2014): *LTE standards*, John Wiley and sons Inc, New York.
- Jiles, D. C. (1998): *Introduction to Magnetism and Magnetic Materials*. 2nd edition. CRC U.S
- John D. kraus and Ronald J. Marhefka (2001): *Antannas*. 3rd edition, McGrawhill, New York.
- John D. J (1998): *Classical Electrodynamics*, 3rd edition Wiley and sons, inc., publication, New York.
- Jose E. V B, Salil S., Mutaz S.and Ishwinder S. (2013): Performance of CS fallback from LTE to UMTS. *IEEE Communications*. 0163-6804
- Jung-Sim R, Yong-Seung C, Tae J. K. and Sang-Wook N. (2008): Electromagnetic Shielding Effectiveness of Multifunctional Metal Composite Fabrics. *Textile Research Journal*, Volume: 78 issue: 9, page(s): 825-835

- Khadar M. A. B and Sneha T (2017): Design and Testing of Biconical Antenna. *International journal of research trends in Engineering and research*. 139-144.
- Knoll G. F. (1979): *Radiation detection and measurement*. John Wiley and Sons, New York
- Konya, J and Nagy, N. M. (2012): *Nuclear and Radio-chemistry*. 1st edition, John Wiley and Sons, New York.
- Krane K. S. (1988): *Introductory Nuclear Physics*. John Wiley and Sons, New York.
- Kyriacou E, S. Pavlopoulos, A. Berler, M. Neophytou, A. Bourka, A. Georgoulas, A. Anagnostaki, D. Karayiannis, C. Schizas, C. Pattichis, A. Andreou and D. Koutsouris (2003): Multi-purpose HealthCare Telemedicine Systems with mobile communication link support. *Biomed Eng*; 2: 7. doi: 10.1186/1475-925X-2-7
- Kyung-Taek R. and Cheol-Hong L. (2014): Biologically Hazardous Agents at Work and Efforts to Protect Workers' Health: A Review of Recent Reports. *Saf Health Work*; 5(2): 43–52.
- Lav G. I. (2014): Voice over LTE: Status and Migration Trends. *International Journal of Applied Research*; 2(12): 431-435

- Liao, D. and Sarabandi, K. (2005): Near-earth wave propagation characteristics of electric dipole in presence of vegetation or snow layer. *IEEE Transactions on Antennas and Propagation*, 53(11):3747–3756.
- Lin, J. C. (2002): Microwave exposure and safety associated with personal wireless telecommunication base stations. *IEEE Microwave magazine*, 3(3):28–32.
- Lusekelo K. (2013): Analysis of the Effects of Rectangular Ground Plane on Radiation Pattern of the Monopole Antenna. *International Journal of Scientific and Research Publications*, Volume 3, Issue 11.
- Lusekelo K. (2013): Gain enhancement of the monopole antenna. *International journal of software and hardware research in Engineering*. Vol. 1, Issue 4.
- Mao, G., Anderson, B. D., and Fidan, B. (2007): Path loss exponent estimation for wireless sensor network localization. *Computer Networks*, 51(10):2467–2483.
- Martin C., Chris D., and William W. (2007): *Modern Spectrum Management*, Cambridge University Press, U.S.A
- MathWorks (2016). Matlab 2016a. release 2016a. software, The MathWorks, Inc, Natick, Massachusetts, United States.

- May, T. C and Woods, M. H. (1979): "Alpha-particle-induced soft errors in dynamic memories. *IEEE Transactions on Electron Devices*, Volume: 26 , Issue: 1
- Mekala H. R., Sai J and Nayakanti V. P. (2016): Evolution of Mobile Networks: From 1G to 4G. *Advanced Research in Electrical and Electronic Engineering*, Volume 3, Issue 4, pp. 307-310
- Mimoza I, Enver H, Luan A, Rreze H, Besa D. (2017): *Comparative Analysis of Downlink Signal Levels Emitted by GSM 900, GSM 1800, UMTS, and LTE Base Stations*. 16th Annual Mediterranean Ad Hoc Networking Workshop, Budva, 2017, pp. 1-5. Doi:10.1109/MedHocNet.2017.8001655
- Moulder, J. E. (2007): Static Electric and Magnetic Fields and Human Health *American Journal of Industrial Medicine*. 50:227e33
- Mushiake, Y (1999): Log-Periodic Structure Provides no broad-band property for antennas. *Journal of The Institute of Electronics, Information and Communication Engineers*, Vol. 82, No. 5, pp. 510-511
- National Communication Authority (2011): *Press Release*. Retrived from <http://www.nca.org.gh/Download-Documents.html>
- Neto, J and Yang, Y. and Glover, I. (2010): *Plausibility of practical low-cost location using wsn path-loss law inversion*. International conference on Wireless Sensor Network. University of Huddersfield
- Nicola Green and Leslie Haddon (2009): *Mobile Communications: An Introduction to New Media*. 1st edition, Berg,Oxford, New York.

- Ochala, I and Okeme, I.C (2011): Design and Implementation of a High-Gain Compound Yagi Antenna. *Journal of Advances in Applied Science Research*, 2 (6):41-50
- Okene E. D. and Okhueleigbe E.I. (2017): Roadmap and Challenges to the Deployment of 4g Lte Network: The Nigerian Experience. *American Journal of Networks and Communications*. Vol. 6, No. 5, 2017, pp. 74-78
- Okumura, Y., Ohmori, E., Kawano, T., and Fukuda, K. (1968): Field strength and its variability in VHF and UHF land-mobile radio service. *Rev. Elec. Commun. Lab*, 16(9):825–73.
- Pabari, J. P., Acharya, Y. B., Desai, U. B., Merchant, S. N., Krishna, B. G. (2010): Radio Frequency Modelling for Future Wireless Sensor Network on Surface of the Moon. *Int. J. Communications, Network and System Sciences*, 395-401
- Pande, M., Choudhari, N., and Pathak, S. (2012): Energy efficient hybrid architecture and positioning of sensors in wsn for precision agriculture. *In Proceedings of the CUBE International Information Technology Conference*, pages 198–203. ACM.
- Parsons, J. D. (2000): *The mobile radio propagation channel*. 2nd edition John Wiley and Sons, New York.
- Pattanaik S (2012): Biological effects of RF/ MW radiations on human. *Journal of Applied Science Research*, 4 (1):381-387

- Petersen, J. K. (2002): *The telecommunications illustrated dictionary*. CRC Press, U.S.A
- Purcell E. M. (2011): *Electricity and Magnetism*, 2nd edition Cambridge University Press, New York.
- Purcell E. M. and Morin D. J. (2013): *Electricity and Magnetism*, 3rd edition. Cambridge University Press, New York.
- Rappaport Theodore S. (2002): *Wireless Communications: Principles and practice*, 2nd Edition. Prentice-Hall, U.S
- Sesia S, Toufik I. and Baker M (2011): *LTE-The UTMS long term evolution, from theory to practice*. 2nd edition, John Wiley and Sons, New York.
- Sharmila (2015): A Review of Wireless Mobile Technology. *International Journal of Science and Research*, Volume 5 Issue 11.
- Singh R. K. (2016): 4G LTE Cellular Technology: Network Architecture and Mobile Standards. *International Journal of Emerging Research in Management and Technology*, Volume-5, Issue-12
- Simon R. Saunders and Alejandro Aragon-Zavala (2007): *Antennas and propagation for wireless communication systems*. 2nd edition, John Wiley and Sons, New York.
- Seybold J. S. (2005): *Introduction to RF Propagation*. John Wiley and Sons, New York.

- Sreedhar K. V. S. (2014): Antennas. *International Journal of Engineering Inventions* Volume 3, 2319-6491.
- Stutzman W. L. and Thiele G. A. (2012): *Antenna Theory and Design*. 3rd edition, John Wiley and Sons, New York.
- Sudesh R. A, Kshitij A. Land Amit A. D (2015): Review on Printed Log Periodic and Yagi MSA. *International Journal of Computer*. Volume 126 – No.8
- Tara A.Y. (2011): Understanding LTE and its performance. *International Journal of Communication Networks and Information Security*. Vol. 9, No. 1.
- Tipler P. A. (1999): *Physics for Scientists and Engineers: Vol. 1: Mechanics, Oscillations and Waves, Thermodynamics*. MacMillan U.S.
- Vladimir N. B and Prato F S. (2017): Biological effects of the hypomagnetic field: An analytical review of experiments and theories. *Journal of PLoS One*, 12 (6): e0179340.
- Weltner K, Grosjean J., Schuster P., and Weber W.J. (1986): *Mathematics for Engineers and Scientists*. Nelson Thornes Ltd, UK
- Willis S. L and Kikkert C. J. (2005): Radio propagation model for long-range ad hoc wireless sensor network. In wireless networks, communication and mobile computing. 2005 *International conference Wireless Networks, Communications and Mobile Computing*, volume 1 pages 826-832. IEEE.

Woodside G. (1997): *Environmental, Safety, and Health Engineering*. US: John Wiley and Sons, New York.

Xuart S.T., Ziolkowski R. W and Park I. (2015): Crossed Dipole Antennas: A review. *IEEE Antennas and Propagation Magazine*, 57(5), 107-122.

APPENDICES

APPENDIX 1A: GREATER ACCRA REGION; ELECTRIC FIELD STRENGTH AND POWER DENSITIES.

SITE	ELECT. FIELD ST. (MIN)	ELECT. FIELD ST. (MEAN)	ELECT. FIELD ST. (MAX)	POWER DENSITY (MIN)	POWER DENSITY (MEAN)	POWER DENSITY (MAX)
1	2.23E-10±2.3E-11	3.89E-09±3.89E-10	8.04E-09±8.04E-10	8.95E-10	1.56E-08	3.23E-08
2	4.74E-10±4.74E-11	3.22E-09±3.22E-10	5.73E-09±5.73E-10	1.90E-09	1.29E-08	2.30E-08
3	1.81E-10±1.81E-11	7.88E-10±7.88E-11	2.20E-09±2.20E-10	7.27E-10	3.16E-09	8.82E-09
4	6.17E-08±6.17E-09	1.14E-06±1.14E-07	5.07E-06±5.07E-07	2.48E-07	4.59E-06	2.04E-05
5	1.85E-07±1.85E-08	6.37E-07±6.37E-08	1.47E-06±1.47E-08	7.42E-07	2.55E-06	5.88E-06
6	8.10E-10±8.10E-11	1.24E-09±1.24E-10	1.69E-09±1.69E-10	3.25E-09	4.99E-09	6.79E-09
7	3.02E-10±3.02E-11	5.33E-09±5.33E-10	1.36E-08±1.36E-09	1.21E-09	2.14E-08	5.44E-08
8	1.70E-10±1.70E-11	3.71E-10±3.71E-11	7.54E-10±7.54E-11	6.82E-10	1.49E-09	3.02E-09
9	8.40E-10±8.40E-11	3.26E-09±3.26E-10	5.07E-09±5.07E-10	3.37E-09	1.31E-08	2.04E-08
10	8.68E-09±8.68E-10	9.68E-09±9.68E-10	1.07E-08±1.07E-09	3.48E-08	3.88E-08	4.28E-08
11	4.53E-08±4.53E-09	7.05E-07±7.05E-08	2.40E-06±2.40E-07	1.28E-06	2.83E-06	9.61E-06
12	3.52E-08±3.52E-09	1.17E-06±1.17E-07	2.34E-06±2.34E-07	1.41E-07	4.71E-06	9.37E-06
13	7.12E-08±7.12E-09	1.04E-06±1.04E-07	3.32E-06±3.32E-07	2.86E-07	4.19E-06	1.33E-05
14	8.62E-09±8.62E-10	9.02E-09±9.02E-10	9.89E-09±9.89E-10	3.46E-08	3.62E-08	3.97E-08
15	3.02E-10±3.02E-11	4.34E-10±4.34E-11	6.33E-10±6.33E-11	1.21E-09	1.74E-09	2.54E-09
16	9.51E-08±9.51E-09	1.20E-06±1.20E-07	4.38E-06±4.38E-07	3.82E-07	4.79E-06	1.76E-05
17	2.00E-09±2.00E-10	7.82E-08±7.82E-09	3.10E-07±3.10E-08	6.85E-09	3.14E-07	1.24E-06
18	1.36E-08±1.36E-09	2.11E-07±2.11E-08	5.06E-07±5.06E-08	5.45E-08	8.45E-07	2.03E-06
19	9.51E-09±9.51E-10	1.11E-08±1.11E-09	1.27E-08±1.27E-09	3.82E-08	4.46E-08	5.08E-08
20	2.01E-10±2.01E-11	1.67E-09±1.67E-10	7.08E-09±7.08E-10	8.05E-10	6.72E-09	2.84E-08
21	8.48E-09±8.48E-10	1.02E-08±1.02E-09	1.16E-08±1.16E-09	3.40E-08	4.08E-08	4.67E-08
22	1.18E-08±1.18E-09	1.84E-07±1.84E-08	4.83E-07±4.83E-08	4.75E-08	7.39E-07	1.94E-06
23	9.49E-09±9.49E-10	1.14E-08±1.14E-09	1.21E-08±1.21E-09	3.81E-08	4.56E-08	4.88E-08
24	9.89E-09±9.89E-10	1.10E-08±1.10E-09	1.24E-08±1.24E-09	3.97E-08	4.40E-08	4.96E-08
25	9.36E-09±9.36E-10	1.07E-08±1.07E-09	1.25E-08±1.25E-09	3.76E-08	4.31E-08	5.00E-08
26	9.23E-08±9.23E-09	8.54E-07±8.54E-08	2.57E-06±2.57E-07	3.70E-07	3.43E-06	1.03E-05
27	5.97E-08±5.97E-09	4.47E-07±4.47E-08	7.95E-07±7.95E-08	2.40E-07	1.79E-06	3.19E-06
28	3.94E-10±3.94E-11	1.22E-09±1.22E-10	2.27E-09±2.27E-10	1.58E-09	4.89E-09	9.11E-09
29	1.25E-07±1.25E-08	5.32E-06±5.32E-07	1.04E-05±1.04E-06	5.02E-07	2.14E-05	4.17E-05
30	8.23E-09±8.23E-10	2.26E-07±2.26E-08	1.04E-06±1.04E-07	3.30E-08	9.07E-07	4.16E-06
31	9.94E-09±9.94E-10	1.12E-08±1.12E-09	1.35E-08±1.35E-09	3.89E-08	4.39E-08	5.28E-08
32	1.15E-08±1.15E-09	1.27E-08±1.27E-09	1.36E-08±1.36E-09	4.52E-08	4.97E-08	5.30E-08
33	1.00E-08±1.00E-09	1.12E-08±1.12E-09	1.24E-08±1.24E-09	3.91E-08	4.39E-08	4.84E-08
34	5.40E-11±5.40E-12	1.23E-09±1.23E-10	2.28E-09±2.28E-10	2.11E-10	4.82E-09	8.91E-09
35	7.02E-08±7.02E-09	4.10E-07±4.10E-08	1.08E-06±1.08E-07	2.75E-07	1.60E-06	4.21E-06
36	5.14E-11±5.14E-12	1.97E-10±1.97E-11	2.91E-10±2.91E-11	2.01E-10	7.69E-10	1.14E-09
37	7.22E-11±7.22E-12	8.37E-10±8.37E-11	1.36E-09±1.36E-10	2.90E-10	3.36E-09	5.44E-09
38	1.49E-09±1.49E-10	1.27E-08±1.27E-09	3.58E-08±3.58E-09	5.99E-09	5.08E-08	1.44E-07
39	1.23E-07±1.23E-08	8.64E-07±8.64E-08	1.88E-06±1.88E-07	4.94E-07	3.47E-06	7.53E-06
40	5.65E-06±5.65E-07	8.30E-06±8.30E-07	1.17E-05±1.17E-06	2.27E-05	3.33E-05	4.71E-05
41	1.10E-09±1.10E-10	2.56E-08±2.56E-09	9.30E-08±9.30E-09	4.43E-09	1.03E-07	3.73E-07
42	2.77E-11±2.77E-12	1.41E-09±1.41E-10	5.14E-09±5.14E-10	1.11E-10	5.64E-09	2.06E-08
43	3.52E-08±3.52E-09	2.30E-06±2.30E-07	7.33E-06±7.33E-07	1.41E-07	9.24E-06	2.94E-05
44	4.21E-09±4.21E-10	8.05E-08±8.05E-09	2.36E-07±2.36E-08	1.69E-08	3.23E-07	9.48E-07
45	3.09E-09±3.09E-10	1.30E-08±1.30E-09	3.74E-08±3.74E-09	1.24E-08	5.22E-08	1.50E-07
46	3.85E-11±3.85E-12	1.42E-10±1.42E-11	3.14E-10±3.14E-11	1.54E-10	5.68E-10	1.26E-09
47	2.53E-11±2.53E-12	2.82E-10±2.82E-11	9.02E-10±9.02E-11	1.02E-10	1.13E-09	3.62E-09
48	7.63E-10±7.63E-11	7.53E-08±7.53E-09	3.34E-07±3.34E-08	3.06E-09	3.02E-07	1.34E-06

SITE	ELECT. FIELD ST. (MIN)	ELECT. FIELD ST. (MEAN)	ELECT. FIELD ST. (MAX)	POWER DENSITY (MIN)	POWER DENSITY (MEAN)	POWER DENSITY (MAX)
49	1.44E-10±1.44E-11	2.72E-09±2.72E-10	7.23E-09±7.23E-10	5.78E-10	1.09E-08	2.90E-08
50	3.09E-08±3.09E-09	2.34E-07±2.34E-08	5.54E-07±5.54E-08	1.24E-07	9.37E-07	2.22E-06

APPENDIX 1B: ASHANTI REGION; ELECTRIC FIELD STRENGTH AND POWER DENSITIES.

SITE	ELECT. FIELD ST. (MIN)	ELECT. FIELD ST. (MEAN)	ELECT. FIELD ST. (MAX)	POWER DENSITY (MIN)	POWER DENSITY (MEAN)	POWER DENSITY (MAX)
1	6.72E-09±6.72E-10	2.11E-08±2.11E-09	4.16E-08±4.16E-09	2.70E-08	8.47E-08	1.67E-07
2	4.58E-08±4.58E-09	7.09E-06±7.09E-07	1.58E-05±1.58E-06	1.84E-07	2.84E-05	6.35E-05
3	1.17E-06±1.17E-07	2.34E-06±2.34E-07	3.10E-06±3.10E-07	4.71E-06	9.39E-06	1.24E-05
4	4.68E-11±4.68E-12	9.52E-10±9.52E-11	2.30E-09±2.30E-10	1.88E-10	3.82E-09	9.24E-09
5	6.64E-09±6.64E-10	5.21E-08±5.21E-09	8.44E-08±8.44E-09	2.66E-08	2.09E-07	3.39E-07
6	9.58E-11±9.58E-12	2.33E-10±2.33E-11	4.15E-10±4.15E-11	3.84E-10	9.33E-10	1.67E-09
7	1.04E-10±1.04E-11	6.14E-10±6.14E-11	1.09E-09±1.09E-10	4.18E-10	2.46E-09	4.37E-09
8	1.49E-10±1.49E-11	8.96E-09±8.96E-10	3.88E-08±3.88E-09	5.97E-10	3.59E-08	1.56E-07
9	1.17E-07±1.17E-08	1.78E-06±1.78E-07	4.03E-06±4.03E-07	4.68E-07	7.16E-06	1.62E-05
10	3.68E-09±3.68E-10	2.80E-08±2.80E-09	5.95E-08±5.95E-09	1.48E-08	1.12E-07	2.39E-07
11	3.83E-07±3.83E-08	1.23E-05±1.23E-06	3.80E-05±3.80E-06	1.54E-06	4.93E-05	1.52E-04
12	8.68E-11±8.68E-12	4.03E-10±4.03E-11	8.76E-10±8.76E-11	3.48E-10	1.61E-09	3.51E-09
13	6.69E-11±6.69E-12	4.87E-09±4.87E-10	1.75E-08±1.75E-09	2.68E-10	1.96E-08	7.01E-08
14	5.20E-09±5.20E-10	9.67E-07±9.67E-08	3.81E-06±3.81E-07	2.09E-08	3.88E-06	1.53E-05
15	7.66E-11±7.66E-12	2.69E-09±2.69E-10	8.44E-09±8.44E-10	3.07E-10	1.08E-08	3.39E-08
16	2.53E-08±2.53E-09	4.71E-06±4.71E-07	1.52E-05±1.52E-06	1.02E-07	1.89E-05	6.10E-05
17	1.16E-09±1.16E-10	2.15E-06±2.15E-07	7.44E-06±7.44E-07	4.65E-09	8.62E-06	2.98E-05
18	7.50E-09±7.50E-10	2.66E-06±2.66E-07	6.03E-06±6.03E-07	3.01E-08	1.07E-05	2.41E-05
19	6.14E-09±6.14E-10	1.14E-06±1.14E-07	5.07E-06±5.07E-07	2.46E-08	4.56E-06	2.04E-05
20	1.63E-08±1.63E-09	3.20E-07±3.20E-08	8.40E-07±8.40E-08	6.56E-08	1.29E-06	3.37E-06
21	8.12E-09±8.12E-10	2.58E-08±2.58E-09	7.33E-08±7.33E-09	8.97E-09	1.03E-07	2.94E-07
22	5.59E-11±5.59E-12	2.34E-09±2.34E-10	5.60E-09±5.60E-10	2.24E-10	9.37E-09	2.25E-08
23	1.43E-11±1.43E-12	1.46E-10±1.46E-11	4.46E-10±4.46E-11	5.74E-11	5.86E-10	1.79E-09
24	1.27E-06±1.27E-07	6.95E-06±6.95E-07	1.27E-05±1.27E-06	5.08E-06	2.79E-05	5.10E-05
25	2.68E-07±2.68E-08	7.53E-06±7.53E-07	2.81E-05±2.81E-06	1.08E-06	3.04E-05	1.13E-04
26	2.60E-09±2.60E-10	2.10E-08±2.10E-09	5.30E-08±5.30E-09	1.04E-08	8.41E-08	2.13E-07
27	3.78E-10±3.78E-11	4.76E-10±4.76E-11	6.99E-10±6.99E-11	1.52E-09	1.91E-09	2.80E-09
28	7.25E-10±7.25E-11	1.82E-08±1.82E-09	5.10E-08±5.10E-09	2.91E-09	7.29E-08	2.04E-07
29	5.65E-09±5.65E-10	2.57E-08±2.57E-09	5.40E-08±5.40E-09	2.27E-08	1.03E-07	2.17E-07
30	2.28E-07±2.28E-08	2.34E-06±2.34E-07	7.47E-06±7.47E-07	9.13E-07	9.39E-06	3.00E-05
31	1.57E-08±1.57E-09	9.42E-08±9.42E-09	1.54E-07±1.54E-08	6.30E-08	3.78E-07	6.19E-07
32	3.37E-10±3.37E-11	4.41E-10±4.41E-11	5.35E-10±5.35E-11	1.35E-09	1.77E-09	2.15E-09
33	4.66E-07±4.66E-08	1.76E-06±1.76E-07	5.95E-06±5.95E-07	8.70E-07	7.06E-06	2.39E-05

SITE	ELECT. FIELD ST. (MIN)	ELECT. FIELD ST. (MEAN)	ELECT. FIELD ST. (MAX)	POWER DENSITY (MIN)	POWER DENSITY (MEAN)	POWER DENSITY (MAX)
34	3.76E-10±3.76E-11	4.28E-10±4.28E-11	4.69E-10±4.69E-11	1.51E-09	1.72E-09	1.88E-09
35	4.67E-10±4.67E-11	3.00E-09±3.00E-10	5.96E-09±5.96E-10	1.87E-09	1.20E-08	2.39E-08
36	1.83E-08±1.83E-09	9.41E-08±9.41E-09	3.19E-07±3.19E-08	1.00E-07	3.78E-07	1.28E-06
37	3.56E-10±3.56E-11	3.56E-09±3.56E-10	7.59E-09±7.59E-10	1.43E-09	1.43E-08	3.05E-08
38	9.07E-08±9.07E-09	5.83E-06±5.83E-07	1.87E-05±1.87E-06	3.55E-07	2.28E-05	7.32E-05
39	6.07E-09±6.07E-10	4.53E-07±4.53E-08	1.43E-06±1.43E-07	2.44E-08	1.82E-06	5.75E-06
40	9.30E-07±9.30E-08	7.57E-06±7.57E-07	1.83E-05±1.83E-06	3.73E-06	3.04E-05	7.32E-05
41	5.98E-10±5.98E-11	2.41E-09±2.41E-10	6.20E-09±6.20E-10	2.34E-09	9.48E-09	2.42E-08
42	7.33E-10±7.33E-11	1.68E-09±1.68E-10	2.84E-09±2.84E-10	2.94E-09	6.75E-09	1.14E-08
43	1.40E-08±1.40E-09	7.20E-08±7.20E-09	1.76E-07±1.76E-08	5.63E-08	2.89E-07	7.06E-07
44	3.68E-10±3.68E-11	4.79E-10±4.79E-11	8.08E-10±8.08E-11	1.48E-09	1.92E-09	3.24E-09
45	3.80E-10±3.80E-11	4.07E-10±4.07E-11	4.36E-10±4.36E-11	1.53E-09	1.63E-09	1.75E-09
46	3.98E-10±3.98E-11	2.96E-09±2.96E-10	7.37E-09±7.37E-10	1.60E-09	1.19E-08	2.96E-08
47	8.88E-10±8.88E-11	7.13E-09±7.13E-10	2.89E-08±2.89E-09	3.56E-09	2.86E-08	1.16E-07
48	8.88E-10±8.88E-11	7.13E-09±7.13E-10	2.89E-08±2.89E-09	3.56E-09	2.86E-08	1.16E-07
49	4.91E-09±4.91E-10	5.68E-08±5.68E-09	1.54E-07±1.54E-08	1.97E-08	2.28E-07	6.19E-07
50	5.24E-10±5.24E-11	2.82E-09±2.82E-10	6.78E-09±6.78E-10	2.10E-09	1.13E-08	2.72E-08

APPENDIX 1C: WESTERN REGION; ELECTRIC FIELD STRENGTH AND POWER DENSITIES.

SITE	ELECT. FIELD ST. (MIN)	ELECT. FIELD ST. (MEAN)	ELECT. FIELD ST. (MAX)	POWER DENSITY (MIN)	POWER DENSITY (MEAN)	POWER DENSITY (MAX)
1	1.64E-11±1.64E-12	1.82E-11±1.82E-12	2.07E-11±2.07E-12	6.57E-11	7.32E-11	8.29E-11
2	2.00E-11±2.00E-12	2.29E-11±2.29E-12	2.62E-11±2.62E-12	8.03E-11	9.18E-11	1.05E-10
3	2.13E-09±2.13E-10	1.36E-07±1.36E-08	4.60E-07±4.60E-08	8.56E-09	5.47E-07	1.84E-06
4	3.41E-10±3.41E-11	3.69E-10±3.69E-11	4.13E-10±4.13E-11	1.37E-09	1.48E-09	1.66E-09
5	3.56E-10±3.56E-11	4.34E-10±4.34E-11	4.94E-10±4.94E-11	1.43E-09	1.74E-09	1.98E-09
6	2.55E-10±2.55E-11	2.50E-09±2.50E-10	5.79E-09±5.79E-10	1.02E-09	1.00E-08	2.32E-08
7	9.17E-12±9.17E-13	1.41E-11±1.41E-12	2.98E-11±2.98E-12	3.68E-11	5.67E-11	1.20E-10
8	1.50E-09±1.50E-10	2.54E-07±2.54E-08	1.20E-06±1.20E-07	6.02E-09	1.02E-06	4.82E-06
9	4.86E-09±4.86E-10	4.52E-07±4.52E-08	1.97E-06±1.97E-07	1.95E-08	1.81E-06	7.90E-06
10	7.30E-10±7.30E-11	4.37E-09±4.37E-10	8.30E-09±8.30E-10	2.93E-09	1.75E-08	3.33E-08
11	1.06E-09±1.06E-10	3.04E-09±3.04E-10	6.60E-09±6.60E-10	4.26E-09	1.22E-08	2.65E-08
12	3.58E-10±3.58E-11	3.95E-10±3.95E-11	4.16E-10±4.16E-11	1.43E-09	1.58E-09	1.67E-09
13	3.85E-10±3.85E-11	1.20E-09±1.20E-10	2.60E-09±2.60E-10	1.54E-09	4.80E-09	1.04E-08
14	4.83E-10±4.83E-11	2.12E-07±2.12E-08	8.30E-07±8.30E-08	1.49E-09	8.49E-07	3.33E-06

SITE	ELECT. FIELD ST. (MIN)	ELECT. FIELD ST. (MEAN)	ELECT. FIELD ST. (MAX)	POWER DENSITY (MIN)	POWER DENSITY (MEAN)	POWER DENSITY (MAX)
15	3.71E-10±3.71E-11	4.28E-10±4.28E-11	5.13E-10±5.13E-11	1.49E-09	1.72E-09	2.06E-09
16	1.12E-09±1.12E-10	1.33E-07±1.33E-08	5.71E-07±5.71E-08	4.50E-09	5.33E-07	2.29E-06
17	1.10E-08±1.10E-09	1.55E-07±1.55E-08	6.04E-07±6.04E-08	4.42E-08	6.21E-07	2.42E-06
18	9.54E-12±9.54E-13	6.65E-11±6.65E-12	1.38E-10±1.38E-11	3.83E-11	2.67E-10	5.54E-10
19	8.52E-12±8.52E-13	9.05E-12±9.05E-13	9.87E-12±9.87E-13	3.42E-11	3.63E-11	3.96E-11
20	8.98E-12±8.98E-13	9.83E-12±9.83E-13	1.05E-11±1.05E-12	3.60E-11	3.94E-11	4.20E-11
21	3.37E-10±3.37E-11	4.13E-10±4.13E-11	5.42E-10±5.42E-11	1.35E-09	1.66E-09	2.18E-09
22	7.75E-12±7.75E-13	9.49E-12±9.49E-13	1.04E-11±1.04E-12	3.11E-11	3.81E-11	4.16E-11
23	2.19E-10±2.19E-11	6.63E-10±6.63E-11	1.28E-09±1.28E-10	8.80E-10	2.66E-09	5.12E-09
24	2.93E-10±2.93E-11	3.57E-10±3.57E-11	4.77E-10±4.77E-11	1.18E-09	1.43E-09	1.91E-09
25	1.32E-11±1.32E-12	3.32E-10±3.32E-11	5.42E-10±5.42E-11	5.29E-11	1.33E-09	1.65E-09
26	3.49E-10±3.49E-11	4.11E-10±4.11E-11	4.61E-10±4.61E-11	1.40E-09	1.65E-09	1.85E-09
27	2.12E-11±2.12E-12	2.30E-11±2.30E-12	2.53E-11±2.53E-12	8.49E-11	9.23E-11	1.01E-10
28	1.86E-11±1.86E-12	2.17E-11±2.17E-12	2.38E-11±2.38E-12	7.48E-11	8.69E-11	9.54E-11
29	2.03E-11±2.03E-12	2.14E-11±2.14E-12	2.27E-11±2.27E-12	8.14E-11	8.57E-11	9.09E-11
30	2.04E-11±2.04E-12	2.41E-11±2.41E-12	2.65E-11±2.65E-12	8.18E-11	9.65E-11	1.06E-10
31	2.39E-11±2.39E-12	2.52E-11±2.52E-12	2.64E-11±2.64E-12	9.59E-11	1.01E-10	1.06E-10
32	1.96E-11±1.96E-12	2.18E-11±2.18E-12	2.47E-11±2.47E-12	7.88E-11	8.75E-11	9.90E-11
33	1.85E-11±1.85E-12	2.40E-11±2.40E-12	3.33E-11±3.33E-12	7.41E-11	9.65E-11	1.34E-10
34	1.94E-11±1.94E-12	2.43E-11±2.43E-12	3.87E-11±3.87E-12	7.79E-11	9.74E-11	1.55E-10
35	1.76E-09±1.76E-10	3.62E-09±3.62E-10	8.04E-09±8.04E-10	7.04E-09	1.45E-08	3.23E-08
36	3.77E-10±3.77E-11	1.99E-09±1.99E-10	4.02E-09±4.02E-10	1.51E-09	7.98E-09	1.61E-08
37	3.68E-09±3.68E-10	4.70E-08±4.70E-09	2.06E-07±2.06E-08	1.47E-08	1.88E-07	8.27E-07
38	7.68E-12±7.68E-13	4.88E-10±4.88E-11	1.53E-09±1.53E-10	3.08E-11	1.96E-09	6.12E-09
39	3.40E-10±3.40E-11	3.77E-10±3.77E-11	4.68E-10±4.68E-11	1.31E-09	1.51E-09	1.88E-09
40	2.45E-11±2.45E-12	2.59E-10±2.59E-11	9.92E-10±9.92E-11	9.81E-11	1.04E-09	3.98E-09
41	3.87E-10±3.87E-11	4.25E-07±4.25E-08	1.83E-06±1.83E-07	1.55E-09	1.70E-06	7.36E-06
42	1.21E-08±1.21E-09	4.93E-08±4.93E-09	1.08E-07±1.08E-08	4.84E-08	1.98E-07	4.33E-07
43	2.08E-09±2.08E-10	2.38E-07±2.38E-08	9.47E-07±9.47E-08	8.35E-09	9.57E-07	3.80E-06
44	3.68E-10±3.68E-11	3.97E-10±3.97E-11	4.54E-10±4.54E-11	1.20E-09	1.59E-09	1.82E-09
45	1.52E-08±1.52E-09	7.86E-08±7.86E-09	2.04E-07±2.04E-08	6.10E-08	3.15E-07	8.20E-07
46	3.58E-10±3.58E-11	3.93E-10±3.93E-11	4.27E-10±4.27E-11	1.43E-09	1.58E-09	1.71E-09

SITE	ELECT. FIELD ST. (MIN)	ELECT. FIELD ST. (MEAN)	ELECT. FIELD ST. (MAX)	POWER DENSITY (MIN)	POWER DENSITY (MEAN)	POWER DENSITY (MAX)
47	4.99E-10±4.99E-11	1.59E-08±1.59E-09	4.51E-08±4.51E-09	2.00E-09	6.36E-08	1.81E-07
48	1.29E-08±1.29E-09	2.85E-08±2.85E-09	5.65E-08±5.65E-09	5.18E-08	1.14E-07	2.27E-07
49	2.39E-10±2.39E-11	1.63E-07±1.63E-08	8.06E-07±8.06E-08	1.70E-09	6.55E-07	3.23E-06
50	1.30E-10±1.30E-11	1.40E-09±1.40E-10	6.13E-09±6.13E-10	5.21E-10	5.61E-09	2.46E-08

APPENDIX 2A: SITES WHERE MEASUREMENTS WERE TAKEN IN GREATER ACCRA REGION

SITE	TOWER NAME	LATITUDE	LONGITUDE
1	37 Military Hospital	5.59	-0.183056
2	Abelemkpe	5.61084	-0.22026
3	Adabraka_3	5.56258333	-0.21461111
4	Adenta_1	5.710996	-0.170968
5	Agbogba_2	5.70238	-0.18697
6	Agyiriganor	5.65192	-0.12515
7	Airport_1	5.60886	-0.18099757
8	Airpot_West	5.61838	-0.18126
9	Ashiyie	5.74683	-0.15053
10	Ashongman_3	5.69737	-0.23109
11	Ashonmang_4	5.70725	-0.22612
12	Asly_Botwe	5.68436	-0.13888
13	Cantonment_3	5.58405	-0.16459
14	Cantonments_4	5.57608	-0.179
15	Dome_2	5.64276	-0.23721
16	East Legon_1	5.642	-0.16024
17	East_Legon_3	5.64027778	-0.13658333
18	Emef_Estate Mataheko	5.75398	0.00321
19	EPP_Books	5.54771	-0.2045
20	GBC	5.58262	-0.18879
21	Geowas	5.54811	-0.21294
22	Haatso_2	5.67585	-0.20685
23	Kanda	5.58628	-0.19075
24	Kingdom_Bks	5.55392	-0.18754
25	Kokomlemle_3	5.57693	-0.20445
26	Kokomlemle_4	5.574722	-0.212222
27	Kotobabi_2	5.59927	-0.20601
28	Kwabanya_4	5.69962778	-0.25200556
29	Lashibi_2	5.63226	-0.07446

SITE	TOWER NAME	LATITUDE	LONGITUDE
30	Madina_Esta	5.6693055	-0.1558888
31	Makola	5.54529	-0.20706
32	Mamobi_2	5.59285	-0.196799
33	Mamobi_2	5.59418	-0.19357
34	Nungua_Boade	5.61575	-0.0862
35	New_Achimota	5.62425	-0.23561
36	Nun_Adogon	5.61069444	-0.088
37	Nungu_Barie	5.61672222	-0.0770277
38	Nungua 4	5.593247222	-0.078811111
39	Regimanuel	5.626472	-0.125972
40	Sakomono	5.62943	-0.06061
41	Sakomono_2	5.62038	-0.0681
42	Sakumono_4	5.614417	-0.053667
43	Tebiibiano	5.59688	-0.12118
44	Tem_Com_2C	5.63225	-0.00535
45	Tema_Com_20	5.65734	-0.07495
46	Tem_Kpone_Rd	5.677469	-0.027385
47	T_Industry_4	5.679444	-0.001389
48	Tema_Com1_C	5.65052	-0.0020616
49	Tema_Office	5.65563	-0.00874
50	University	5.649001	-0.198365

APPENDIX 2B: SITES WHERE MEASUREMENTS WERE TAKEN IN ASHANTI REGION

SITE	TOWER NAME	LATITUDE	LONGITUDE
1	Aboabo_3	6.69965	-1.60328
2	Adako_Jachi	6.72837	-1.50935
3	Adukrom_Ksi	6.70241	-1.58624
4	Ahenbrunum	6.73244	-1.61839
5	Akaporiso	6.19811	-1.62697
6	Anwomaso	6.68626	-1.53077
7	Atimatim	6.76971175	-1.610332
8	Ayiduase_2	6.67907	-1.5484
9	Ayigya_2	6.69086	-1.57234
10	Ayigya_3	6.68909	-1.57865
11	Ayigya	6.69706	-1.57949
12	Bekwai_2	6.45324	-1.58025
13	Bremang	6.73579	-1.63668
14	Bremang UGC2	6.75038	-1.63128
15	Kronum	6.75511111	-1.638

SITE	TOWER NAME	LATITUDE	LONGITUDE
16	Bomso	6.68192	-1.58182
17	Buoho	6.79405435	-1.641385
18	Buokrom_4	6.72591	-1.59792
19	Deduako	6.65545	-1.54674
20	Emena	6.67077	-1.54285
21	Kum_Academy	6.71163	-1.56032
22	Mampong	7.06323	-1.40602
23	Meduma_2	6.76753	-1.58641
24	Mosizngo2	6.71844444	-1.601722
25	Mossi_Zongo	6.72536111	-1.60503
26	Abuakwa_3	6.69266	-1.71814
27	Adum_4	6.6895	-1.620556
28	Adwoato	6.70726	-1.64653
29	ejisu_4	6.7285	-1.47852
30	ash_kenyase	6.7467	-1.5552
31	Apire	6.6558	-1.65836
32	Atwima_Kdua	6.74916	-1.75437
33	Bohyen	6.72434	-1.65659
34	Bonsaaso	6.2425	-1.99229
35	Central_Mkt	6.69439	-1.62005
36	Danyame	6.677889	-1.632722
37	Kdso_Wamasi	6.6624167	-1.664833
38	Kejetia	6.70155	-1.62344
39	Kromuse	6.6683888	-1.680111
40	Kwada_Agric	6.67222222	-1.658944
41	Kwadaso	6.70264	-1.65836
42	Kwadaso_3	6.69014	-1.66522
43	Kwadaso_5	6.70112	-1.65171
44	Kwadaso_Stp	6.69313	-1.66046
45	Nwinim_NO1	6.57831	-1.79291
46	Odumasi_Ob	6.16375	-1.654944
47	Suame_3	6.71457	-1.62952
48	Tafo_Hosptl	6.72414	-1.61246
49	Tafo_School	6.74197	-1.60931
50	Tafo_Zongo	6.73091	-1.61243

APPENDIX 2C: SITES WHERE MEASUREMENTS WERE TAKEN IN WESTERN REGION

SITE	TOWER NAME	LATITUDE	LONGITUDE
1	Boinso	5.55472	-2.7264
2	DaTanuo	6.3141	-2.8707
3	Assakae	4.93354	-1.80037
4	Awaso	6.2296	-2.2691
5	Axim_3	4.87436111	-2.2040389
6	Half_Asin_2	5.0526	-2.87929
7	Jewi_Wharf	5.086	-2.9393
8	Ketan	4.95674	-1.73704
9	Kwesimtm_SS	4.9218	-1.7932
10	Kwsimntm_2	4.93546944	-1.7915806
11	Ntakoful	4.95041944	-1.7595889
12	Nzma_Akropn	5.07618889	-2.2946111
13	Sek_Navy_SS	4.93531111	-1.74025
14	Skondi_Rige	4.94859	-1.72512
15	Takoradi 6	4.87863889	-1.7652389
16	Takradi_SS	4.9217	-1.765322
17	Windy_Ridge	4.90725	-1.7605833
18	Aboadze_2	4.98506111	-1.6392611
19	Adabokrom	6.82166667	-3.0191667
20	Akwidaa	4.76092	-2.03408
21	Anagye	4.90374	-2.11665
22	Anhwiaso	6.33172222	-2.2562778
23	Bibiani_4	6.4424	-2.3121
24	Bibiani_5	6.3369	-2.2713
25	Sefi_Awaso	6.2468	-2.2876
26	SefwiI_Merwa	6.2882	-2.13635
27	Mumuni	5.48718	-2.46679
28	Nsuopun	5.86231944	-1.9855194
29	Punikrom	6.32249	-2.50431
30	Sfwi_Bkwi_3	6.19351111	-2.3271111
31	Sfwi_Bkwi_4	6.20278889	-2.3277194
32	Sefwi_Camp	6.35201	-2.54365
33	Wsa_Dadso_2	5.87401111	-2.0552389
34	Wassa_Dunkwa	5.77427	-2.53815
35	Akango	5.0347	-2.234183
36	Apollo	4.90532	-1.79619
37	Atieku	5.56844444	-1.6930833
38	Bensu_Subrinso	5.2074	-1.8854
39	Ekumfo_eku	5.026	-1.6872222
40	Ituma_3	5.0713	-1.6568

SITE	TOWER NAME	LATITUDE	LONGITUDE
41	Bogoso	5.51293	-2.05705
42	Bondaye	5.39968	-2.16964
43	Bonsu_Konta	6.31945	-3.01743
44	Kwafukaa	6.28416	-2.74362
45	New_Yakasi	5.79781	-2.85865
46	Sureso	5.73591	-2.37777
47	Yiwabra	5.76078	-2.66073
48	Nkontompo_2	4.92036	-1.74413
49	Salman	5.00361	-2.24385
50	Tkw_Akwenm	5.28133	-1.99414

APPENDIX 3: MATLAB PROGRAMME CODE

```
function varargout = MSCalculator(varargin)

% MSCALCULATOR MATLAB code for MSCalculator.fig

% MSCALCULATOR, by itself, creates a new MSCALCULATOR or raises
the existing

% singleton*.

%

% H = MSCALCULATOR returns the handle to a new MSCALCULATOR or
the handle to

% the existing singleton*.

%

% MSCALCULATOR('CALLBACK',hObject,eventData,handles,...) calls the
local

% function named CALLBACK in MSCALCULATOR.M with the given
input arguments.

%

% MSCALCULATOR('Property','Value',...) creates a new
MSCALCULATOR or raises the

% existing singleton*. Starting from the left, property value pairs are
% applied to the GUI before MSCalculator_OpeningFcn gets called. An
% unrecognized property name or invalid value makes property application
% stop. All inputs are passed to MSCalculator_OpeningFcn via varargin.
```

```

%
%   *See GUI Options on GUIDE's Tools menu. Choose "GUI allows only one
%   instance to run (singleton)".
%
% See also: GUIDE, GUIDATA, GUIHANDLES
% Edit the above text to modify the response to help MSCalculator
% Last Modified by GUIDE v2.5 02-Jul-2020 09:13:29
% Begin initialization code - DO NOT EDIT
gui_Singleton = 1;
gui_State = struct('gui_Name',    mfilename, ...
                  'gui_Singleton', gui_Singleton, ...
                  'gui_OpeningFcn', @MSCalculator_OpeningFcn, ...
                  'gui_OutputFcn', @MSCalculator_OutputFcn, ...
                  'gui_LayoutFcn', [] , ...
                  'gui_Callback', []);
if nargin && ischar(varargin{1})
    gui_State.gui_Callback = str2func(varargin{1});
end
if nargout
    [varargout{1:nargout}] = gui_mainfcn(gui_State, varargin{:});
else
    gui_mainfcn(gui_State, varargin{:});
end
% End initialization code - DO NOT EDIT
% --- Executes just before MSCalculator is made visible.
function MSCalculator_OpeningFcn(hObject, eventdata, handles, varargin)
% This function has no output args, see OutputFcn.
% hObject    handle to figure

```

```

% eventdata reserved - to be defined in a future version of MATLAB
% handles structure with handles and user data (see GUIDATA)
% varargin command line arguments to MSCalculator (see VARARGIN)
% Choose default command line output for MSCalculator
handles.output = hObject;
% Update handles structure
guidata(hObject, handles);
% UIWAIT makes MSCalculator wait for user response (see UIRESUME)
% uiwait(handles.figure1);
% --- Outputs from this function are returned to the command line.
function varargout = MSCalculator_OutputFcn(hObject, eventdata, handles)
% varargout cell array for returning output args (see VARARGOUT);
% hObject handle to figure
% eventdata reserved - to be defined in a future version of MATLAB
% handles structure with handles and user data (see GUIDATA)
% Get default command line output from handles structure
varargout{1} = handles.output;
function TxtHumanHeight_Callback(hObject, eventdata, handles)
% hObject handle to TxtHumanHeight (see GCBO)
% eventdata reserved - to be defined in a future version of MATLAB
% handles structure with handles and user data (see GUIDATA)
% Hints: get(hObject,'String') returns contents of TxtHumanHeight as text
% str2double(get(hObject,'String')) returns contents of TxtHumanHeight as a
double
HumanHeight=str2double(get(handles.TxtHumanHeight,'string'));
% --- Executes during object creation, after setting all properties.
function TxtHumanHeight_CreateFcn(hObject, eventdata, handles)
% hObject handle to TxtHumanHeight (see GCBO)
% eventdata reserved - to be defined in a future version of MATLAB

```

```

% handles empty - handles not created until after all CreateFcns called
% Hint: edit controls usually have a white background on Windows.
% See ISPC and COMPUTER.
if ispc && isequal(get(hObject,'BackgroundColor'),
get(0,'defaultUicontrolBackgroundColor'))
    set(hObject,'BackgroundColor','white');
end

function TxtNumberOfTransmitter_Callback(hObject, eventdata, handles)
% hObject handle to TxtNumberOfTransmitter (see GCBO)
% eventdata reserved - to be defined in a future version of MATLAB
% handles structure with handles and user data (see GUIDATA)
% Hints: get(hObject,'String') returns contents of TxtNumberOfTransmitter as
text
% str2double(get(hObject,'String')) returns contents of
TxtNumberOfTransmitter as a double
NumberOfTransmitter=str2double(get(handles.TxtNumberOfTransmitter,'string'))
;
% --- Executes during object creation, after setting all properties.
function TxtNumberOfTransmitter_CreateFcn(hObject, eventdata, handles)
% hObject handle to TxtNumberOfTransmitter (see GCBO)
% eventdata reserved - to be defined in a future version of MATLAB
% handles empty - handles not created until after all CreateFcns called
% Hint: edit controls usually have a white background on Windows.
% See ISPC and COMPUTER.
if ispc && isequal(get(hObject,'BackgroundColor'),
get(0,'defaultUicontrolBackgroundColor'))
    set(hObject,'BackgroundColor','white');
end

function TxtTransmitterPower_Callback(hObject, eventdata, handles)
% hObject handle to TxtTransmitterPower (see GCBO)

```

```

% eventdata reserved - to be defined in a future version of MATLAB
% handles structure with handles and user data (see GUIDATA)
% Hints: get(hObject,'String') returns contents of TxtTransmitterPower as text
% str2double(get(hObject,'String')) returns contents of TxtTransmitterPower
as a double
TransmitterPower=str2double(get(handles.TxtTransmitterPower,'string'));
% --- Executes during object creation, after setting all properties.
function TxtTransmitterPower_CreateFcn(hObject, eventdata, handles)
% hObject handle to TxtTransmitterPower (see GCBO)
% eventdata reserved - to be defined in a future version of MATLAB
% handles empty - handles not created until after all CreateFcns called
% Hint: edit controls usually have a white background on Windows.
% See ISPC and COMPUTER.
if ispc && isequal(get(hObject,'BackgroundColor'),
get(0,'defaultUicontrolBackgroundColor'))
    set(hObject,'BackgroundColor','white');
end
function TxtDistanceFromTransmitter_Callback(hObject, eventdata, handles)
% hObject handle to TxtDistanceFromTransmitter (see GCBO)
% eventdata reserved - to be defined in a future version of MATLAB
% handles structure with handles and user data (see GUIDATA)
% Hints: get(hObject,'String') returns contents of TxtDistanceFromTransmitter as
text
% str2double(get(hObject,'String')) returns contents of
TxtDistanceFromTransmitter as a double
DistanceFromTransmitter=str2double(get(handles.TxtDistanceFromTransmitter,'s
tring'));
% --- Executes during object creation, after setting all properties.
function TxtDistanceFromTransmitter_CreateFcn(hObject, eventdata, handles)
% hObject handle to TxtDistanceFromTransmitter (see GCBO)

```

```

% eventdata reserved - to be defined in a future version of MATLAB
% handles empty - handles not created until after all CreateFcns called
% Hint: edit controls usually have a white background on Windows.
% See ISPC and COMPUTER.
if ispc && isequal(get(hObject,'BackgroundColor'),
get(0,'defaultUicontrolBackgroundColor'))
    set(hObject,'BackgroundColor','white');
end

function TxtHeightOfAntenna_Callback(hObject, eventdata, handles)
% hObject handle to TxtHeightOfAntenna (see GCBO)
% eventdata reserved - to be defined in a future version of MATLAB
% handles structure with handles and user data (see GUIDATA)
% Hints: get(hObject,'String') returns contents of TxtHeightOfAntenna as text
% str2double(get(hObject,'String')) returns contents of TxtHeightOfAntenna
as a double
HeightOfAntenna=str2double(get(handles.TxtHeightOfAntenna,'string'));
% --- Executes during object creation, after setting all properties.
function TxtHeightOfAntenna_CreateFcn(hObject, eventdata, handles)
% hObject handle to TxtHeightOfAntenna (see GCBO)
% eventdata reserved - to be defined in a future version of MATLAB
% handles empty - handles not created until after all CreateFcns called
% Hint: edit controls usually have a white background on Windows.
% See ISPC and COMPUTER.
if ispc && isequal(get(hObject,'BackgroundColor'),
get(0,'defaultUicontrolBackgroundColor'))
    set(hObject,'BackgroundColor','white');
end
% --- Executes on button press in TxtVerticalHPBW.
function TxtVerticalHPBW_Callback(hObject, eventdata, handles)

```

```

% hObject    handle to TxtVerticalHPBW (see GCBO)
% eventdata reserved - to be defined in a future version of MATLAB
% handles    structure with handles and user data (see GUIDATA)
VerticalHPBW=str2double(get(handles.TxtVerticalHPBW,'string'));
% --- Executes during object creation, after setting all properties.
function TxtVerticalHPBW_CreateFcn(hObject, eventdata, handles)
% hObject    handle to TxtVerticalHPBW (see GCBO)
% eventdata reserved - to be defined in a future version of MATLAB
% handles    empty - handles not created until after all CreateFcns called
% --- Executes on button press in TxtHorizontalHPBW.
function TxtHorizontalHPBW_Callback(hObject, eventdata, handles)
% hObject    handle to TxtHorizontalHPBW (see GCBO)
% eventdata reserved - to be defined in a future version of MATLAB
% handles    structure with handles and user data (see GUIDATA)
HorizontalHPBW=str2double(get(handles.TxtHorizontalHPBW,'string'));
% --- Executes during object creation, after setting all properties.
function TxtHorizontalHPBW_CreateFcn(hObject, eventdata, handles)
% hObject    handle to TxtHorizontalHPBW (see GCBO)
% eventdata reserved - to be defined in a future version of MATLAB
% handles    empty - handles not created until after all CreateFcns called
function TxtTiltAngle_Callback(hObject, eventdata, handles)
% hObject    handle to TxtTiltAngle (see GCBO)
% eventdata reserved - to be defined in a future version of MATLAB
% handles    structure with handles and user data (see GUIDATA)
% Hints: get(hObject,'String') returns contents of TxtTiltAngle as text
%    str2double(get(hObject,'String')) returns contents of TxtTiltAngle as a
double
TiltAngle=str2double(get(handles.TxtTiltAngle,'string'));
% --- Executes during object creation, after setting all properties.

```

```

function TxtTiltAngle_CreateFcn(hObject, eventdata, handles)
% hObject    handle to TxtTiltAngle (see GCBO)
% eventdata  reserved - to be defined in a future version of MATLAB
% handles    empty - handles not created until after all CreateFcns called
% Hint: edit controls usually have a white background on Windows.
%         See ISPC and COMPUTER.
if ispc && isequal(get(hObject,'BackgroundColor'),
get(0,'defaultUicontrolBackgroundColor'))
    set(hObject,'BackgroundColor','white');
end

function TxtOperatingFrequency_Callback(hObject, eventdata, handles)
% hObject    handle to TxtOperatingFrequency (see GCBO)
% eventdata  reserved - to be defined in a future version of MATLAB
% handles    structure with handles and user data (see GUIDATA)
% Hints: get(hObject,'String') returns contents of TxtOperatingFrequency as text
%        str2double(get(hObject,'String')) returns contents of
TxtOperatingFrequency as a double
OperatingFrequency=str2double(get(handles.TxtOperatingFrequency,'string'));
% --- Executes during object creation, after setting all properties.
function TxtOperatingFrequency_CreateFcn(hObject, eventdata, handles)
% hObject    handle to TxtOperatingFrequency (see GCBO)
% eventdata  reserved - to be defined in a future version of MATLAB
% handles    empty - handles not created until after all CreateFcns called
% Hint: edit controls usually have a white background on Windows.
%         See ISPC and COMPUTER.
if ispc && isequal(get(hObject,'BackgroundColor'),
get(0,'defaultUicontrolBackgroundColor'))
    set(hObject,'BackgroundColor','white');
end

```

```

% --- Executes on button press in ButtonReset.
function ButtonReset_Callback(hObject, eventdata, handles)
% hObject    handle to ButtonReset (see GCBO)
% eventdata  reserved - to be defined in a future version of MATLAB
% handles    structure with handles and user data (see GUIDATA)
set(handles.TxtOperatingFrequency,'string','');
set(handles.TxtNumberOfTransmitter,'string','');
set(handles.TxtHumanHeight,'string','');
set(handles.TxtTransmitterPower,'string','');
set(handles.TxtDistanceFromTransmitter,'string','');
set(handles.TxtDistanceFromTransmitter,'string','');
set(handles.TxtHeightOfAntenna,'string','');
set(handles.TxtVerticalHPBW,'string','');
set(handles.TxtHorizontalHPBW,'string','');
set(handles.TxtTiltAngle,'string','');
set(handles.TxtAntenaGain,'string','');
set(handles.TxtElectricFieldStrength,'string','');
set(handles.TxtPowerDensity,'string','');
set(handles.TxtCompliance,'string','');
% set(handles.axes1,'string','');
% --- Executes on button press in ButtonEFieldGreaph.
function ButtonEFieldGreaph_Callback(hObject, eventdata, handles)
% hObject    handle to ButtonEFieldGreaph (see GCBO)
% eventdata  reserved - to be defined in a future version of MATLAB
% handles    structure with handles and user data (see GUIDATA)
HumanHeight=str2double(get(handles.TxtHumanHeight,'string'));
DistanceFromTransmitter=str2double(get(handles.TxtDistanceFromTransmitter,'s
tring'));
HeightOfAntenna=str2double(get(handles.TxtHeightOfAntenna,'string'));

```

```

TransmitterPower=str2double(get(handles.TxtTransmitterPower,'string'));
dh=HeightOfAntenna-HumanHeight;
r=sqrt(power(dh,2)+power(DistanceFromTransmitter,2));
u=(r-2:0.1:r+2);
VerticalHPBW=str2double(get(handles.TxtVerticalHPBW,'string'));
HorizontalHPBW=str2double(get(handles.TxtHorizontalHPBW,'string'));
TiltAngle=str2double(get(handles.TxtTiltAngle,'string'));
theta=(VerticalHPBW-TiltAngle);
phi=HorizontalHPBW;
G=100./(theta*phi);
D=(10*log10(G))-2.14;
D=10*log10(D);
[DistanceFromTransmitter,HeightOfAntenna] =
meshgrid(20:0.2:DistanceFromTransmitter);
r=sqrt(power(HeightOfAntenna,2)+power(DistanceFromTransmitter,2));
EFS=abs(((1./sqrt(2)).*sqrt(TransmitterPower).*D)./r));
axes(handles.axes1);
% plot(DT,HOA,EFP)
mesh(EFS);
title('Electric field strength');
zlabel('Electric Field Strength');
xlabel('height of mast (m)');
ylabel ('Mast Distance(m)');
% view (-20,60)
colorbar;
% rotate3d on;
Rotate3d(0.3, [0, 0, 0], [0, 0, 1])
% --- Executes on button press in ButtonGain.
function ButtonGain_Callback(hObject, eventdata, handles)

```

```

% hObject   handle to ButtonGain (see GCBO)
% eventdata reserved - to be defined in a future version of MATLAB
% handles   structure with handles and user data (see GUIDATA)
% Directivity results
VerticalHPBW=str2double(get(handles.TxtVerticalHPBW,'string'));
HorizontalHPBW=str2double(get(handles.TxtHorizontalHPBW,'string'));
TiltAngle=str2double(get(handles.TxtTiltAngle,'string'));
theta=(VerticalHPBW-TiltAngle);
phi=HorizontalHPBW;
G=100./(theta*phi);
D=(10*log10(G))-2.14;
D=10*log10(D);
set(handles.TxtAntenaGain,'string',D)
% --- Executes on button press in ButtonElectricFieldStrength.
function ButtonElectricFieldStrength_Callback(hObject, eventdata, handles)
% hObject   handle to ButtonElectricFieldStrength (see GCBO)
% eventdata reserved - to be defined in a future version of MATLAB
% handles   structure with handles and user data (see GUIDATA)
HumanHeight=str2double(get(handles.TxtHumanHeight,'string'));
DistanceFromTransmitter=str2double(get(handles.TxtDistanceFromTransmitter,'s
tring'));
HeightOfAntenna=str2double(get(handles.TxtHeightOfAntenna,'string'));
TransmitterPower=str2double(get(handles.TxtTransmitterPower,'string'));
dh=HeightOfAntenna-HumanHeight;
r=sqrt(power(dh,2)+power(DistanceFromTransmitter,2));
u=(r-2:0.1:r+2);
VerticalHPBW=str2double(get(handles.TxtVerticalHPBW,'string'));
HorizontalHPBW=str2double(get(handles.TxtHorizontalHPBW,'string'));
TiltAngle=str2double(get(handles.TxtTiltAngle,'string'));

```

```

theta=(VerticalHPBW-TiltAngle);
phi=HorizontalHPBW;
G=100./(theta*phi);
D=(10*log10(G))-2.14;
D=10*log10(D);
EFS=abs(((1./sqrt(2)).*sqrt(TransmitterPower).*D)./r)+0.1*randn(size(u));
EFS1 = min(EFS);
set(handles.TxtElectricFieldStrength,'string',EFS1)
% --- Executes on button press in ButtonPowerDensity.
function ButtonPowerDensity_Callback(hObject, eventdata, handles)
% hObject    handle to ButtonPowerDensity (see GCBO)
% eventdata  reserved - to be defined in a future version of MATLAB
% handles    structure with handles and user data (see GUIDATA)
NumberOfTransmitter=str2double(get(handles.TxtNumberOfTransmitter,'string'))
;
HumanHeight=str2double(get(handles.TxtHumanHeight,'string'));
DistanceFromTransmitter=str2double(get(handles.TxtDistanceFromTransmitter,'s
tring'));
HeightOfAntenna=str2double(get(handles.TxtHeightOfAntenna,'string'));
TransmitterPower=str2double(get(handles.TxtTransmitterPower,'string'));
dh=HeightOfAntenna-HumanHeight;
r=sqrt(power(dh,2)+power(DistanceFromTransmitter,2));
u=(r-2:0.1:r+2);
VerticalHPBW=str2double(get(handles.TxtVerticalHPBW,'string'));
HorizontalHPBW=str2double(get(handles.TxtHorizontalHPBW,'string'));
TiltAngle=str2double(get(handles.TxtTiltAngle,'string'));
theta=(VerticalHPBW-TiltAngle);
phi=HorizontalHPBW;
G=100./(theta*phi);

```

```

D=(10*log10(G))-2.14;
D=10*log10(D);
EFS=abs(((1./sqrt(2)).*sqrt(TransmitterPower).*D)./r)+0.1*randn(size(u));
PD = (NumberOfTransmitter/2)*(1./377)*power(EFS,2);
PD1 = min(PD);
set(handles.TxtPowerDensity,'string',PD1)
% --- Executes on button press in ButtonCompliance.
function ButtonCompliance_Callback(hObject, eventdata, handles)
% hObject    handle to ButtonCompliance (see GCBO)
% eventdata  reserved - to be defined in a future version of MATLAB
% handles    structure with handles and user data (see GUIDATA)
NumberOfTransmitter=str2double(get(handles.TxtNumberOfTransmitter,'string'))
;
HumanHeight=str2double(get(handles.TxtHumanHeight,'string'));
DistanceFromTransmitter=str2double(get(handles.TxtDistanceFromTransmitter,'s
tring'));
HeightOfAntenna=str2double(get(handles.TxtHeightOfAntenna,'string'));
TransmitterPower=str2double(get(handles.TxtTransmitterPower,'string'));
dh=HeightOfAntenna-HumanHeight;
r=sqrt(power(dh,2)+power(DistanceFromTransmitter,2));
u=(r-2:0.1:r+2);
VerticalHPBW=str2double(get(handles.TxtVerticalHPBW,'string'));
HorizontalHPBW=str2double(get(handles.TxtHorizontalHPBW,'string'));
TiltAngle=str2double(get(handles.TxtTiltAngle,'string'));
theta=(VerticalHPBW-TiltAngle);
phi=HorizontalHPBW;
G=100./(theta*phi);
D=(10*log10(G))-2.14;
D=10*log10(D);

```

```

EFS=abs(((1./sqrt(2)).*sqrt(TransmitterPower).*D)./r)+0.1*randn(size(u));
PD = (NumberOfTransmitter/2)*(1./377)*power(EFS,2);
PD1 = min(PD);
C = PD1./4;
set(handles.TxtCompliance,'string',C)
function TxtAntenaGain_Callback(hObject, eventdata, handles)
% hObject    handle to TxtAntenaGain (see GCBO)
% eventdata  reserved - to be defined in a future version of MATLAB
% handles    structure with handles and user data (see GUIDATA)
% Hints: get(hObject,'String') returns contents of TxtAntenaGain as text
%         str2double(get(hObject,'String')) returns contents of TxtAntenaGain as a
double
AntenaGain=str2double(get(handles.TxtAntenaGain,'string'));
% --- Executes during object creation, after setting all properties.
function TxtAntenaGain_CreateFcn(hObject, eventdata, handles)
% hObject    handle to TxtAntenaGain (see GCBO)
% eventdata  reserved - to be defined in a future version of MATLAB
% handles    empty - handles not created until after all CreateFcns called
% Hint: edit controls usually have a white background on Windows.
%         See ISPC and COMPUTER.
if ispc && isequal(get(hObject,'BackgroundColor'),
get(0,'defaultUicontrolBackgroundColor'))
    set(hObject,'BackgroundColor','white');
end
function TxtElectricFieldStrength_Callback(hObject, eventdata, handles)
% hObject    handle to TxtElectricFieldStrength (see GCBO)
% eventdata  reserved - to be defined in a future version of MATLAB
% handles    structure with handles and user data (see GUIDATA)
% Hints: get(hObject,'String') returns contents of TxtElectricFieldStrength as text

```

```

%    str2double(get(hObject,'String')) returns contents of
TxtElectricFieldStrength as a double

% --- Executes during object creation, after setting all properties.
function TxtElectricFieldStrength_CreateFcn(hObject, eventdata, handles)
% hObject    handle to TxtElectricFieldStrength (see GCBO)
% eventdata  reserved - to be defined in a future version of MATLAB
% handles    empty - handles not created until after all CreateFcns called

% Hint: edit controls usually have a white background on Windows.

%    See ISPC and COMPUTER.

if ispc && isequal(get(hObject,'BackgroundColor'),
get(0,'defaultUicontrolBackgroundColor'))
    set(hObject,'BackgroundColor','white');
end

function TxtPowerDensity_Callback(hObject, eventdata, handles)
% hObject    handle to TxtPowerDensity (see GCBO)
% eventdata  reserved - to be defined in a future version of MATLAB
% handles    structure with handles and user data (see GUIDATA)

% Hints: get(hObject,'String') returns contents of TxtPowerDensity as text
%    str2double(get(hObject,'String')) returns contents of TxtPowerDensity as a
double

% --- Executes during object creation, after setting all properties.
function TxtPowerDensity_CreateFcn(hObject, eventdata, handles)
% hObject    handle to TxtPowerDensity (see GCBO)
% eventdata  reserved - to be defined in a future version of MATLAB
% handles    empty - handles not created until after all CreateFcns called

% Hint: edit controls usually have a white background on Windows.

%    See ISPC and COMPUTER.

if ispc && isequal(get(hObject,'BackgroundColor'),
get(0,'defaultUicontrolBackgroundColor'))
    set(hObject,'BackgroundColor','white');

```

```

end

function TxtCompliance_Callback(hObject, eventdata, handles)
% hObject    handle to TxtCompliance (see GCBO)
% eventdata  reserved - to be defined in a future version of MATLAB
% handles    structure with handles and user data (see GUIDATA)
% Hints: get(hObject,'String') returns contents of TxtCompliance as text
%    str2double(get(hObject,'String')) returns contents of TxtCompliance as a
double

% --- Executes during object creation, after setting all properties.
function TxtCompliance_CreateFcn(hObject, eventdata, handles)
% hObject    handle to TxtCompliance (see GCBO)
% eventdata  reserved - to be defined in a future version of MATLAB
% handles    empty - handles not created until after all CreateFcns called
% Hint: edit controls usually have a white background on Windows.
%    See ISPC and COMPUTER.
if ispc && isequal(get(hObject,'BackgroundColor'),
get(0,'defaultUicontrolBackgroundColor'))
    set(hObject,'BackgroundColor','white');
end

```

ANALYSIS OF ELECTRIC FIELD STRENGTHS AND POWER DENSITIES OF 4G LTE BASE STATIONS IN THE GREATER ACCRA REGION OF GHANA

A. R. Fuseini^{1*}, J. K. Amoako¹ and A. Twum²

¹Health Physics and Instrumentation Centre, Ghana Atomic Energy Commission, P.O. Box LG 80, Accra,

²Department of Physics, University of Cape Coast, Cape Coast.

ABSTRACT

The analysis of electric field strengths and power densities at Fifty (50) Fourth Generation Long Time Evolution (4G LTE) telecommunication base stations in the Greater Accra region, which is an urban and densely populated area was carried out using an Anritsu Spectrum Master coupled to a handheld log-periodic antenna. Measurements were made at five different locations at a height of between 1.5 m above ground level around each of the base stations at a transmission peak period during the day. The measurements were however made at public access points around sites near schools, hospitals and highly populated residential areas. The results of the compliance electric field measurement for the various base stations in the Greater Accra region used for this work varied from as low as 3.85E-08 mV/m at site 46 to as high as 1.17E-02 mV/m at site 40 with corresponding power densities of 1.54E-07 mW/m² and 4.71E-02 mW/m² respectively. The results however comply with the ICNIRP recommended values of 38.89 V/m and 4 W/m² for electric field strength and power density for 800 MHz frequency band respectively.

INTRODUCTION

Mobile communication technology has dominated the telecommunication industry in the world (Olatinwo et. al, 2014). In Ghana most of the telephone mast are installed near hospitals, schools and in densely populated residential areas. There is evidence that the high number of these base stations are of significant concern to the general public (Chitranshi et. al, 2014). It is envisaged that there will be an increase in the number of usage of moibe phones in the near future (Singh, 2012). This will bring about an increase in the number of base stations and will lead to more agitations with regards to the health and safety concerns associated with these base stations (Bello, 2010). There have been reports of dizziness, sleeping problems and nausea, due to RF radiations associated with these base stations (Eger et. al, 2009).

Ghana has adopted the ICNIRP reference limits as it does not currently have its own national guidelines. Therefore

the results of this work were compared to that of the ICNIRP safety limits on electromagnetic field.

STUDY AREA

This region has the smallest area of Ghana's 10 administrative regions, occupying a total land mass of 3,245 square kilometres or 1.4 per cent of the total land area of Ghana (<https://www.stasghana.gov.gh>). It is located at 5.8143° N latitude and 0.0747° E longitude and bordered on the north by the Eastern Region, on the east by the Volta Region, on the south by the Gulf of Guinea, and on the west by the Central Region (<https://www.ghana.gov.gh>). This is the second most populated region, after the Ashanti Region, with a population of 4,010,054 in 2010, accounting for 16.3 per cent of Ghana's total population. Below is a map that shows the sites where measurements were taken in the region (<https://www.stasghana.gov.gh>).

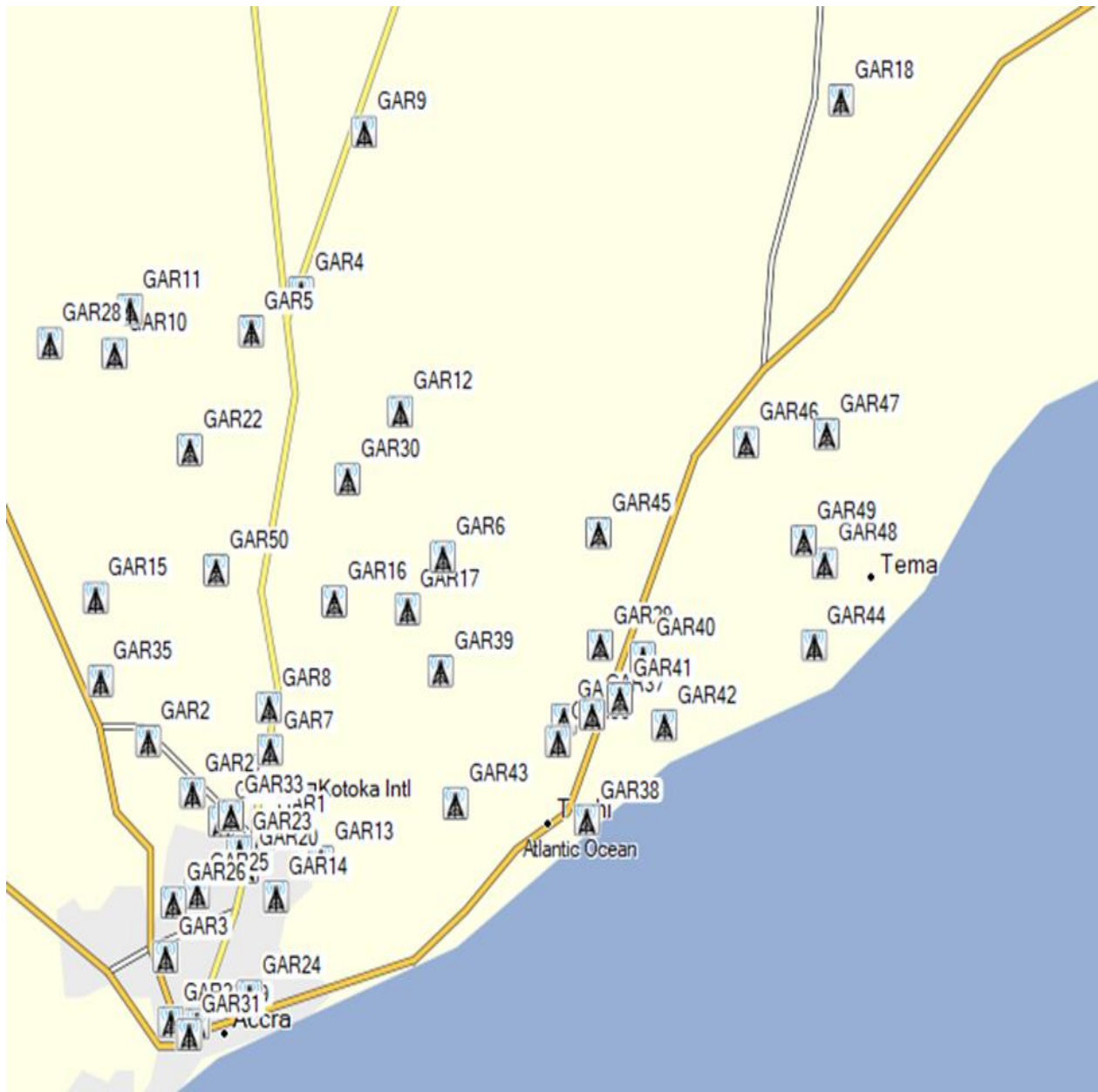


Figure 1: Map that showing sites where measurements were taken in Greater Accra region

MATERIALS AND METHODS

Radiofrequency (RF) signals were measured around fifty (50) Fourth Generation Long Term Evolution (4G LTE) base stations in the Greater Accra region of Ghana, which is an urban and densely populated areas.

The measurements were carried out at five (5) different locations around each mast using an Anritsu Spectrum Master, model MS2720T which was coupled to a handheld Log Periodic Antenna (LPA) model TS-6021.

The spectrum master had an in-built antenna factors and associated cable factors that were able to correct the measured electric field strength. The points at which the measurement were taken around the base stations were chosen based on the direction of the antennae (sector). Also, all the measurements were made at public access points and the points were chosen to represent the highest levels of exposure to which a person might be subjected to, considering the positions of antennas and also to make sure that there were little or no reflecting objects and as few overhead conductors like power lines and buildings with metal roofs much as possible. These locations were however found by a quick sweep of the area using the measuring equipment. The selected sites were chosen to cover schools, hospitals and highly populated residential areas.

The antenna was connected to the spectrum master with the aid of a RF cable which had a load impedance of 50Ω . The data was then downloaded after each day's measurement onto a lap-top computer. The spectrum master software that had been installed on the lap top was then used to determine the corresponding electric field strength in dB (mV/m) which is a quantitative expression of the intensity of an electric field at a particular location.

$$E = V_o + K + A_c \quad [1]$$

Where; E is the electric field strength in dB (mV/m), V_o is the output voltage of the antenna in dB (mV), K is the antenna factor in dB (m^{-1}) and A_c is the attenuation of the antenna signal path in dB.

An average of all the 5 points at which the measurements were taken at each site was then calculated using the formula:

$$\text{Mean, } \bar{x} = \sum_{j=1}^n \frac{x_j}{n} \quad [2]$$

The intention of the measurements was to determine if the RF EME over the frequency bands of 800 MHz of the cell sites comply with the public exposure limits of 38.89 V/m recommended by the International Commission on Non-ionising Radiation Protection (ICNIRP) (ICNIRP, 2010).

The power density (in Wm^{-2}) which is the amount of power (time rate of energy transfer) per unit volume was calculated using the relations:

$$S = \frac{E^2}{Z_o} \quad [3]$$

Where: E is the electric field strength in V/m, S is the power density in W/m^2 and Z_o is the impedance in Ω . For free space, impedance is 377Ω . In determining compliance with ICNIRP, the relation below was used:

$$\sum_{i=1}^N \frac{S_i^{\text{meas}}}{S_{\text{guid}}^{\text{meas}}} = \frac{S_1^{\text{meas}}}{S_{\text{guid}}^{\text{meas}}} + \frac{S_2^{\text{meas}}}{S_{\text{guid}}^{\text{meas}}} + \dots + \frac{S_N^{\text{meas}}}{S_{\text{guid}}^{\text{meas}}} < 1 \quad [4]$$

Where S_{meas} is the measured (calculated) power density and S_{guid} is the guidance or reference power density and checked with the public exposure limits of $4 W/m^2$ as recommended by the International Commission on Non-ionising Radiation Protection (ICNIRP), (ICNIRP, 2010).

RESULTS AND DISCUSSIONS

The results of the compliance electric field strength measurement for the various base stations in the region varied from as low as $3.85E-08$ mV/m at site 46 which had a mean value of $1.42E-07$ mV/m and a maximum value of $3.14E-07$ mV/m to as high as $1.17E-02$ mV/m at site 40 which had a mean value of $8.30E-03$ mV/m and a minimum

value of $5.65E-03$ mV/m. The corresponding power densities of site 46 were; a minimum of $1.54E-07$ mW/m², a mean of $5.68E-07$ mW/m² and a maximum of $6.39E-07$ the area is mainly a residential area with few factories.

Whereas the corresponding power densities of site 40 were $3.33E-02$ mW/m² as the mean and $2.27E-02$ mW/m² and

mW/m². The site is located along the Tema-Aflao highway and

$4.71E-02$ mW/m² as the minimum and maximum respectively. The mast is located in a sect of estate buildings and it's close to a beach and a lagoon. It's originally a fishing village.

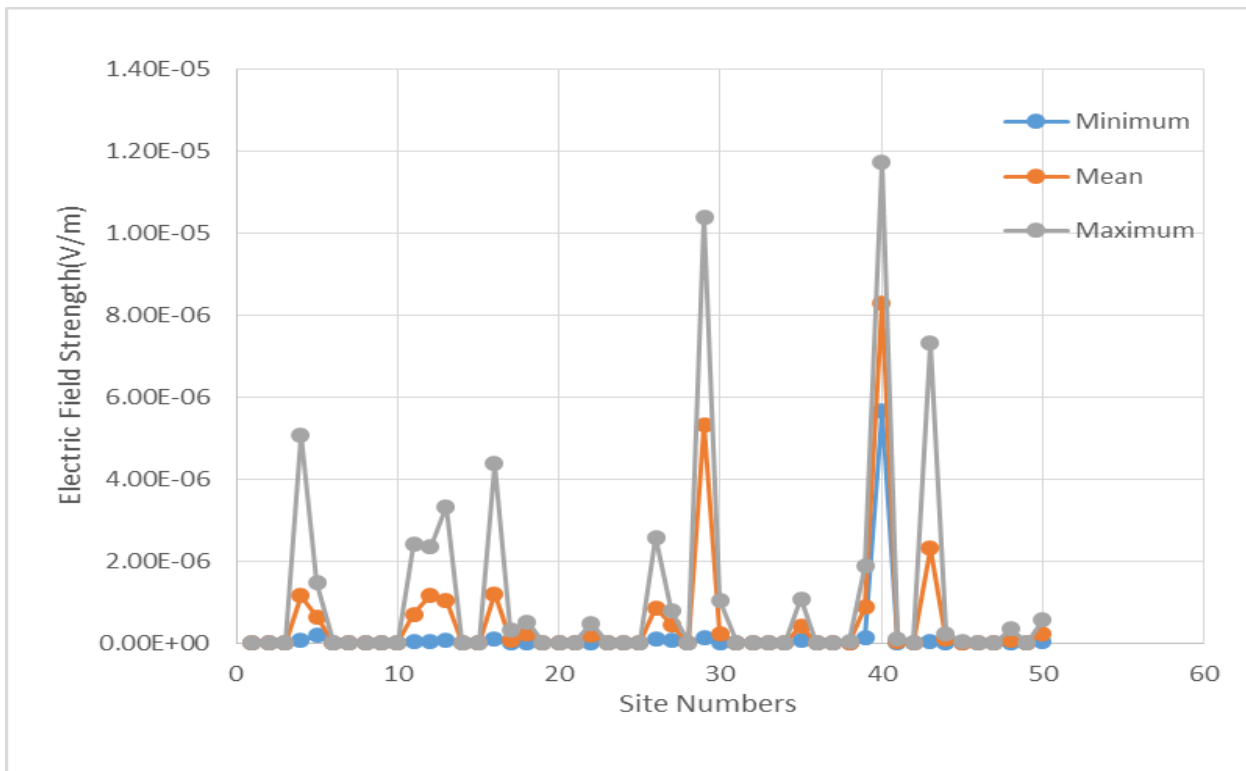


Figure 1: Graph of electric field strength variation with site numbers

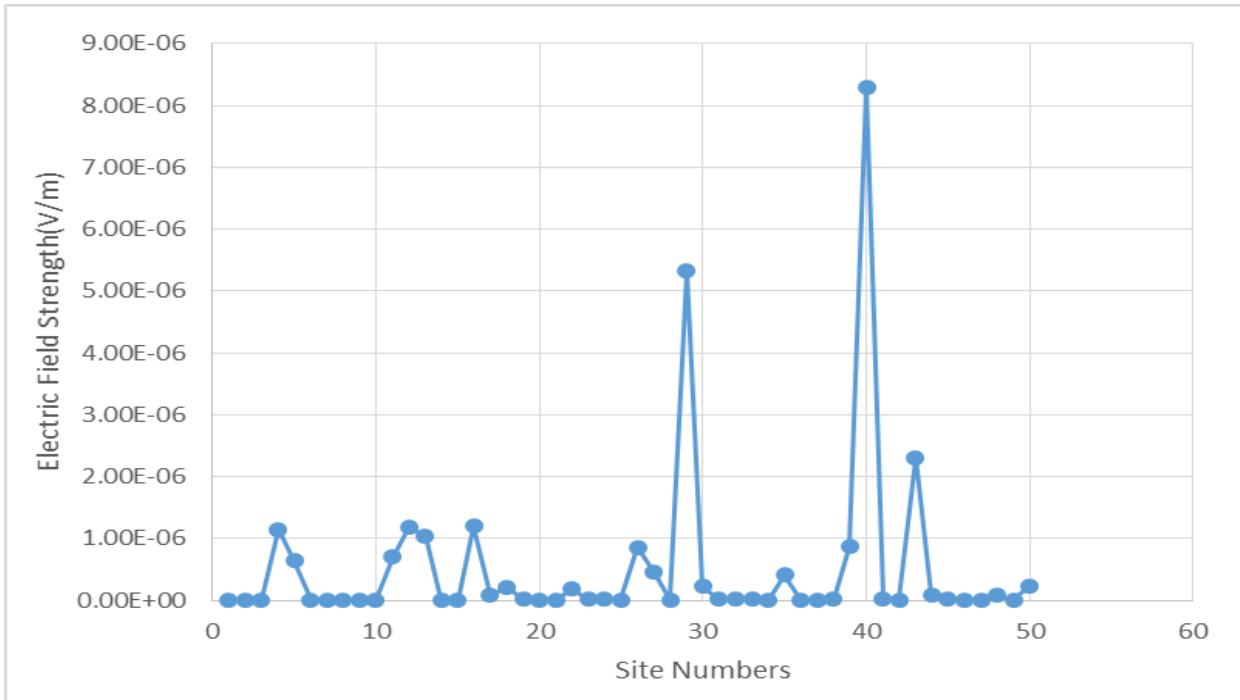


Figure 2: Graph of mean electric field strength variation with site numbers

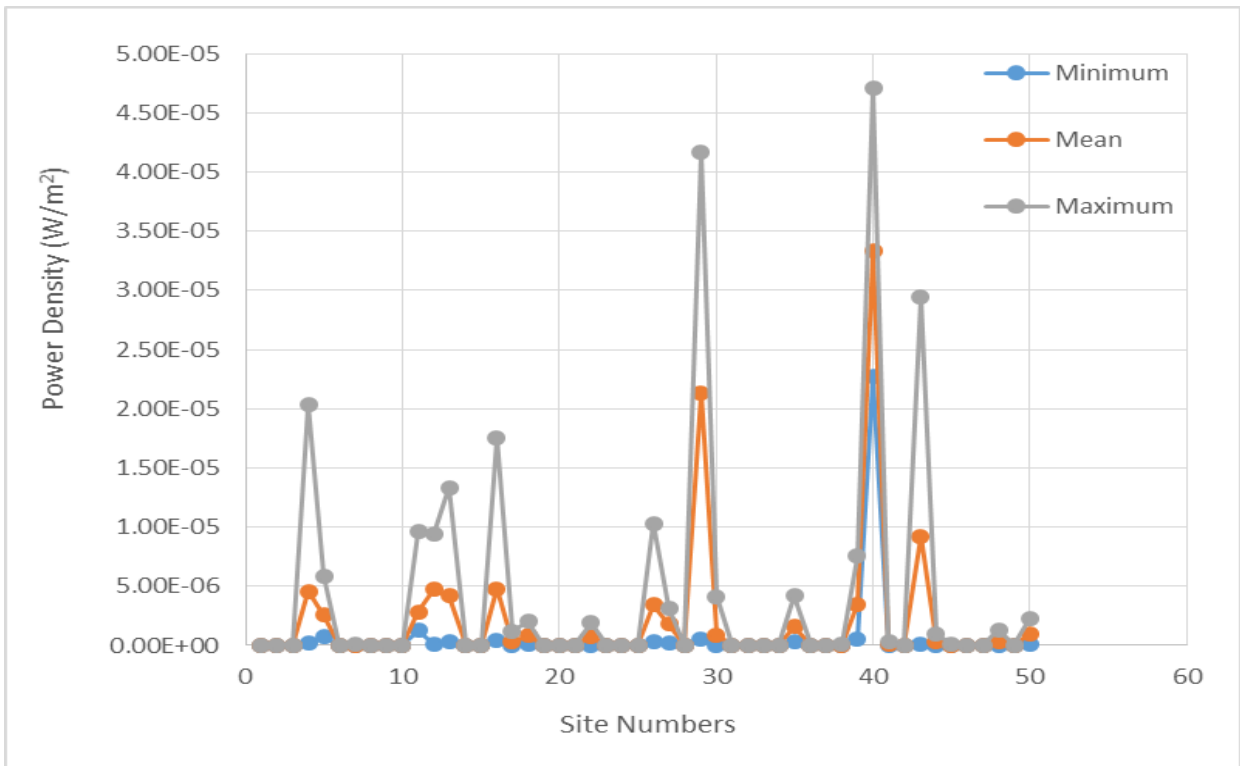


Figure 3: Graph of power density variation with site numbers

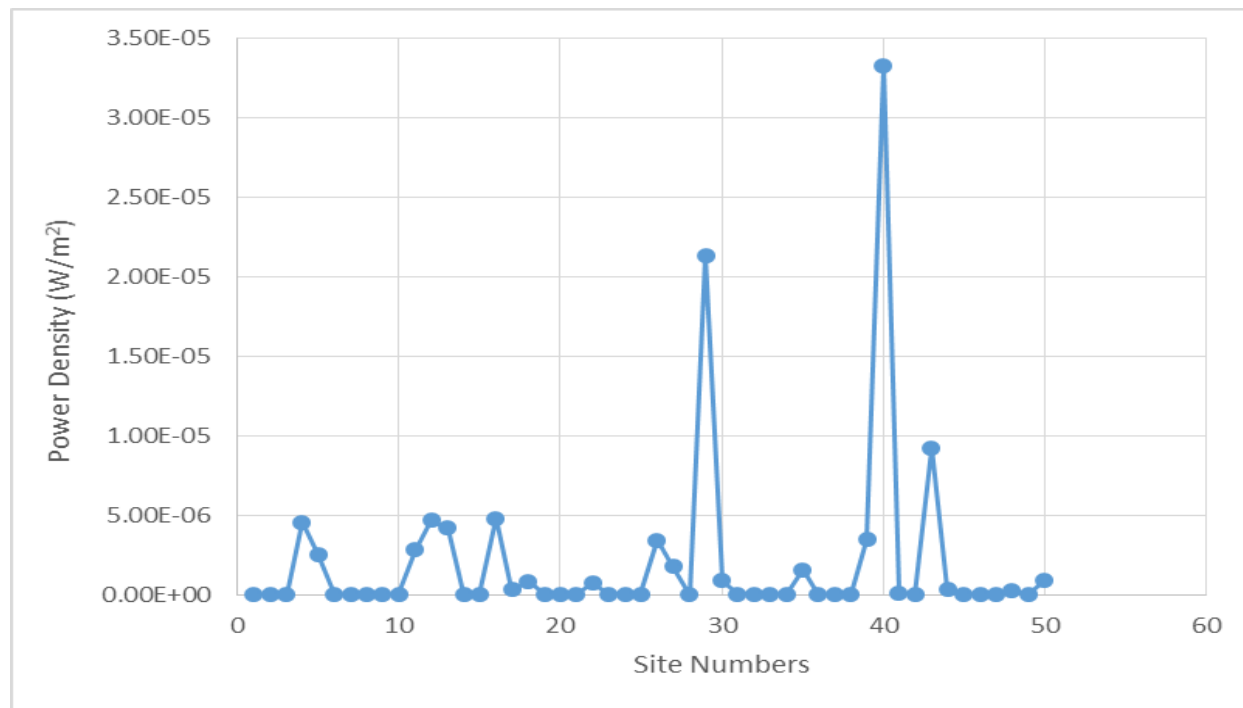


Figure 4: Graph of mean power density variation with site numbers

Specifically, the highest electric field strength is 0.001% of the recommended limit of 38.89 V/m and the highest power density measured within the vicinity of the masts was 4.71E-02 mW/m² of the recommended limit of 4 W/m².

The results of this work were compared to Deatanyah et.al, (2018) who also measured and analyzed radiofrequency radiations from selected base station in Ghana. Their average electric field strength for GSM 900 was 266.13 mV/m, GSM 1800 was 414.43 mV/m and UMTS 2100 was 366.54 mV/m. The average power densities from Deatanyah et.al, (2018) were GSM 900 was 0.1879mW/m², GSM 1800 was 0.4556 mW/m² and UMTS 2100 was 0.3564 mW/m². This indicates that the results from this work were relatively lower than theirs and could be attributed to the fact that the technology used in the 4 G LTE is much better than that in the 1G, 2G and 3G and also had a lower operating frequency than their work.

The results of the power density were also compared to Chen and Lin, (2014). They also measured Electric fields emitted from a LTE Base Station in an Urban Area in Taiwan and their maximum power density was 1.853 mW/m² and so appeared higher than this work.

Also, there is generally a higher level of compliance of the results with the ICNIRP limits. But this does not mean that there is no possibility of a biological effect from these sites when one is exposed to them for long.

CONCLUSION

From the study, there will surely be an increase in the number of base stations and also an introduction of new and sophisticated technologies into the telecommunication industry as far as Ghana is concern. And so the levels of public exposures to radiofrequency radiations is expected to increase.

This work should be replicated in the other regions that were not studied. This will therefore be a base point as far as the study of 4G LTE base stations are concern in Ghana.

ACKNOWLEDGEMENTS

The researcher would like to thank the Radiation Protection Institute of the Ghana Atomic Energy Commission and the University of Cape Coast for the provision of funds.

REFERENCES

1. Bello M. O. (2010) "Effects of the Location of GSM Base Stations on Satisfaction of Occupiers and Rental Value of Proximate Residential Property," *Computer and Information Science*, vol. 3, pp. 159-170.
2. Chen Hsing-Yi and Lin Tsung-Han (2014): Simulations and Measurements of Electric Fields Emitted from a LTE Base Station in an Urban Area. *International Journal of Antennas and Propagation*. Volume 2014, Article ID 147341, 10 pages
3. Chitranshi R., Mehrotra R. K. and Pancoli P. (2014) "Analysis of Cell Tower Radiation, RF Safety and Practical Realization of Compliance Distance," *International Journal of Scientific and Research Publications*, vol. 4, pp. 1 – 6.
4. Deatanyah P., Amoako J.K, Abavare E.K.K and Menyeh A. (2017): Analysis of electric field strength and power around selected mobile base stations. *Radiation Protection Dosimetry* (2018), pp. 1–8
5. <https://www.stasghana.gov.gh-09/01/2019>
6. <https://www.ghana.gov.gh-09/01/2019>
7. ICNIRP (2010): guidelines for limiting exposure to time varying Electric, Magnetic field and Electromagnetic fields (up to 300 GHz). *Journal of Health Phys* 99(6):818-836
8. Linhares, A., Terada M. A. B. and Soares A. J. M. (2013) "Estimating the Location of Maximum Exposure to Electromagnetic Fields Associated with a Radiocommunication Station," *Journal of Microwaves, Optoelectronics and Electromagnetic Application*, vol. 12, pp. 141-157,
9. Olatinwo S. O., Shoewu, O. and Makanjuola N. T. (2014) "Radio Wave Signal Attenuation in a GSM Network (EPE as a Case Study)," *The Pacific Journal of Science and Technology*, vol. 15, pp. 114 - 124.
10. Singh R. K. (2012) "Assessment of Electromagnetic Radiation from Base Station Antennas," *Indian Journal of Radio and Space Physics*, vol. 41, pp. 557-565.